SCIENCE CHINA
Information Sciences

• REVIEW •

May 2026, Vol. 69, Iss. 5, 151102:1–151102:44
https://doi.org/10.1007/s11432-025-4819-5

Continuous representation methods, theories, and applications: an overview and perspective

Yisi LUO[1], Xile ZHAO[2*] & Deyu MENG[1,3*]

[1]*School of Mathematics and Statistics, Ministry of Education Key Lab of Intelligent Networks and Network Security, Xi'an Jiaotong University, Xi'an 710049, China*
[2]*School of Mathematical Sciences, University of Electronic Science and Technology of China, Chengdu 611731, China*
[3]*Macao Institute of Systems Engineering, Macau University of Science and Technology, Macao 999078, China*

Received 20 May 2025/Revised 4 October 2025/Accepted 24 November 2025/Published online 14 April 2026

Abstract Recently, continuous representation methods have emerged as novel paradigms that characterize the intrinsic structures of real-world data through function representations that map positional coordinates to their corresponding values in the continuous space. As compared with the traditional discrete framework, the continuous framework demonstrates inherent superiority for data representation and reconstruction (e.g., image restoration, novel view synthesis, and waveform inversion) by offering inherent advantages including resolution flexibility, cross-modal adaptability, inherent smoothness, and parameter efficiency. In this review, we systematically examine recent advancements in continuous representation frameworks, focusing on three aspects: (i) continuous representation method designs, such as basis function representation, statistical modeling, tensor function decomposition, and implicit neural representation; (ii) theoretical foundations of continuous representations, such as approximation error analysis, convergence property, and implicit regularization; (iii) real-world applications of continuous representations derived from computer vision, graphics, bioinformatics, and remote sensing. Furthermore, we outline future directions and perspectives to inspire exploration and deepen insights to facilitate continuous representation methods, theories, and applications.

Keywords continuous representation, implicit neural representation, tensor decomposition, compressed sensing, optimization, convergence and generalization

Citation Luo Y S, Zhao X L, Meng D Y. Continuous representation methods, theories, and applications: an overview and perspective. Sci China Inf Sci, 2026, 69(5): 151102, https://doi.org/10.1007/s11432-025-4819-5

1 Introduction

In the era of big data, reconstructing high-quality data information from incomplete measurements, noisy observations, or physical rules and attributes remains a fundamental challenge across diverse domains [1–4], such as medical imaging reconstruction [5], satellite remote sensing [6], scene reconstruction in graphics [7], and numerical scientific computing [8]. Traditional data reconstruction methods often rely on discrete grid-based representations (e.g., vectors, matrices, or higher-order tensors [9]) and handcrafted priors (e.g., sparsity or low-rankness [10]), which may be inadequate for capturing intrinsic geometric or topological structures of complex real-world data. In particular, these limitations are encountered when handling irregularly sampled, heterogeneous modalities, or cross-resolution tasks, such as arbitrary-resolution imaging [11], 3D medical image registration [12], graphics [7], radar imaging geometry [13], and irregular spatial transcriptomics (ST) [14].

To address these challenges, continuous representation methods (see [2, 11, 15–18] for classical examples) have emerged as transformative paradigms for general data reconstruction problems. The continuous representation refers to the type of methods that leverage a continuous function representation for discrete data, which maps positional information (e.g., spatial coordinates, temporal index, or view directions) to the corresponding responses (e.g., image pixels, physical fields, or volume intensities) through certain parametric models, such as basis functions or deep neural networks (DNNs). To enhance the effectiveness of continuous representation, regularization terms can be further developed by imposing implicit or explicit structural constraints for the continuous representation function, such as differential operators in loss functions [19] and functional decomposition [2]. By embedding discrete data into such smooth, resolution-independent continuous spaces, these methods enable many advantages, such as global feature modeling, adaptability to irregular multi-dimensional data, resolution independence, and

* Corresponding author (email: xlzhao122003@163.com, dymeng@mail.xjtu.edu.cn)

interpretable learning theories. For instance, the implicit neural representations (INRs) [11, 16, 20] parameterize signals as continuous functions using neural networks, enabling seamless interpolation and super-resolution. Tensor functional decomposition frameworks [2,21] exploit the multilinear structure of high-dimensional data through low-rank factorizations of multivariate functions. Statistical continuous representation methods [21–23] encode temporal correlations in continuous time-indexed domains that are important for streaming or time series data analysis. Such continuous approaches inherently avoid discretization errors and achieve parameter efficiency—the discrete data can be implicitly represented by a parametric model that holds much fewer parameters[1)] [24]. The parameter efficiency is critical for tasks with large-scale datasets, e.g., 5D seismic data interpolation [25] or video space-time super-resolution [26]. The continuous representation also holds advantages for further integrating domain-specific knowledge, such as the physics-informed constraints for full-waveform inversion (FWI) [27], or quasi-static motion priors for magnetic resonance imaging (MRI) [28], bridging the gap between generic parametric models and application-driven requirements. Overall, continuous representation methods have emerged as increasingly effective paradigms for diverse data reconstruction tasks.

Despite rapid progress, the field remains generally fragmented. Existing studies often focus on isolated aspects, such as general continuous representation designs (e.g., Chebyshev expansions for functions [29], Fourier features INR [20], and wavelet INRs [30]), theoretical-oriented analyses (e.g., convergence analyses for DNNs, e.g., from the neural tangent kernel (NTK) theory [20,31,32] or implicit regularization perspective [2,33]), or domain-specific applications (e.g., continuous hyperspectral imaging (HSI) [34], deformable registration [12], and functional decomposing partial differential equations (PDEs) [35]), without synthesizing their interplay. These interplay parts are important for gaining deeper insights into these methods and developing further improvements. For example, the widely-studied INR-based arbitrary-scale image super-resolution [11] actually holds similar training paradigms to the neural operator (NO) [36,37], a way to approximate numerical PDE using neural networks, since both of them take some low-dimensional inputs (coordinates and latent vectors) and synthesize high-resolution responses. For another example, the tensorial radiance fields [38] used for 3D scene reconstruction actually hold intrinsic similarity with a bunch of tensor decomposing functional representations [2, 29, 39, 40] analyzed in scientific computing. The classical Fourier basis functional representation [8] holds similar ideas with more recent INR methods in Fourier basis-enhanced neural representations [20], to name but a few. More specifically, the "interplay" refers to the interplay among various types of methodologies, theoretical frameworks, and insights across different scientific domains that utilize continuous data representations. This interplay primarily includes two dimensions. (i) (Methodological interplay) A model architecture or algorithm developed for a specific problem in a sub-area (e.g., NO learning [37] in scientific computing) demonstrates potential to be effectively applied or adapted to solve challenges in another area (e.g., continuous image representation in computer vision [41] using operator learning). This creates a way for transferring efficient and robust algorithmic designs among sub-areas. (ii) (Theoretical interplay) Theoretical tools established in one domain (e.g., NTK theory for analyzing multilayer perceptrons [31]) can be leveraged to interpret, explain, or inspire the development of models in a different area (e.g., understanding the spectral bias of INRs [42] or the training dynamics of physics-informed neural networks [19]), boosting a deeper understanding of diverse methods and frameworks. In Subsection 2.7, we explicitly highlight representative examples of such interplay in the continuous representation field.

1.1 Contributions

The main aim of this work is to provide a comprehensive review of continuous representation methods including continuous representation parametric models and structural modeling designs, theoretical frameworks and current results that formally analyze the mathematical properties of continuous methods, and diverse domain-specific data reconstruction applications of continuous representation methods. The expectation is to bridge the information gap between different subareas within the continuous representation research field, thus enabling new exciting and transformative research directions unexplored before. An overview of the advancements in continuous representation methods, theories, and applications introduced in this work is summarized in Figure 1, and the fundamental concepts and advantages of continuous representation approaches are illustratively presented in Figure 2. We outline the main contributions of this review as follows.

• We provide a systematic review of continuous representation methods for data representation and reconstruction, structured around three parts—review of continuous methodology designs, theoretical insights of these

1) This advantage can be shown using tensor representation. Consider a tensor $\mathcal{A} \in \mathbb{R}^{n_1 \times n_2 \times n_3}$ and a parametric model $f(x, y, z) : \mathbb{R}^3 \to \mathbb{R}$ that maps the index of $\mathcal{A}$ to its value. According to the universal approximation theorem [24], a two-layer DNN can approximate this continuous function with small error, which holds much fewer parameters than the tensor $\mathcal{A}$ itself (i.e., less than $n_1 n_2 n_3$ parameters).

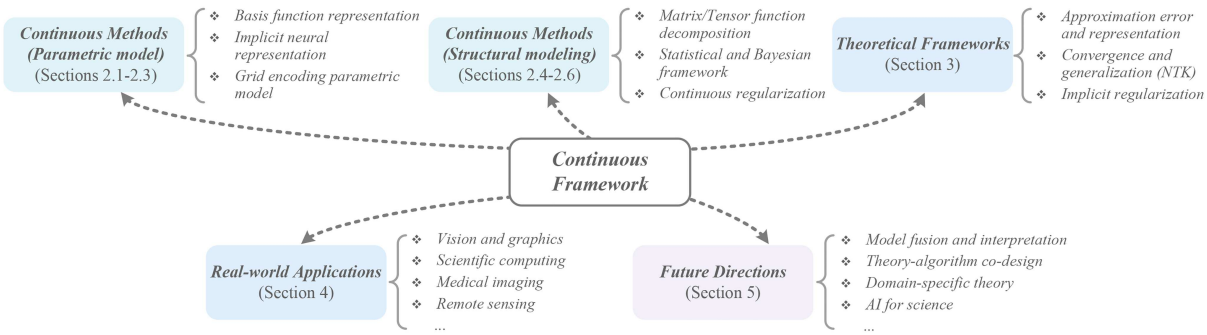

Figure 1 (Color online) This work is structured to provide a comprehensive overview of continuous representation methods through three perspectives. First, we systematically review continuous representation methods including parametric model architectures and data structural modeling strategies (Section 2). Second, we review representative theoretical frameworks for formally analyzing the properties and capabilities of continuous representation methods (Section 3). Third, we review real-world applications of continuous representation methods derived from diverse fields (Section 4). Finally, we discuss future research directions and perspectives aimed at further enhancing the effectiveness, theoretical insights, and applicability of continuous representation frameworks (Section 5).

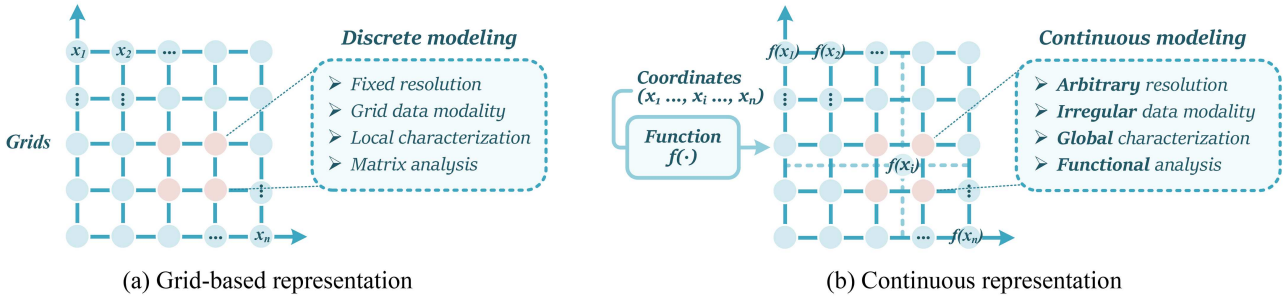

Figure 2 (Color online) A comparative analysis between discrete grid modeling and emerging continuous representation modeling approaches. In contrast to conventional grid representations, the novel continuous representation paradigm employs a parametric mapping function $f(\cdot)$ that maps continuous-domain coordinates to their corresponding values, deriving intrinsic advantages such as resolution flexibility, irregular data modeling ability, global characterization of data structures, and interpretable learning theories (such as functional decomposition analysis [2]) that extends beyond discrete grids.

continuous methods, and corresponding applications across diverse fields, deciphering the rapid evolution of related fields.

• We highlight promising future directions and chart a prospect for addressing open challenges for continuous method designs, theoretical developments for continuous frameworks, and utilizing them to facilitate real-world applications. We aim to inspire interdisciplinary collaborations to advance the data reconstruction methods inspired by continuous representation frameworks.

Several reviews of continuous representation methods in different areas exist in the literature. Xie et al. [43] provided a comprehensive review of neural fields (referred to as INRs in this work) and their applications in different domains of computer vision and graphics, such as neural radiance field, signed distance function (SDF) representation, and robotics. Recently, Gao et al. [44] provided a comprehensive review of neural radiance fields (NeRF) in 3D vision, covering both neural fields and 3D Gaussian splatting (3DGS)-based methods [45]. Essakine et al. [46] proposed a comprehensive survey of INR methods, including their structure designs and network optimization strategies. Recently, Irshad et al. [47] presented a comprehensive survey on neural fields in the field of robotics. Sun et al. [48] proposed a comprehensive survey of medical image registration via neural fields. As compared with these reviews, the proposed work summarizes from a more general and broader perspective, i.e., the continuous representation perspective. Specifically, existing reviews have centered on sub-fields of continuous representations, such as NeRF [44] and medical imaging analysis based on neural fields [48]. In this work, we identify field fragmentation and integrate fragmented knowledge under a unified continuous representation framework, thereby establishing a more comprehensive methodological perspective on continuous representations. As a result, our paper presents a more comprehensive and systematic review of continuous representation methods, whereas earlier surveys such as NeRF and medical image analysis constitute sub-fields within our broader investigation. Therefore, the proposed review is believed to be novel and presents a higher-level overview for researchers entering this rapidly evolving area.

1.2 Recent trends and challenges

In this subsection, we review recent trends and open challenges in the field of continuous representations, aiming to provide an overview of current research directions and identify potential areas for future exploration. Recent trends in continuous representations mainly include three aspects.

• The first dominant trend is that researchers gradually move away from isolated parametric model designs, and develop towards hybrid frameworks that combine the strengths of different continuous representation methods. Representative examples include (i) combining INRs with interpretable basis function representations, such as positional encoding (PE) INR [20] based on Fourier features, wavelet INR [30] based on wavelets, and Kolmogorov-Arnold network (KAN)-based methods [49] based on splines, (ii) incorporating computational mathematical tools with continuous representations to enhance interpretability and robustness, such as neural ordinary differential equation-based continuous representation [22], (iii) integrating low-rank matrix/tensor decomposition methods with continuous representations to enhance efficiency, such as low-rank tensor function representation (LRTFR) [2], functional tensor decomposition-based INRs [35,50], and tensor NeRF [38], and (iv) incorporating grid encoding with INRs to enhance convergence efficiency and high-frequency components characterization, such as InstantNGP [51], DVGO [52], and RHINO [53].

• Theoretically, there is a growing effort to build a rigorous theoretical foundation for continuous methods, bridging machine learning and applied mathematics. The NTK framework [31] is widely used to explain the spectral bias of INRs and the convergence properties of various architectures [54–56]. Studies are revealing the implicit regularization of over-parameterized models (e.g., over-parameterized INRs) towards low-complexity solutions (e.g., low-rankness), explaining their generalization capabilities [33,57]. Studies are also characterizing the function classes that specific INR architectures can represent, formulating them as structured dictionaries [58] or through harmonic analysis [59], enhancing theoretical understanding.

• Moreover, continuous representations are increasingly being used as backbones to resolve challenges in diverse scientific applications. For instance, the physics-informed neural networks and neural operators solve PDEs by using continuous representations to represent solution fields [36, 60]. In computer vision and graphics, continuous representations are widely used in shape representation [61], novel view synthesis [15, 62], and continuous image representation [11]. In medical imaging and bioinformatics, applications of continuous representations include MRI reconstruction [63], deformable image registration [12], and modeling ST data [64]. Remote sensing and geoscience tasks such as hyperspectral image super-resolution [65], seismic data interpolation [25,66], and spectral unmixing [67] also benefit from the continuous framework's efficiency and flexibility.

Despite the rapid progress of continuous representations, we identify several key challenges that remain open and present important potential for future research.

• (Scalability and efficiency) Training INRs for very high-dimensional data (e.g., 4D light fields, 5D seismic data) can be computationally intensive. Developing more efficient optimization schemes and model architectures are critical needs. Developing methods that can enhance the computational efficiency of modern continuous models (e.g., matrix/tensor function representations) for complex non-grid data (e.g., point clouds and ST) is an open challenge.

• (Spectral bias) The inherent bias of standard INRs towards learning low-frequency components remains a fundamental limitation. Although methods like PE and SIREN [16] mitigate this, robustly capturing complex and high-frequency signal details, especially in the presence of noise, is still an important challenge.

• (Theoretical gap) While theoretical progress has been made for linear models (e.g., matrix factorization) and linear optimization regimes (e.g., NTK), a comprehensive theory for the implicit regularization, generalization, and approximation capabilities of nonlinear continuous models (like INR architectures) and nonlinear optimization regimes is still underdeveloped. Using theoretical understanding of spectral bias or implicit regularization to actively design better optimization strategies, activation functions, and network architectures, rather than just using theory as a post hoc explanation, is an important future direction.

• (Generalization and robustness) It is challenging to ensure the generalization of continuous representations to unseen data coordinates, out-of-domain distributions, and different resolutions. These challenges include overfitting to the training coordinates and sensitivity to initialization. Techniques to improve robustness and generalization for continuous representations are important.

Future research will likely be driven by a deeper integration of continuous parametric model design, mathematical theories, and domain-specific applications, leading to more efficient and reliable tools for continuous data representation across fields. The remainder of this paper is structured as follows. In Section 2, we review the developments of various continuous representation models and structural modeling methods. In Section 3, we delve into the theoretical foundations of continuous representation methods such as approximation error analysis and NTK theories.

Table 1 Key terminologies used in this paper.

Terminology	Description
Continuous representation	A function that maps positional coordinates to their corresponding values in the continuous space.
Implicit regularization	The implicit bias of an optimization algorithm towards certain solutions, without explicit regularization.
INR (implicit neural representation)	An implicit neural network that parameterizes a continuous function, mapping coordinates to values.
PE	A technique to map input coordinates to a higher-dimensional space using Fourier features or other mappings.
SIREN (sinusoidal representation network)	An INR that uses sinusoidal activation functions for continuous representation [16].
SDF	A function mapping coordinate to its distance to a surface, with sign indicating whether the point is inside or outside the surface.
NeRF	A method for scene representation that uses an INR to map 3D coordinates and viewing directions to color and density.
InstantNGP (instant neural graphics primitives)	A method for efficient training of INRs using a multi-resolution hash table encoding [51].
3DGS	A method for parameterizing neural fields with a collection of Gaussian functions with learnable parameters [45].
NMF (nonnegative matrix factorization)	A matrix factorization technique that factorizes a nonnegative matrix into two low-rank nonnegative matrices.
MoE (mixture-of-experts)	A neural architecture that consists of multiple expert networks and a gating network that assigns inputs to suitable experts.
NeurTV (neural total variation)	A regularization method by penalizing the directional derivatives of INR outputs with respect to input coordinates.
LIIF (local implicit image function)	A method for arbitrary-scale image super-resolution that uses an INR to map coordinates and latent features to RGB values.
CP (canonical polyadic), Tucker, TT (tensor-train)	Tensor decomposition methods for factorizing tensors into simpler components.
PINN (physics-informed neural network)	A neural network trained to solve PDEs by incorporating physical laws into the loss function.
NTK	A kernel that describes the behavior of neural networks during training in the infinite-width limit.
ST	A type of bioinformatics data that measures gene expressions with spatial locations within tissues.
FWI	A geophysical imaging method that predicts subsurface properties from observed seismic data.

Table 2 Key notations used in this paper.

Notation	Description	Notation	Description
$f(\mathbf{v})$	Function mapping coordinate $\mathbf{v}$ to value.	Θ	Parameters of a neural network.
$\sum$	Summation.	$\prod$	Scalar product.
$\triangle$	Tensor face-wise product.	ω_0	Frequency parameter in activation function.
$\mathcal{L}$	Loss function.	$\gamma(\mathbf{v})$	Positional encoding function.
$x, \mathbf{x}, \mathbf{X}, \mathcal{X}$	Scalar, vector, matrix, tensor.	$\mathbf{W}_i, \mathbf{b}_i$	Weight matrix and bias vector in DNN.
$\times_n$	Mode-n tensor-matrix product.	$\Theta^{(L)}$	NTK of a DNN with depth L.
$\|\cdot\|_F$	Frobenius norm.	$\otimes$	Outer product.
∇	Gradient operator.	∂	Partial derivative.
$\mathcal{N}$	Differential operator in a PDE.	u	Solution of a PDE.

In Section 4, we review various applications of continuous representation methods such as medical imaging, remote sensing, and bioinformatics. In Section 5, we introduce promising future directions and perspectives to inspire further explorations of continuous representation methods. Key terminologies and notations used in this paper are summarized in Tables 1 and 2.

Table 3 Review of some representative continuous representation parametric models.

Category	Method	Description	Year	Ref.
Basis function representation	(NMF) Smooth nonnegative matrix factorization	Utilize Gaussian basis functions to parameterize nonnegative matrix factorization for multi-way data analysis.	2015	[68]
	(STD) Smooth tensor decomposition	Introduce smoothed Tucker decomposition represented by Fourier basis functions to incorporate smoothness.	2017	[69]
	(Chebfun) Chebfun in three dimensions	Trivariate function representation based on low-rank tensor decomposition through finite Chebyshev expansions.	2017	[29]
	(TT) Functional tensor-train	Functional TT decomposition parameterized by Gaussian kernels for regression problems.	2018	[70]
	(CPD) CP decomposition of multivariate functions	Generalize the CPD from tensors to multivariate functions by finite multi-dimensional Fourier series.	2021	[8]
Implicit neural representation	(PE) Fourier features positional-encoding INR	Propose Fourier feature mapping for PE that enables INR to learn high-frequency details.	2020	[20]
	(SIREN) INR with periodic activation functions	Leverage periodic activation functions for INR and verify the effectiveness of SIREN for continuous representation.	2020	[16]
	Meta-learning for INR initialization	Apply meta-learning to learn initial weights for INRs based on signal classes for faster convergence and better generalization.	2021	[71]
	(WIRE) Wavelet INR	Use the complex Gabor wavelet function as the activation function of INR to improve robustness.	2023	[30]
	(FINER) Flexible spectral-bias tuning for INR	Introduce variable-periodic activation functions and initialize INR bias differently for flexible spectral-bias tuning.	2024	[72]
	(FR-INR) Fourier reparameterization for INR weights	Learn the coefficient matrix of fixed Fourier bases for linear weights of INR to alleviate spectral bias.	2024	[42]
Grid parametric encoding	(InstantNGP) Multi-resolution hash grid encoding	Use a smaller INR augmented by a multi-resolution hash table of trainable feature vectors on grids.	2022	[51]
	(DVGO) Direct voxel grid optimization	A density voxel grid for scene geometry and a feature voxel grid for view-dependent appearance.	2022	[52]
	(Plenoxels) Sparse 3D grid encoding	Efficient scene representation as a sparse 3D grid with spherical harmonics.	2022	[73]
	(DINER) Disorder-invariant hash-based INR	Disorder-invariant INR by projecting coordinates into a learnable hash table, alleviating spectral bias.	2024	[74]
	(RHINO) Regularized grid encoding	Regularizing hash-based grid encoding using coordinate INR concatenated with parametric grid input.	2025	[53]

2 Continuous representation: parametric model and structural modeling

In this section, we systematically review the advancements of continuous representation methods, focusing on two groups: parametric model design and data structural modeling methods. The parametric models, including basis function representation models, INRs, and grid encoding-based models, aim to construct effective parameterization schemes for the continuous functions, hence enhancing data representation and reconstruction accuracy. The structural modeling approaches, such as matrix/tensor function decomposition, statistical and Bayesian frameworks, and continuous regularization methods based on continuous representations, encode prior knowledge of data and structural constraints to further enhance robustness and generalization abilities of continuous representations. An overview of continuous parametric model designs and structural modeling methods is shown in Tables 3 [8, 16, 20, 29, 30, 42, 51–53, 68–74] and 4 [2, 17, 18, 21–23, 50, 75–81].

2.1 Basis function representation

The concept of basis function continuous representation lies in the core idea of decomposing a multivariate function into a series of low-dimensional functions (in most cases, univariate functions), which are parameterized by some predefined basis functions such as Gaussian kernels or Fourier series. These basis function representations enjoy good interpretability and solid theoretical properties, e.g., existence and identifiability [8], allowing for a wide range of data science problems.

Table 4 Review of some representative structural modeling methods based on continuous representation.

Category	Method	Description	Year	Ref.
Matrix or tensor decomposition	(CoordX) Matrix decomposition	Introduce CoordX based on matrix decomposition to accelerate conventional INRs.	2022	[75]
	(LRTFR) Tensor Tucker decomposition	Low-rank tensor function representation based on Tucker decomposition for multi-dimensional data.	2024	[2]
	(F-LRTF) Tensor SVD	Learnable functional transform-based low-rank tensor factorization for continuous interpolation.	2024	[76]
	(DRO-TFF) Rank-one decomposition	Parameter-efficient deep rank-one tensor functional factorization for multi-dimensional data.	2025	[77]
	(F-INR) Functional tensor decomposition	Functional Tucker, CP, and TT decomposition-based INR for efficient continuous representation.	2025	[50]
Statistical framework	(SFTL) Factor trajectory learning	Streaming factor trajectory learning for tensor decomposition by using Gaussian processes to model factor trajectory.	2023	[78]
	(FunBaT) Functional Bayesian decomposition	Functional Bayesian Tucker decomposition with Gaussian processes for continuous-indexed tensor data.	2024	[21]
	(BayOTIDE) Online functional decomposition	Functional Tucker decomposition with Gaussian processes for online inference of time-series data imputation.	2024	[23]
	(GRET) Temporal tensor decomposition	Tensor decomposition with continuous spatial indexes and temporal trajectories via neural ODEs.	2025	[22]
Continuous regularization	(IDIR) Jacobian regularization	Introduce Jacobian regularizer and hyperelastic regularizer based on INR for deformable registration.	2022	[17]
	(INRR) Regularize INR by itself	Learning the Dirichlet energy parameterized by another tiny INR to improve the generalization of the backbone INR.	2023	[79]
	(CRNL) Nonlocal self-similarity	Continuous representation-based nonlocal method with coupled tensor factorization for data reconstruction.	2024	[80]
	(NeurTV) Neural total variation	Higher-order and directional total variation regularization based on continuous neural representation.	2025	[18]
	Isometric regularization for functional data	Isometric regularization to preserve geometric quantities between latent space of INR and functional data manifold.	2025	[81]

Yokota et al. [68] proposed the smooth nonnegative matrix and tensor factorizations for robust multi-way data analysis. This model is based on the matrix or tensor factorization parameterized by Gaussian basis functions in the form of

$$\Phi(i,n)=\exp\left[-\frac{(i-n\Delta t)^2}{2\sigma^2}\right],$$

where i,n are indexes, and then solves an optimization model based on the NMF to recover information from an observed data $\mathbf{Y}$:

$$\min_{\mathbf{W},\mathbf{X}}\frac{1}{2}\|\mathbf{Y}-\Phi\mathbf{W}\mathbf{X}\|_F^2,\quad \text{s.t. } \Phi\mathbf{W}\geqslant 0,\ \mathbf{X}\geqslant 0.$$

This NMF model encodes smoothness constraints on nonnegative factors using smooth basis functions, hence facilitating better physical interpretation and robustness with respect to noise. Debals et al. [82] proposed the NMF using nonnegative polynomial approximations, in which the factors of NMF are modeled by a parametric representation of finite-interval nonnegative polynomials to obtain an optimization problem without external nonnegativity constraints, which can be solved using quasi-Newton or nonlinear least-squares methods. The polynomial model also guarantees smooth solutions for noise reduction through smooth basis function representations.

Similarly, Imaizumi et al. [69] proposed the smooth tensor decomposition using the Tucker functional tensor decomposition parameterized by basis functions, which leverages smoothness using the sum of a few Fourier basis functions. They theoretically showed that, under the smoothness assumption of the tensor, the smooth tensor decomposition achieves a better reconstruction error bound for tensor recovery and interpolation.

Gorodetsky and Jakeman [70] proposed functional TT decomposition-based continuous representation model for

regression problems, in the form of

$$f(x_1, x_2, \ldots, x_d) = \sum_{i_0=1}^{r_0} \sum_{i_1=1}^{r_1} \cdots \sum_{i_d=1}^{r_d} f_1^{(i_0 i_1)}(x_1) f_2^{(i_1 i_2)}(x_2) \cdots f_d^{(i_{d-1} i_d)}(x_d),$$

where the univariate factor functions $f_k^{ij}(x_k)$ are parameterized by Gaussian kernels $\Phi_k(x) = \exp(-\frac{(x-\theta_k)^2}{\sigma^2})$ with learnable Gaussian coefficients θ optimized by stochastic gradient descent or quasi-Newton methods. The functional TT model excels in the task of low-multilinear-rank regression.

Kargas and Sidiropoulos [83] proposed the nonlinear system identification via tensor completion, which identifies a general nonlinear function $y = f(x_1, \ldots, x_N)$ from input-output pairs via a tensor completion problem. Their later work [8] proposed the functional formulation of the CP tensor decomposition using Fourier basis functions in the form of

$$\Phi_0(x) = 1,\ \Phi_k(x) = \sqrt{2}\cos(k\pi x),$$

where only the cosine extension is used for efficiency. Then the CPD of a multivariate function f parameterized by such basis functions has the form

$$f(\mathbf{x}) = \sum_{k_1=0}^{K-1} \cdots \sum_{k_N=0}^{K-1} \sum_{r=1}^{R} \prod_{n=1}^{N} a_n^r[k_n] \Phi_{k_n}(\mathbf{x}[n]),$$

where the Fourier coefficients a_n^r are optimized towards fitting the training data. The authors provided an existence and uniqueness guarantee for the CP functional decomposition model from the finite multidimensional Fourier series perspective, and showed that the model can be empirically effective for real-world data regression problems. Similarly, Sort et al. [39] proposed to represent a high-dimensional functional tensor as a low-dimensional set of functions and feature matrices in the form of CPD with Fourier basis functions, along with a probabilistic latent model in the decomposition to enable sparse and irregular sampling, with applications to longitudinal data modeling.

Earlier theoretical studies showed that some specific types of multivariate functions can be exactly factorized into explicit forms of low-dimensional functions. For instance, Kunkel and Mehrmann [84] studied the numerical factorization of matrix-valued functions, and applied it in the numerical solution of differential algebraic Riccati equations. Oseledets [85] proposed constructive approximation (explicit representation) of some specific multivariate functions (e.g., the polynomial and sine functions) in the TT decomposition format:

$$f(x_1, \ldots, x_d) \approx \sum_{\alpha=1}^{r} u_1(x_1, \alpha) u_2(x_2, \alpha) \cdots u_d(x_d, \alpha).$$

For example, for a function $f(x_1, \ldots, x_d) = \sin(x_1 + x_2 + \cdots + x_d)$, the functional TT decomposition has the form

$$f = \begin{pmatrix} \sin x_1 & \cos x_1 \end{pmatrix} \begin{pmatrix} \cos x_2 & -\sin x_2 \\ \sin x_2 & \cos x_2 \end{pmatrix} \cdots \begin{pmatrix} \cos x_{d-1} & -\sin x_{d-1} \\ \sin x_{d-1} & \cos x_{d-1} \end{pmatrix} \begin{pmatrix} \cos x_d \\ \sin x_d \end{pmatrix}.$$

The TT decompositions of some other functions, e.g., the polynomial function, were also obtained [85]. The obtained functional decompositions are useful for the construction of efficient algorithms in high-dimensional problems. Similarly, Tichavský and Straka [86] proposed an alternating least squares method for fitting a TT to an arbitrary number of tensor fibers, allowing robust and flexible modeling of multivariate functions that contain noise. They provided examples of the algorithm for decomposing the Rosenbrock function and the quadratic function. Chen et al. [87] studied the collaborative filtering problem and formalized the problem as a general functional matrix factorization, which learns feature functions based on training data, and the learnable feature functions are parameterized by piecewise linear functions.

Hashemi and Trefethen [29] studied Tucker factorization of trivariate functions and proposed constructive algorithms for approximating trivariate functions in Tucker format, e.g.,

$$f(x, y, z) \approx \mathcal{T} \times_1 A(x) \times_2 B(y) \times_3 C(z),$$

where the factor one-dimensional functions are represented by finite sum of Chebyshev polynomials and the core tensor $\mathcal{T}$ is an $m \times n \times p$ tensor. For instance, the multivariate function

$$f(x, y, z) = 3x^7 z + yz + yz^2 + \log(2 + y)z^3 - 2z^5 \tag{1}$$

has an exact decomposition formulation in the Tucker decomposition format

$$A(x) = \left[1,\ x^7\right],\ B(y) = \left[1,\ y,\ \log(2+y)\right],\ C(z) = \left[z^5,\ z+z^2,\ z^3,\ z\right]. \tag{2}$$

Using the Chebyshev polynomial representation algorithm can construct the Tucker decomposition for (1) numerically to obtain the decomposition result (2) [29]. From the decomposition we can see the trilinear rank of f is $(2,3,4)$: these three numbers are the x-rank, the y-rank, and the z-rank. The $2\times3\times4$ discrete core tensor $\mathcal{T}$ has the following mode-1 unfolding:

$$\mathcal{T}_{(1)} = \left[\begin{array}{ccc|ccc|ccc|ccc} -2 & 0 & 0 & 0 & 1 & 0 & 0 & 0 & 1 & 0 & 0 & 0 \\ 0 & 0 & 0 & 0 & 0 & 0 & 0 & 0 & 0 & 3 & 0 & 0 \end{array}\right] \in \mathbb{R}^{2\times12}.$$

The Tucker decomposition using Chebyshev polynomial representations would benefit fundamental numerical computations of multivariate functions such as differentiation, Laplacian operators, definite and indefinite integrals [29]. Recently, the KAN [49] emerged as a new alternative for function approximation, showing particular interpretability and robustness for scientific applications. Each layer of KAN can be viewed as a combination of spline basis functions, hence linking traditional basis function representation with modern neural representations.

Basis function representations provide principal ways to approximate multivariate continuous functions using predefined basis functions with learnable coefficients, which benefits multi-way data analysis and reconstruction tasks. Nevertheless, predefined basis function representation methods may lack strong representation abilities for depicting complex and irregular real-world data structures. In future work, the spirit of basis function methods can be combined with modern neural representation (such as randomized neural network [88] and KAN-based approaches [49]) to enable better characterization of data in signal processing and high-dimensional regression problems in machine learning. Studying the theoretical advantage of basis function methods (such as implicit smoothness [69, 89] and fast inference) could facilitate understanding and inspire further explorations on the utility of basis functions for more complex continuous representations. For instance, the 3DGS has emerged as a popular framework for continuous scene representation in computer vision. 3DGS models radiance fields with a collection of continuous 3D Gaussian basis functions, each parameterized by learnable mean, covariance, color, and opacity, and can be seen as a type of basis function representation learning. It offers significant advantages in training efficiency and robust geometry reconstruction compared to neural networks, enabling real-time rendering for applications such as novel view synthesis [15, 45].

2.2 Implicit neural representation

Implicit neural representation has emerged as a transformative parametric model for representing complex, irregular data through continuous coordinate-based mappings using DNNs. Specifically, INRs map spatial coordinates to the corresponding values using DNNs. By parameterizing signals as continuous functions of spatial or temporal coordinates, INRs overcome the limitations of discrete sampling, enabling representation at arbitrary resolution, natural interpolation between samples, and compact modeling of high-dimensional data, which benefits many downstream applications.

The two most classical INRs are the Fourier feature PE-based INR [20] and the sinusoidal periodic activation function-based INR [16]. The PE-based INR [20] showed that passing input coordinates through a simple Fourier feature mapping enables a multilayer perceptron (MLP) to learn high-frequency functions in low-dimensional domains. More specifically, given a coordinate vector $\mathbf{v}\in\mathbb{R}^d$, the Fourier mapping maps it to the surface of a higher dimensional hypersphere with a set of sinusoids:

$$\gamma(\mathbf{v}) = \mathrm{PE}(\mathbf{v}) = \left[a_1\cos\left(2\pi\mathbf{b}_1^{\mathrm{T}}\mathbf{v}\right), a_1\sin\left(2\pi\mathbf{b}_1^{\mathrm{T}}\mathbf{v}\right), \ldots, a_m\cos\left(2\pi\mathbf{b}_m^{\mathrm{T}}\mathbf{v}\right), a_m\sin\left(2\pi\mathbf{b}_m^{\mathrm{T}}\mathbf{v}\right)\right]^{\mathrm{T}}.$$

Then passing the positional encoded vector $\gamma(\mathbf{v})$ through a ReLU-based MLP results in effective continuous learning for the low-dimensional input domain of $\mathbf{v}$. The underlying reason for the effectiveness of PE is that an MLP with PE (under certain conditions) is equivalent to a kernel regression with a diagonal shift-invariant kernel from the NTK perspective (see Section 3 for details), while a conventional MLP without PE leads to a non-diagonal kernel. The kernel regression with a diagonal shift-invariant kernel tends to more easily capture high-frequency information, thus allowing more effective continuous representation using PE.

Similarly, the sinusoidal periodic activation function-based INR [16] (termed SIREN) is also a widely utilized INR method. It was shown that leveraging periodic activation functions for INRs (instead of using conventional

activations such as ReLU) are ideally suited for continuously representing complex natural signals and their derivatives. The authors also proposed principled initialization schemes for SIREN and demonstrated the representation abilities of SIREN for images, wavefields, video, sound, and their derivatives. The SIREN is constructed by stacking sinusoidal layers in the form of

$$\mathbf{x}_i \mapsto \phi_i\left(\mathbf{x}_i\right) = \sin\left(\omega_0(\mathbf{W}_i\mathbf{x}_i + \mathbf{b}_i)\right),$$

where $\mathbf{W}_i$ and $\mathbf{b}_i$ are learnable weights and biases, ω_0 is a frequency hyperparameter (in most times setting $\omega_0 = 30$). The differentiability of sinusoidal function naturally allows SIREN to tackle physical modeling problems such as surface representation and numerical PDE modeling (e.g., Helmholtz and wave equations considered in [16]). The underlying rationale of the effectiveness of SIREN is similar to that of the PE from the NTK perspective. Subsequently, Fathony et al. [90] suggested that simply multiplying some sinusoidal or Gabor wavelet basis functions applied to the input coordinates yields comparable performance against PE and SIREN-based INRs.

Later, researchers started to constantly develop more powerful INR paradigms from various aspects. Inspired by harmonic analysis, Saragadam et al. [30] developed a new INR (termed WIRE) with continuous complex Gabor wavelet activation functions, i.e.,

$$\phi_i(\mathbf{x}_i) = \psi(\mathbf{W}_i\mathbf{x}_i + \mathbf{b}_i; \omega_0, s_0),\ \psi(x; \omega_0, s_0) = \mathrm{e}^{\mathrm{j}\omega_0 x}\mathrm{e}^{-|s_0 x|^2}, \tag{3}$$

where ω_0 controls the frequency of the wavelet and s_0 controls the spread (or width). WIRE enjoys the advantages of periodic nonlinearities such as SIREN due to the complex exponential term and the spatial compactness from the Gaussian window term $\mathrm{e}^{-|s_0 x|^2}$. Unlike SIREN, WIRE does not require a carefully chosen set of initial weights due to the Gaussian window, and thus enables robust continuous representation learning with respect to the choice of hyperparameters. Li et al. [91] proposed the collaged Fourier bases for INR, which utilizes spatial masks to modulate each global Fourier feature and collages the frequency patches to form a better reconstruction of the image's local pattern. Liu et al. [72] proposed the variable-periodic activation functions for INRs, where each layer is formulated as

$$\mathbf{x}_i \mapsto \phi_i\left(\mathbf{x}_i\right) = \sin\left(\omega_0\alpha_i(\mathbf{W}_i\mathbf{x}_i + \mathbf{b}_i)\right),\ \alpha_i = |\mathbf{W}_i\mathbf{x}_i + \mathbf{b}_i| + 1.$$

It uses the variable-periodic activation function $\sin((|x|+1)x)$ to flexibly tune the supported frequency set of INR to improve performance in continuous signal representation. Jayasundara et al. [92] proposed the prolate spheroidal wave function (PSWF)-based INR, which exploits the optimal space-frequency domain concentration of PSWF as the nonlinear mechanism in INRs to better generalize to unseen coordinates. The PSWF $\psi_n(c,t)$ here is the eigenfunction of an integral operator problem

$$\int_{-t_0}^{t_0} \psi_n(c,t)\frac{\sin\Omega(x-t)}{\pi(x-t)}dt = \psi_n(c,x)\lambda_n(c),$$

which is numerically solved by the expansion of Legendre polynomial $P_k(t)$, i.e., parameterizing the solution as $\psi_n(c,t) = \sum_{k=0}^{\infty}\beta_k^n P_k(t)$ and determining the Legendre coefficients β_k^n using recursions. Ramasinghe and Lucey [93] proposed a unified perspective on the activation function design of INR, and showed that a large number of non-periodic functions are suitable for continuous representation using INR, such as Laplacian and quadratic functions.

Recently, Shi et al. [42] proposed the Fourier reparameterized training for INR, which learns coefficient matrix of fixed Fourier bases to compose the weights of the MLP. The reparameterized training leads to a more balanced eigenvalue distribution of the NTK, hence leading to improved convergence speed for continuous representation by alleviating the spectral-bias of INR. Hao et al. [94] proposed the levels-of-experts (LoE) framework. For each linear layer of the MLP, the LoE employs multiple candidate values of its weight matrix, with different layers replicating at different frequencies. For each input, only one of the weight matrices is chosen for each layer. This LoE structure greatly increases the INR model capacity without incurring extra computation. Similarly, Ben-Shabat et al. [95] proposed the mixture of experts (MoE) INR that learns local piecewise continuous functions that simultaneously learns to subdivide the domain and fit it locally. They also introduced novel conditioning and pretraining methods for the gating network of the MoE that improve convergence. Vyas et al. [96] proposed to learn transferable representations for INRs by sharing initial encoder layers across multiple INRs with independent decoder layers. At the inference stage, the learned encoder representations are transferred as initialization for another input sample, thus enabling knowledge transfer. Zhang et al. [97] proposed a nonparametric teaching scheme for INRs, where the teacher selects signal fragments for iterative training of the MLP to achieve fast convergence. They unveiled the link between the evolution of INR and that of a function using functional gradient descent in nonparametric teaching, thus expanding the applicability of nonparametric teaching towards deep learning using INRs.

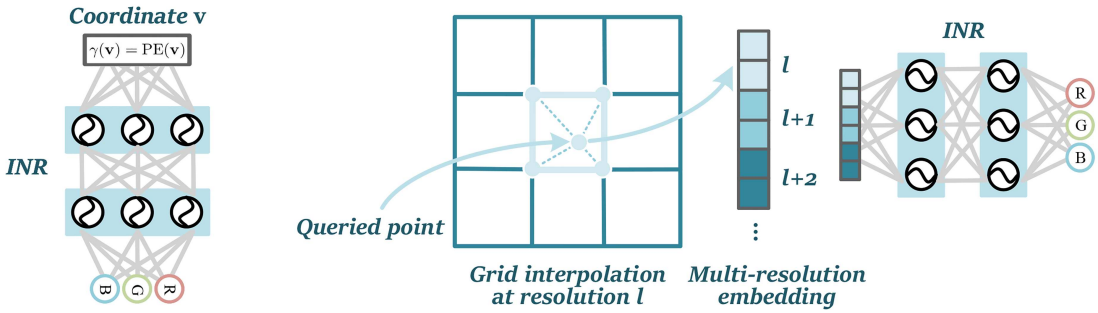

Figure 3 (Color online) The structures of the PE-based INR [20] and the multi-resolution grid encoding-based INR [51]. (a) The PE-based INR maps the input coordinate through a Fourier mapping layer before passing through an MLP for effective continuous representation; (b) the multi-resolution grid encoding-based INR (e.g., InstantNGP [51]) constructs learnable feature vectors stored on grids with multiple resolutions. To query the point outside grids, linear interpolation is computed and the interpolated results of different grid resolutions are concatenated and passed through an MLP. Here, the learnable feature vectors are efficiently stored in hash tables.

Other external structure designs are also incorporated into INRs for efficient continuous learning. Fang et al. [98] proposed the CycleINR, which samples unseen points from the learned INR and uses these points to train another INR, and then imposes cycle-consistency loss between the sampled points of two INRs, leading to higher accuracy for super-resolution. Saragadam et al. [99] proposed the multi-scale INR, which decomposes the signal into multi-scale orthogonal parts in terms of Laplacian pyramid, and represents small disjoint patches of the pyramid at each scale with small MLPs, leading to increased coarse-to-fine approximation using INR. Li et al. [100] proposed the superpixel-informed INR model for multi-dimensional data, which exploits the semantic information within and across generalized superpixels for improved continuous representation. Cai et al. [101] studied the effect of batch normalization for alleviating the spectral bias of INR from the NTK eigenvalue distribution perspective. The cross-frequency INR [102] explicitly disentangles the multi-frequency characteristics of data by using the Haar wavelet transform, thus achieving superior accuracy for continuous data representation. Kazerouni et al. [103] proposed to use another network to dynamically adjust key parameters (such as frequencies and phases) of the activation function of the INR, enabling more accurate continuous representations.

The internal iterative learning process of INR for each observed data from scratch can also be relaxed by using the meta learning method [104], which builds suitable model parameters for the INR through one step forward propagation for each data. Besides, Tancik et al. [71] proposed to use meta learning to learn specific initialization schemes for INR parameters for a particular group of signals. The meta learning strategy coupled with dictionary learning of INR [58] could further uncover improved representation abilities and convergence efficiency across instances. It is a promising future direction to use advancing meta learning methods to generalize INR methods or using INRs as meta learners to enable fine tuning of larger models, such as by using the low-rank adaptation (LoRA) [105].

2.3 Grid encoding parametric model

In recent years, parametric models based on grid encoding have achieved remarkable progress in continuous representation, especially in scene representation [15, 51, 106]. By integrating sparse or multi-resolution grids with learnable feature encodings (e.g., hash tables, voxel grids) and interpolation, these methods efficiently capture fine-grained details while accelerating the convergence of continuous models as compared with conventional INRs. We introduce several representative studies along this line.

Müller et al. [51] proposed the iconic multi-resolution hash encoding method for continuous representation, especially focusing on image or scene representation using NeRF (termed InstantNGP). It uses a smaller INR augmented by a multi-resolution hash table of trainable feature vectors on grids (see Figure 3). To use the hash table, InstantNGP maps a cascade of grids to corresponding fixed size arrays of trainable feature vectors. The array is treated as a hash table and indexed using a spatial hash function, e.g.,

$$h(\mathbf{x}) = \left(\bigoplus_{i=1}^{d} \mathbf{x}_i \pi_i\right) \mod T,$$

where $\mathbf{x}$ denotes the spatial index of grids, $\bigoplus$ is the exclusive-or operation, π_i are large prime numbers, and T denotes the size of the hash table. The returning value $h(\mathbf{x})$ indexes the position of the grid $\mathbf{x}$ in the hash table.

The hash table automatically prioritizes the sparse areas with the most important fine scale detail. Then, any point in the continuous domain can be inferred by using linear interpolation of its neighboring grid feature vectors and passing the interpolated results through an MLP to output the corresponding value. Notably, the InstantNGP can be seen as imposing learnable PE for INR, where the learnable parameters are stored in discrete grids and those PE points beyond grids are obtained by linear interpolation using its neighboring grids; see Figure 3. From another perspective, the InstantNGP can be understood as a complex composite form of linear interpolation functions. It excels in learning fine details of images (scenes) and faster convergence due to the flexibility of learnable PE embeddings. Some numerical examples are shown in Figure 4.

Similarly, Sun et al. [52] proposed the DVGO for continuous scene representation, which uses a density voxel grid for scene geometry and a feature voxel grid for view-dependent appearance encoding. The authors also developed post-activation interpolation on voxel density for producing sharp surfaces in lower grid resolution, and imposed special initialization and learning rate schedule to enhance robustness. Yu et al. [107] proposed the PlenOctrees, a method to quickly render novel view images under the scene representation, by training spherical harmonic functions to model view-dependent appearance on the sphere. The color of the novel view image $c(\mathbf{d})$ is calculated by summing the weighted spherical harmonic bases evaluated at the corresponding ray direction $\mathbf{d}$:

$$c(\mathbf{d}) = \left[1 + \exp\left(-\sum_{\ell=0}^{\ell_{\max}} \sum_{m=-\ell}^{\ell} k_\ell^m Y_\ell^m(\mathbf{d})\right)\right]^{-1},$$

where $Y_\ell^m(\mathbf{d})$ are spherical harmonic basis functions and k_ℓ^m are harmonics coefficients learned by an INR. The trained model can be sampled around the volume to create an octree structure, which can be fine-tuned to improve quality. Fridovich-Keil et al. [73] extended PlenOctrees to Plenoxels for efficient scene representation as a sparse 3D grid with spherical harmonics. It achieves end-to-end training of spherical harmonic function representation within a sparse voxel grid without neural networks. The grid encoding coupled with spherical harmonics largely enhances the convergence speed and quality of scene representation for novel view synthesis.

Recently, Zhu et al. [74] proposed the disorder-invariant INR (DINER) by projecting coordinates into a learnable hash table, alleviating spectral bias of conventional INRs. The hash table rearranges the coordinates of an image where the rearranged image has much lower frequency and thus can be better represented using the subsequent INR. The optimization target of DINER has the form of

$$\arg\min_{\theta, \mathcal{H}_M} \mathcal{L}\left[P\left(\{f_\theta(\mathcal{H}_M^i)\}_{i=1}^N\right), P\left(\{\vec{y}_i\}_{i=1}^N\right)\right],$$

where f_θ is an INR, $\mathcal{H}_M^i$ denotes the i-th hash key of the hash table, $\vec{y}_i$ denotes the target value, and P is a physical process (e.g., phase retrieval and refractive index reconstruction considered in [74]). However, it may not hold generalization to unseen coordinates due to the discontinuity of hash key. To address this limitation, Zhu et al. [53] proposed the hybrid RHINO framework, which utilizes an additional coordinate MLP concatenated with the parametric grid input to regularize hash grid encoding-based methods, enhancing the generalization ability for methods such as DINER [74] and InstantNGP [51].

Grid encoding parametric models have achieved significant success for continuous representation. Future research could address the generalization limitations of current studies by integrating advanced interpolation techniques (e.g., cubic splines), low-rank decomposed structures, or more robust hybrid architectures (e.g., the RHINO framework [53]) for broader applications such as operator learning [36] and FWI [108]. These improvements would further amplify the practical value of these grid encoding parametric models, paving the way for broader applications in science and engineering fields.

2.4 Matrix and tensor function decomposition

Matrix and tensor function decomposition methods have been widely studied to incorporate structural constraints (such as low-rankness) into the continuous function representation [2, 75, 77]. Integrating function decomposition paradigms with INRs has also been an emerging type of structural modeling methods for continuous representation. The superiority of such structure lies in its computational efficiency brought by the compact low-rank factorization and coordinate decomposition, and the encoded low-rankness would benefit many data reconstruction problems.

Liang et al. [75] proposed the CoordX, which uses a split structure of MLP for INR. In this method, the initial layers of the MLP are split to learn each dimension of the input coordinates separately. The intermediate features are then fused by the last layers through outer product to generate the learned signal at the corresponding coordinate. It significantly reduces the computational costs and leads to a speedup in training and inference, while

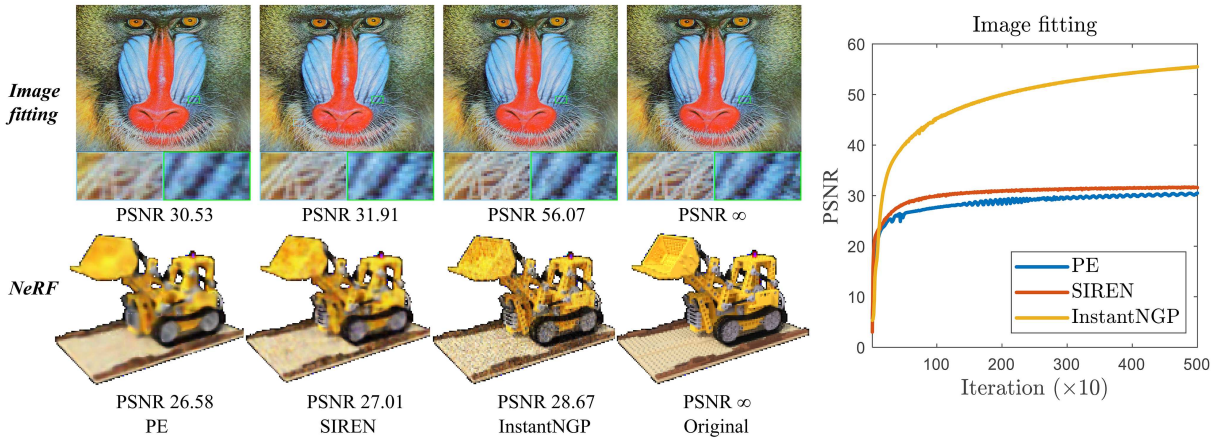

Figure 4 (Color online) The grid encoding-based method InstantNGP [51] achieves faster convergence and captures fine details better as compared with classical INR methods, including PE [20] and SIREN [16]. The top row shows image fitting and the bottom shows novel view synthesis using NeRF [15] of different models with the same iteration step.

achieving similar accuracy as the baseline INR. Luo et al. [2] proposed the LRTFR, which learns a low-rank Tucker decomposition parameterized by univariate INRs to generate the factor matrices of the tensor decomposition. It holds superior computational efficiency for grid-structured data and enjoys effectiveness for multi-dimensional data reconstruction problems. Specifically, given an input coordinate $\mathbf{v}$, the LRTFR is formulated as

$$[\mathcal{C}; f_x, f_y, f_z](\mathbf{v}) := \mathcal{C} \times_1 f_x(\mathbf{v}_{(1)}) \times_2 f_y(\mathbf{v}_{(2)}) \times_3 f_z(\mathbf{v}_{(3)}),$$

where $\mathcal{C}$ is the core tensor and f_x, f_y, f_z are three univariate INRs that generate the factor matrices by taking each separate dimension of the coordinate as inputs. For a tensor of size $n_1 \times n_2 \times n_3$, the LRTFR costs $O[\text{mrd}(n_1 + n_2 + n_3) + rn_1n_2n_3]$ in a forward pass while a conventional MLP-based INR would cost $O(m^2dn_1n_2n_3)$, where m denotes the INR width, d denotes the INR depth, and r denotes the Tucker rank. Since r is usually much lower than m^2d, the LRTFR is practically more efficient than conventional INR methods. And the low-rankness inherent in such type of methods improves the robustness and convergence stability for continuous representation.

Recently, Wang and Zhao [76] proposed the functional transform-based low-rank tensor factorization (FLRTF), which parameterizes the mode-3 factor matrix of the tensor factorization with a functional transform parameterized by INR to enable arbitrary-resolution interpolation of multi-dimensional data, such as frame interpolation of videos and spectral super-resolution of multispectral images. For a third-order tensor $\mathcal{X}$, the FLRTF is formulated as

$$\mathcal{X}(\cdot, \cdot, k) := (\mathcal{A} \triangle \mathcal{B}) \times_3 f(\mathbf{z}_{(k)}), \quad k = 1, 2, \ldots, n_3,$$

where $\mathcal{A}, \mathcal{B}$ are two tensor factors, $\triangle$ is the face-wise product between two tensors, $\times_3$ is the mode-3 tensor-matrix product, and $f(\mathbf{z}_{(k)})$ is a functional transform parameterized by an INR. Continuous data reconstruction tasks such as video frame interpolation/extrapolation and multi-spectral image band interpolation demonstrate FLRTF's superior performance brought by the functional transform tensor factorization. More recently, Li et al. [77] proposed the deep rank-one tensor functional factorization (DRO-TFF). For a third-order tensor $\mathcal{X}$, the DRO-TFF model is formulated as

$$\mathcal{X} = \psi\left\{\cdots \psi\left[(f_{\theta_x}(\mathbf{v}_1) \triangle f_{\theta_y}(\mathbf{v}_2)) \times_3 \mathbf{H}_1\right] \times_3 \cdots \times_3 \mathbf{H}_{k-1}\right\} \times_3 f_{\theta_z}(\mathbf{v}_3),$$

where $f_{\theta_x}(\mathbf{v}_1), f_{\theta_y}(\mathbf{v}_2)$ are rank-one factors generated by univariate INRs, $\mathbf{H}$ are weight matrices of the mode-3 deep transform, $f_{\theta_z}(\mathbf{v}_3)$ is the mode-3 functional transform, and $\psi(\cdot)$ is a nonlinear activation. The DRO-TFF excels in lightweight models by virtue of the lightweight rank-one factorization, and thus holds better efficiency among tensor functional factorization methods.

Furthermore, Vemuri et al. [50] proposed the functional tensor decomposition-based INR, which employs TT, Tucker, and CP tensor decompositions to reconstruct INR. The method reduces forward pass complexity while improving accuracy through specialized learning. The authors applied it to image compression, physics simulations, and 3D geometry reconstruction and show superior efficiency. Nie et al. [109] proposed the LRTFR as a generalized traffic data learner, which enables seamless completion of traffic analysis tasks such as state estimation and mesh-based flow estimation.

Matrix or tensor functional decomposition methods significantly improve the efficiency of INR methods, while the encoded structure constraints such as low-rankness benefit downstream applications. In future research, the

combination of low-rank function decomposed INRs with operator learning paradigms [36] and arbitrary-scale imaging problems [11] are promising directions by leveraging the efficiency of these function decomposition methods. Applying the function decomposition to fine tuning large models are also interesting. It is also interesting to explore more expressive tensor decompositions, such as tensor rings or topology-aware tensor networks, to enhance INRs. Exploring adaptive rank selection in the low-rank function decomposition (such as K-means and PCA-based approaches) is also interesting.

2.5 Statistical and Bayesian framework

Recently, several continuous representation methods based on statistical and Bayesian frameworks have been established. These methods model continuous trajectories (such as temporal trajectory) by imposing statistical distribution assumptions, and then inferring the model parameters from the given observed discrete signals. These methods are capable of capturing long-term dependency and periodic patterns underlying data, making the structural modeling more accurate. The core concept of statistical and Bayesian modeling is to approximate the exact posterior $p(\mathcal{U}, \theta|\mathcal{X})$ using a variational distribution $q(\mathcal{U}, \theta)$, where $\mathcal{X}$ denotes the observed tensor data, $\mathcal{U}$ denotes the latent variables, and θ denotes the statistical parameters to be estimated. The model parameters are inferred by efficient variational inference algorithms, such as variational expectation and maximization or Kalman filtering [23].

To be specific, Fang et al. [78] proposed to model streaming tensors by factor trajectory learning parameterized by Gaussian process (GP), so as to flexibly estimate the continuous temporal evolution of factors for online inference of tensor streams. Their later work [21] introduced the functional Bayesian Tucker decomposition, which models continuous-indexed tensor data by Tucker decomposition parameterized by GP. The GP is used as functional priors to model the latent functions of Tucker decomposition, formulated as

$$\begin{aligned} &f(i_1, \ldots, i_K) \approx \mathrm{vec}(\mathcal{W})^{\mathrm{T}} \left(\mathbf{U}^1(i_1) \otimes \cdots \otimes \mathbf{U}^K(i_K)\right), \\ &\mathbf{U}^k(i_k) = \left[u_1^k(i_k), \ldots, u_{r_k}^k(i_k)\right]^{\mathrm{T}}; \quad u_j^k(i_k) \sim \mathcal{GP}(0, \kappa(i_k, i_k')), \quad j = 1, \ldots, r_k. \end{aligned} \tag{4}$$

Here, $\mathcal{W}$ denotes the core tensor, $\mathbf{U}^k(i_k)$ denotes the factor matrix, $\mathcal{GP}(\cdot)$ denotes the GP, and $\kappa(i_k, i_k')$ denotes the Matérn kernel function. To infer the model parameters from an observed tensor data $\mathcal{D}$, the authors transformed the factor GP into state variables $\mathbf{Z}^k$ under the Markov chain, and further assigned a Gamma prior over the noise precision τ and a Gaussian prior over the Tucker core $\mathcal{W}$. The joint probabilities are approximated into fully factorized format under the mean-field assumption:

$$p(\mathbf{\Theta}|\mathcal{D}) \approx q(\mathbf{\Theta}) = q(\tau) q(\mathcal{W}) \prod_{k=1}^{K} q\left(\mathbf{Z}^k\right),$$

and then optimize the approximated posterior through expectation propagation [21]. The algorithm is evaluated on both synthetic and real-world tensor data, and is capable of modeling continuous-indexed tensor data, especially capturing well-documented period patterns underlying tensor data by virtue of the statistical modeling.

Fang et al. [23] further proposed the Bayesian online multivariate time-series imputation method with continuous functional decomposition. Compared with [21], the new online method is capable of dealing with time-series data that evolves within time. They modeled the multivariate time-series as a temporal vector-valued function $\mathbf{X}(t)$ consisting of the weighted combination of trend and seasonality factors over time. It is formulated as

$$\mathbf{X}(t) = \mathbf{U}\mathbf{V}(t) = [\mathbf{U}_{\mathrm{trend}}, \mathbf{U}_{\mathrm{season}}] \begin{bmatrix} \mathbf{v}_{\mathrm{trend}}(t) \\ \mathbf{v}_{\mathrm{season}}(t) \end{bmatrix}, \ \mathbf{v}_{\mathrm{trend}}^i(t) \sim \mathcal{GP}\left(0, \kappa_{\mathrm{Matern}}\right), \ \mathbf{v}_{\mathrm{season}}^j(t) \sim \mathcal{GP}\left(0, \kappa_{\mathrm{periodic}}\right),$$

where $\mathbf{U}_{\mathrm{trend}}, \mathbf{U}_{\mathrm{season}}$ are combination weights and the trend and seasonality factors $\mathbf{v}_{\mathrm{trend}}(t), \mathbf{v}_{\mathrm{season}}(t)$ are modeled by GPs with different kinds of kernels to exploit temporal patterns (i.e., long-term patterns and periodic patterns). Similar to the inference technique considered in [21], the inference of GP can be converted to the solution of a time-invariant stochastic differential equation, which is further discretized as a Markov model to infer the state variable $\mathbf{Z}(t)$ corresponding to the factor $\mathbf{v}(t)$. Given all observations up to time t_n, i.e., $\mathcal{D}_{t_n}$, and a new observation arrived at t_{n+1}, i.e., $\mathbf{y}_{n+1}$, the statistical model parameters $\Theta := \{\mathbf{U}, \mathbf{Z}(t), \tau\}$ are inferred by maximizing the online posterior under the Bayes' rule

$$\begin{aligned} &p(\Theta \mid \mathcal{D}_{t_n} \cup \mathbf{y}_{n+1}) \propto p(\mathbf{y}_{n+1} \mid \Theta, \mathcal{D}_{t_n}) p(\Theta \mid \mathcal{D}_{t_n}), \\ &p(\Theta \mid \mathcal{D}_{t_n}) \approx q(\tau \mid \mathcal{D}_{t_n}) \prod_{d=1}^{D} q(\mathbf{u}^d \mid \mathcal{D}_{t_n}) q(\mathbf{Z}(t) \mid \mathcal{D}_{t_n}), \end{aligned}$$

where the second approximate posterior is formulated by the mean-field factorization. The authors developed a novel approach to update the posterior $p(\Theta \mid \mathcal{D}_{t_n})$ in an online manner by using Kalman filter and message merging techniques [23]. The method can handle imputation over arbitrary timestamps in the time-series data, and also offers uncertainty quantification for time-series from the statistical modeling, particularly benefiting downstream applications.

More recently, Chen et al. [22] proposed an innovative generalized temporal tensor decomposition with rank-revealing latent model for real-world tensor data reconstruction, which integrates statistical modeling with neural representations. This method encodes continuous spatial indexes through an MLP with Fourier feature encoding under the CP tensor decomposition, and employs neural ODEs in latent space to learn the temporal trajectories of factors. Specifically, given a spatial index i_k in the dimension k, the temporal factor $\mathbf{g}^k$ of the CP functional decomposition is modeled by

$$\begin{aligned}&\mathbf{z}^k(i_k,0)=\text{Encoder}\big([\cos(2\pi\mathbf{b}_k i_k);\sin(2\pi\mathbf{b}_k i_k)]\big),\\&\mathbf{z}^k(i_k,t)=\mathbf{z}^k(i_k,0)+\int_0^t h_{\boldsymbol{\theta}_k}\left[\mathbf{z}^k(i_k,s),s\right]\,ds,\ \mathbf{g}^k(i_k,t)=\text{Decoder}\left[\mathbf{z}^k(i_k,t)\right],\end{aligned}$$

where $\mathbf{z}^k$ are latent temporal factors and $h_{\boldsymbol{\theta}_k}$ is a state transition function of the dynamics at each timestamp, which is parameterized by an MLP. The index i_k is firstly encoded through an encoder MLP with Fourier encoding, and the neural ODE is implemented to obtain the latent temporal factor through $\mathbf{z}^k(i_k,t)=\text{ODESolve}[\mathbf{z}^k(i_k,0),h_{\boldsymbol{\theta}_k}]$. Finally, the temporal factor $\mathbf{g}^k$ is obtained by a decoder MLP. A Gaussian-Gamma prior is further imposed to the factor trajectory to automatically reveal the rank of the temporal tensor. The statistical model is also solved by variational inference with respect to the approximated posterior. The method outperforms existing statistical methods for tensor recovery and prediction by virtue of the neural representation coupled with statistical modeling [22].

Statistical and Bayesian continuous representation methods are capable of capturing periodic and long-term patterns that benefit time-series and streaming data analysis. Future research on enhancing the expressiveness of statistical frameworks (particularly integrating these frameworks with more powerful neural representations [22]) is expected to take advantage of both types of methods to better characterize both irregular local variability and long-term dependency underlying signals.

2.6 Continuous regularization for structural modeling

Except for the construction of various continuous representation models, there is also a group of studies that focus on the development of explicit continuous regularization methods conditioned on representations, mainly derived from intrinsic priors of data such as local correlations and nonlocal self-similarity. The explicit constraints lead to more accurate structural modeling of data based on the continuous representation. These continuous regularization methods improve the generalization ability, robustness, and applicability of continuous models. Moreover, continuous regularizations benefit from the resolution-independence and flexibility of continuous representations to handle complex and irregular scenarios that traditional regularization methods (such as NMF and total variation) fail to implement.

As a representative example, Wolterink et al. [17] proposed the INR for deformable image registration, where several regularization terms were introduced to alleviate the ill-posedness of such an inverse problem. The Jacobian regularizer is formulated as

$$S^{\text{jac}}[\Phi]=\int_\Omega |1-\det\nabla\Phi|\,dx,$$

where Φ is the INR and this regularizer limits the Jacobian determinant around 1 to restrict the local shrinkage or expansion of the deformation. The hyperelastic regularizer [17] conditioned on the INR Φ is defined as

$$S^{\text{hyper}}[\Phi]=\int_\Omega\left[\frac{1}{2}\alpha_l|\nabla u|^2+\alpha_a\phi_c(\text{cof}\,\nabla\Phi)+\alpha_v\psi(\det\nabla\Phi)\right]dx,$$

where $\frac{1}{2}\alpha_l|\nabla u|^2$ penalizes the length of the deformation, $\alpha_a\phi_c(\text{cof}\,\nabla\Phi)$ penalizes the expansion of area with the cofactor matrix of the Jacobian $\text{cof}\,\nabla\Phi$, and $\alpha_v\psi(\det\nabla\Phi)$ penalizes the growth and shrinkage of the deformation with a convex function $\psi(v)=\frac{(v-1)^4}{v^2}$. Except for the first-order regularizations, INR can also be facilitated with higher-order regularizations due to the differentiability of activation functions such as SIREN [16]. The second-order

Bending energy regularization [17] is formulated as

$$\mathcal{S}^{\text{bend}}[\Phi] = \int_{-1}^{1}\int_{-1}^{1}\int_{-1}^{1} \left(\frac{\partial^2\Phi}{\partial x^2}\right)^2 + \left(\frac{\partial^2\Phi}{\partial y^2}\right)^2 + \left(\frac{\partial^2\Phi}{\partial z^2}\right)^2 + 2\left(\frac{\partial^2\Phi}{\partial x\partial y}\right)^2 + 2\left(\frac{\partial^2\Phi}{\partial x\partial z}\right)^2 + 2\left(\frac{\partial^2\Phi}{\partial y\partial z}\right)^2 dxdydz,$$

which penalizes the smoothness of the deformation vector field by using second-order derivatives of INR. These regularization methods can be naturally combined into INRs based on standard automatic differentiation techniques, leading to improved accuracy for deformable image registration.

Recently, Li et al. [79] proposed the Dirichlet energy regularization for INR by utilizing another tiny INR to parameterize the Laplacian matrix of Dirichlet energy, termed INR regularization (INRR). Given an output matrix $\mathbf{X}$ obtained by an INR with parameters θ, the INRR is formulated as

$$\begin{cases} \mathcal{R}(\theta) = \operatorname{tr}\left(\mathbf{X}^{\mathrm{T}}\mathbf{L}(\theta)\mathbf{X}\right), \\ \mathbf{L}(\theta) = \mathbf{A}(\theta)\cdot\mathbf{1}_{m'\times m'} \odot \mathbf{I}_{m'} - \mathbf{A}(\theta), \\ \mathbf{A}(\theta) = \dfrac{\exp\left[g^{\mathrm{T}}(\theta;u)g(\theta;u)\right]}{\mathbf{1}_{m'}^{\mathrm{T}}\exp\left[g^{\mathrm{T}}(\theta;u)g(\theta;u)\right]\mathbf{1}_{m'}}, \end{cases}$$

where $\mathcal{R}(\theta)$ is the Dirichlet energy that captures the row/column-wise nonlocal self-similarity of $\mathbf{X}$, $\mathbf{L}(\theta)$ is the Laplacian matrix that constitutes the Dirichlet energy, $\mathbf{A}(\theta)$ is a weighted adjacency matrix that measures the similarity of $\mathbf{X}$, and $g(\theta;u)$ is another tiny INR with input row/column coordinates u. The tiny INR here enforces the implicit smoothness constraint for the Laplacian matrix $\mathbf{L}(\theta)$, which aligns with the piecewise smoothness of natural images. The INRR is especially helpful for improving the generalization abilities of INR for nonuniform sampling coordinates by leveraging the smooth row/column-wise self-similarity underlying signals. Similarly, Luo et al. [80] proposed the continuous representation-based nonlocal method for multi-dimensional data, which captures the nonlocal self-similarity of discrete grid or irregular signals by constructing nonlocal patch groups, implicitly imposing a nonlocal regularization across the signal. In particular, the nonlocal continuous similar cubes of a signal are grouped together, which holds stronger low-rankness than the original data. Then, a coupled LRTFR method was proposed to represent the nonlocal continuous cubes to reconstruct the data [80]. The nonlocal method enjoys superior reconstruction abilities for both grid data such as images and irregular non-grid ones such as point clouds by virtue of the nonlocal low-rankness excavation, and holds better efficiency by the coupled tensor factorization.

Recently, Luo et al. [18] proposed the total variation regularization on the neural domain (termed NeurTV). It uses the directional or higher-order derivatives of INR outputs with respect to input coordinates to capture local directional correlations intrinsically existed in grid and non-grid data, and NeurTV demonstrates superior capabilities then traditional discrete TV for image, point cloud, and ST data reconstruction by avoiding the discretization error inherent in traditional methods. Specifically, the directional NeurTV is defined as

$$\Psi_{\text{NeurDTV}_\theta}(\Theta) := \int_\Omega \left|\frac{\partial f_\Theta(\mathbf{x})}{\partial \mathbf{x}_{(1)}}\cos\theta + \frac{\partial f_\Theta(\mathbf{x})}{\partial \mathbf{x}_{(2)}}\sin\theta\right| d\mathbf{x},$$

where θ is a predefined direction and f_Θ is an INR with input coordinate $\mathbf{x}$. The directional NeurTV can capture local smoothness along a predefined direction θ. Furthermore, the NeurTV can be extended to a space-variant formulation that automatically determines the local directional and scale parameters for each spatial point to better describe local variations

$$\Psi_{\text{NeurTV}^\alpha_\theta}(\Theta) = \int_\Omega \alpha_{\mathbf{x}} \left\| \begin{pmatrix} a_{\mathbf{x}} & 0 \\ 0 & 2-a_{\mathbf{x}} \end{pmatrix} \begin{pmatrix} \cos\theta_{\mathbf{x}} & \sin\theta_{\mathbf{x}} \\ \sin\theta_{\mathbf{x}} & -\cos\theta_{\mathbf{x}} \end{pmatrix} \begin{pmatrix} \dfrac{\partial f_\Theta(\mathbf{x})}{\partial \mathbf{x}_{(1)}} \\ \dfrac{\partial f_\Theta(\mathbf{x})}{\partial \mathbf{x}_{(2)}} \end{pmatrix} \right\|_{\ell_1} d\mathbf{x}, \tag{5}$$

where $\alpha_{\mathbf{x}}, a_{\mathbf{x}}$ are local scale parameters for $\mathbf{x}$ and $\theta_{\mathbf{x}}$ are local directional parameters. The space-variant NeurTV better captures directional variations within a signal, and the directional parameters $\alpha_{\mathbf{x}}, a_{\mathbf{x}}, \theta_{\mathbf{x}}$ are automatically identified and calibrated during optimization. Some numerical examples of the nonlocal method [80] and the space-variant NeurTV [18] regularization are shown in Figure 5 to visually demonstrate the efficacy of these regularization methods for general data reconstruction tasks by merging such intrinsic data priors with continuous representation.

Recently, Heo et al. [81] proposed an isometric regularization technique for INRs with latent space embedding, such as the generative modeling of shapes using SDF [61]. The regularization preserves meaningful geometric quantities (such as distances and angles) between the latent space and the functional data manifold by interpreting the

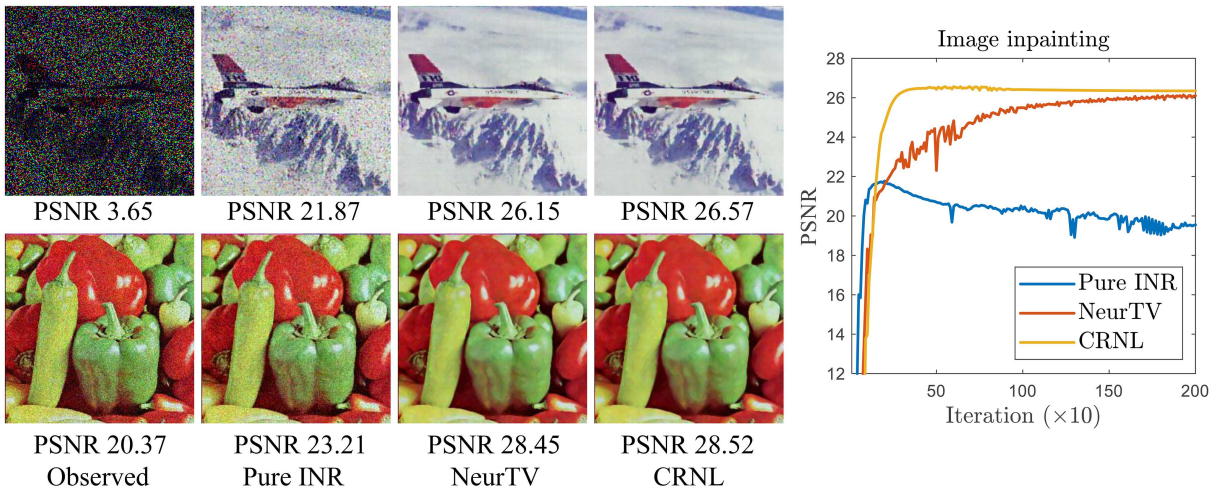

Figure 5 (Color online) Continuous regularization methods such as NeurTV [18] and continuous representation-based nonlocal model (CRNL) [80] alleviate the overfitting phenomenon of pure INR for image reconstruction tasks including image inpainting (top row) and denoising (bottom row) by incorporating intrinsic priors of data.

mapping from latent variables to INRs as a parametrization of a Riemannian manifold. The regularization encourages the manifold to hold minimal intrinsic curvature, hence enabling robust and smooth geometric representations. One can generalize this regularization to a group of latent space-based continuous representations, such as operator learning [36, 81] and arbitrary-scale image representation [11].

In future research, it would be important to scale these effective continuous regularizations to higher-dimensional cases (e.g., extending the directional NeurTV to higher dimensions beyond two), which would benefit multi-directional characterization such as optical flow in videos and spectral smoothness in multispectral images. Meanwhile, it would be interesting to apply these explicit regularizations to more vision and scientific computing problems such as scene representation [15], surface representation [61], and neural physical simulations [110] to enhance their respective robustness.

2.7 Methodological interplay

The continuous methodology design involves many interplays across different domains, which are critical for gaining deeper insights and boosting further improvements of continuous representation methods. For example, modern INR methods have leveraged many techniques and methodologies related to basis function representations, highlighting their interplay. While traditional basis function methods explicitly decompose a function using pre-defined basis functions (e.g., Gaussian, Fourier, Chebyshev), INRs implicitly integrate this idea into the neural network's architecture itself. For instance, the Fourier feature PE [20] maps input coordinates to a set of Fourier basis functions, acting as a fixed basis expansion at the input layer of the INR. The SIREN [16] and WIRE [30] use sinusoidal or wavelet functions as nonlinear activations, parameterizing the INR as a learnable function composed of weighted basis functions. Essentially, INRs inherit the principle of basis functions but replace a fixed, shallow set of global bases with adaptive and hierarchical combinations of basis functions.

The concept of traditional function decomposition [8, 85] has inherent interplay with modern INR-based function decomposition methods [2, 75, 76]. Both approaches decompose a multivariate function as a linear combination of univariate functions. While traditional methods parameterize these univariate functions using predefined basis functions, recent techniques [2, 76] draw inspiration from classical tensor representations and employ INRs to learn the univariate functions adaptively, thereby offering a more flexible framework for representing complex multivariate functions. Computational mathematical tools, such as the neural ordinary differential equation [22], have also become increasingly intertwined with continuous representation frameworks.

For another example, Liu and Tang [41] introduced DiffFNO, a model that integrates the Fourier neural operator (FNO) with a diffusion framework for arbitrary-scale image super-resolution. This application of NO learning [37] to image super-resolution illustrates the growing interplay between methodologies derived from scientific computing and those in the computer vision community. Moreover, the successful integration of InstantNGP and 3DGS into physics-informed neural networks [110–112] highlights the interplay between the computer graphics and scientific computing communities. In particular, efficient continuous representation models from graphics research (e.g., InstantNGP [51] and 3DGS [45]) have demonstrated significant potential in addressing numerical PDE problems,

Table 5 Comparative analysis of some modern continuous representation methods.

Method	Key advantages	Potential trade-off	Primary applications
INR	Concise implementation Parameter efficiency Inherent smoothness	Spectral bias	Neural radiance fields SDF representation Arbitrary-scale super-resolution
Grid encoding	Fast convergence High-frequency capture Memory efficiency	Training overfitting	Novel view synthesis Fast imaging reconstruction
3DGS	Real-time rendering Explicit geometry High-quality scene	Large storage	Graphics 3D reconstruction
Tensor function	Computational efficiency Structural prior Interpretability	Limit expressiveness	Multi-dimensional data Scientific analysis INR acceleration
Statistical framework	Uncertainty quantification Prior incorporation Periodic modeling	Model specification	Time-series analysis Uncertainty analysis

highlighting a promising trend toward interdisciplinary research and investigation. In terms of theoretical interplay, the combination of physics-informed neural networks & neural operators in scientific computing and the NTK theory from classical neural network analysis underscores promising opportunities for interdisciplinary research [19,113,114]. In particular, theoretical tools established in one domain (e.g., NTK theory in classical neural network analysis) can be leveraged to interpret and inspire the development of efficient algorithms in a different domain (e.g., physics-informed neural networks in scientific computing). These interplay parts are important for understanding deepen insights into these methods and developing further improvements.

Here, we further perform a more systematic comparison of some modern continuous representation paradigms by discussing their key advantages and trade-offs. A summary table is shown in Table 5. In particular, INRs [16,20] offer parameter efficiency and implicit smoothness through the continuous representation, which is the most classical continuous representation paradigm nowadays. As compared with INRs, grid encoding methods (e.g., InstantNGP [51]) achieve faster training and superior detail capture by using multi-resolution learnable grids, but may more easily incur overfitting for noisy observations. On the other hand, 3DGS [45] demonstrates computational advantages for real-time continuous representation, such as novel view synthesis, though it may require more storage costs by storing a large number of Gaussian functions [45]. Furthermore, tensor and matrix function decomposition methods [2, 115] introduce beneficial structural priors and improve interpretability & robustness, but may limit expressiveness where low-rank assumption is not satisfied. Statistical and Bayesian approaches [21, 23] provide the distinct ability to model uncertainty and temporal periodic dynamics, while the model specification (e.g., Gaussian processes) may not be suitable for extremely complex data. In summary, it is important to integrate the advantages of different paradigms to promote transformative continuous representation models that are both flexible, efficient, and robust in future research.

3 Theoretical foundations of continuous representations

This section introduces several theoretical frameworks that uncover fundamental insights into continuous representation learning methodologies. Our analysis is primarily based on three groups of theories: approximation error analysis and representational capacity theory for continuous representation models, convergence and generalization analysis of continuous methods from the NTK theory, and implicit regularizations brought by the structures of continuous models and their corresponding optimization dynamics. These theoretical perspectives are summarized in Table 6 [31, 33, 40, 54, 56–59, 116–124].

3.1 Approximation and representation theory

The approximation and representation theory refer to the theoretical framework that quantizes the error of estimating/representing an unknown or complex function using a more tractable continuous function representation by parametric or non-parametric models [29, 40, 116, 117]. The goal is to find or demonstrate that a function from a predefined class (e.g., polynomials, neural networks, Gaussians) could closely match the target function in the continuous domain.

Table 6 Review of representative theoretical foundations related to continuous function representations.

Category	Theory	Description	Year	Ref.
Approximation and representation	Truncation error of SVD for functions	Truncation error estimate and decay rate of SVD approximation for Sobolev smooth bivariate functions.	2018	[116]
	Functional TT decomposition	Propose functional TT (and parameterization error) that represents functions in the TT format.	2019	[40]
	Functional tensor CP decomposition	Propose the functional CPD (and its contractive error bounds) via RKHS-based power iteration.	2021	[117]
	Dictionary analysis for INR	Utilize harmonic analysis to characterize the function class represented by INR using a signal dictionary.	2021	[58]
	Complex wavelets analysis for INR	Characterize the function class represented by wavelet INR using Fourier convolution theorem and Γ-progressiveness.	2024	[59]
	Functional tensor SVD framework	Propose the functional tensor SVD theorem in continuous domains for multi-output regression problem.	2024	[118]
Convergence and generalization	Neural tangent kernel (NTK)	The training of neural nets follows kernel gradient with respect to the NTK, enabling generalization and convergence analysis of neural nets.	2018	[31]
	Convolutional NTK	Propose the NTK computation of CNN and the non-asymptotic proof that wide net is equivalent to NTK regression.	2019	[54]
	Regularized neural nets outperforms NTK	Regularized neural nets has better generalization than NTK and the convergence of ℓ_2-norm regularized neural nets.	2019	[119]
	RKHS norm reg. for neural nets	Use the RKHS norm under the NTK as the function-space regularization of deep neural nets.	2022	[120]
	Modified kernel's spectrum	Propose modified spectrum kernels and a preconditioned method for faster convergence by altering eigenvalues of NTK.	2024	[121]
	NTK analysis for InstantNGP	Demonstrate that InstantNGP recovers fine details better from the NTK eigenvalue perspective.	2025	[56]
Implicit regularization	Implicit reg. in deep matrix factorization	Study the implicit nuclear norm reg. of gradient descent over deep linear neural networks for matrix sensing.	2019	[57]
	Implicit reg. in deep tensor factorization and CNN	Analyze the implicit reg. of hierarchical tensor factorization (equivalent to deep CNN) towards low hierarchical tensor rank.	2022	[122]
	Implicit reg. in deep CP factorization	Establish the polynomial growth of implicit low-rank reg. with respect to the depth of deep tensor CP factorization.	2022	[33]
	Implicit reg. in deep Tucker factorization	Study the implicit reg. of deep Tucker factorization for tensor completion towards solutions with low multilinear rank.	2024	[123]
	Implicit bias of AdamW optimizer	Show that AdamW optimizer converges to a KKT point of the original loss under bounded ℓ_∞-norm constraint.	2024	[124]

First, it is known that deep neural nets serve as universal approximators for any continuous functions in the compact set of Euclidean space.

Theorem 1 (Universal approximation [125,126])**.** Let $K \subset \mathbb{R}^n$ be a compact set, and $f : K \to \mathbb{R}$ be any continuous function. For any $\epsilon > 0$, there exists a single-hidden-layer MLP with activation function σ (any non-polynomial continuous function), such that the network output $N(x)$ satisfies

$$\sup_{x \in K} |f(x) - N(x)| < \epsilon, \ N(x) = \sum_{i=1}^{m} a_i \, \sigma(w_i \cdot x + b_i),$$

where $m \in \mathbb{N}$, $a_i, b_i \in \mathbb{R}$, and $w_i \in \mathbb{R}^n$.

The theorem provides a fundamental theoretical guarantee on the representation abilities of INR. For example, the widely-used SIREN [16] utilizes the sinusoidal activation function, which is a non-polynomial continuous function. Hence, SIREN has the capacity to approximate any continuous functions. However, in practice, INRs such as SIREN still suffer from spectral basis that favors low-frequency information and leads to slower convergence to high-frequency information. This is related to the optimization dynamic and can be well explained by the NTK; see Subsection 3.2.

From the traditional function approximation perspective, many studies have explored the representation capacity of basis function representations. For example, any integrable periodic function can be represented by a unique combination of Fourier series [127]. Any compactly supported non-periodic function can be transformed into a periodic function, and hence can also be represented by Fourier series. Similarly, linear combinations of complete wavelets bases (such as Haar wavelets) are capable of approximating any integrable functions from the multiresolution analysis [128].

Following the function representation theory pipeline, several studies have investigated the function class that could be captured by general INR structures. Yüce et al. [58] proposed a theoretical framework that characterizes the function class represented by an INR. Specifically, INR families are structured signal dictionaries with atoms being integer harmonic functions related to the initial mapping frequencies. The INR f_θ in [58] is formulated as

$$f_\theta(\mathbf{r}) = \mathbf{W}^{(L)}\mathbf{z}^{(L-1)} + \mathbf{b}^{(L)},\ \mathbf{z}^{(\ell)} = \rho^{(\ell)}\left(\mathbf{W}^{(\ell)}\mathbf{z}^{(\ell-1)} + \mathbf{b}^{(\ell)}\right),\ \ell = 1, \ldots, L-1,\ \mathbf{z}^{(0)} = \gamma(\mathbf{r}), \tag{6}$$

where $\mathbf{r}$ is the input coordinate, γ is the first-layer encoding, and ρ is the activation. Such a structure can only capture the following class of functions.

Theorem 2 (Function class represented by INR [58]). Let $\rho^{(\ell)}(\mathbf{z}) = \sum_{k=0}^{K} \alpha_k \mathbf{z}^k$ for $\ell > 1$. Let $\Omega = [\Omega_0, \ldots, \Omega_{T-1}]^{\mathrm{T}}$ and ϕ denote the matrix of frequencies and vector of phases in the encoding layer $\gamma(\mathbf{r}) = \sin(\Omega\mathbf{r} + \phi)$. Then the architecture $f_\theta(\mathbf{r})$ can only represent functions of the form

$$f_\theta(\mathbf{r}) = \sum_{\omega' \in \mathcal{H}(\Omega)} c_{\omega'} \sin\left(\langle \omega', \mathbf{r}\rangle + \phi_{\omega'}\right), \tag{7}$$

where $\mathcal{H}(\Omega) \subseteq \left\{ \sum_{t=0}^{T-1} s_t \Omega_t \middle| s_t \in \mathbb{Z} \wedge \sum_{t=0}^{T-1} |s_t| \leqslant K^{L-1} \right\}$.

The theorem shows that the expressive power of conventional INRs (such as PE-based INR [20] and SIREN [16]) is restricted to functions that can be expressed as a linear combination of certain harmonics related to the feature mapping $\gamma(\mathbf{r})$. Hence, the INR has the same expressive power as a structured signal dictionary whose atoms are sinusoids with frequencies ω' equal to sums and differences of the integer harmonics of the mapping frequencies Ω [58]. Another insight is that the INR represents this function class with degree of freedom $O(TK^L)$ using substantially fewer parameters (i.e., with $O(T^2L)$ parameters in the learnable weights $\mathbf{W}$), indicating that the INR imposes a certain low-rank structure over the coefficients. Furthermore, the authors [58] drew inspirations from meta-learning to construct dictionary atoms of INRs as a combination of examples seen during meta-training. As a result, the target signals would project onto the eigenfunctions of the NTK with the largest eigenvalues, leading to increased convergence speed by meta-learning to reshape the dictionary atoms.

Recently, Roddenberry et al. [59] proposed a wavelet analysis framework that captures the function class represented by wavelet INR [30]. The analysis is based on the Fourier convolution theorem of the atoms of the first-layer feature of the INR. Specifically, the signal is represented from coarse approximations performed in the first layer of the INR. The wavelet INR in [59] is formulated as

$$f_\theta(\mathbf{r}) = \mathbf{W}^{(L)}\mathbf{z}^{(L-1)}(\mathbf{r}) + \mathbf{b}^{(L)},\ \mathbf{z}^{(\ell)}(\mathbf{r}) = \rho^{(\ell)}\left(\mathbf{W}^{(\ell)}\mathbf{z}^{(\ell-1)}(\mathbf{r}) + \mathbf{b}^{(\ell)}\right),\ \mathbf{z}^{(0)}(\mathbf{r}) = \psi\left(\mathbf{W}^{(0)}\mathbf{r} + \mathbf{b}^{(0)}\right),$$

where ρ are polynomials and ψ is the so-called template function in the first layer, considered as complex wavelets in [59]. This class of INR has a Fourier transform that is fully determined by convolutions of the Fourier transforms of the atoms in the first layer, as demonstrated in the representation theorem.

Theorem 3 (Function class represented by INR using template function convolutions [59]). Let a point $\mathbf{r}_0 \in \mathbb{R}^d$ be given and $\Delta = \{\boldsymbol{m} | \sum_{t=1}^{F_1} m_t = k\}$. Under mild assumptions, there exists an open neighborhood $U \ni \mathbf{r}_0$ such that for all $\phi \in \mathcal{C}_0^\infty(U)$

$$\widehat{\phi \cdot f_{\boldsymbol{\theta}}}(\xi) = \left\{ \widehat{\phi} * \sum_{k=0}^{K^{L-1}} \sum_{\boldsymbol{m} \in \Delta} \widehat{\beta}_{\boldsymbol{m}} \ast_{t=1}^{F_1} \left[\mathrm{e}^{\mathrm{i}2\pi \langle \mathbf{W}_t^{-\mathrm{T}} \xi, \mathbf{b}_t \rangle} \widehat{\psi}(\mathbf{W}_t^{-\mathrm{T}} \xi) \right]^{*m_t, \xi} \right\}(\xi), \tag{8}$$

for coefficients $\widehat{\beta}_{\boldsymbol{m}} \in \mathbb{C}$ independent of $\mathbf{r}$, where $(\cdot)^{*m,\xi}$ denotes m-fold convolution of the argument with itself with respect to ξ. The $\mathbf{W}_t^{-\mathrm{T}}$ denotes the transpose of the inverse matrix. Furthermore, the coefficients $\widehat{\beta}_{\boldsymbol{m}}$ are only nonzero when each $t \in [1, \ldots, F_1]$ such that $m_t \neq 0$ also satisfies $\mathbf{W}_t\mathbf{r}_0 + \mathbf{b}_t \in \mathrm{supp}(\psi)$.

This theorem is an application of the Fourier convolution theorem conditioned on the INR function class introduced in Theorem 2. Specifically, the Fourier transform $\widehat{\phi \cdot f_{\boldsymbol{\theta}}}$ is fully determined by the self-convolutions of the Fourier transforms of the atoms in the first layer, which generates integer harmonics by scaled, shifted copies of the template function ψ, i.e., $\psi(\mathbf{W}_t\mathbf{r}_0 + \mathbf{b}_t)$. The support of these scaled and shifted atoms of the first layer, say $\psi(\mathbf{W}_t\mathbf{r}_0 + \mathbf{b}_t)$, is preserved as the support of ψ, so that the INR output at a given coordinate $\mathbf{r}$ is dependent only on the atoms in the first layer whose support contains $\mathbf{r}$ [59]. Moreover, the authors [59] used the Γ-progressiveness analysis tool to show the advantages of using complex wavelets for INR. The Γ-progressiveness refers to the property of a function that the support of its Fourier transform lies in a convex conic set of $\mathbb{R}^d$. They demonstrated that the wavelet INR is a Γ-progressive function. Thus, any advantages/limitations of approximating functions using Γ-progressive template functions are maintained. And if the atoms in the first layer of an INR using a template function ψ have vanishing Fourier transform in some neighborhood of the origin, then the output of the INR has Fourier support that also vanishes in that neighborhood (i.e., band-pass property). Hence, the authors designed a split INR structure that utilizes two INRs to respectively serve as low-pass and high-pass filters for signal representation, which holds good performance. These INR theories would provide solid foundations for further developments of continuous representation theories, algorithms, and applications for diverse fields.

Furthermore, we shift our focus to the representation and approximation analysis of a class of functional decomposition studies, which are related to the INR-based functional tensor decomposition methods [2, 35, 75, 129]. INR-based functional tensor decomposition methods currently lack sufficient theoretical explanations on their representation and approximation abilities. We suppose that existing frameworks from the harmonic and Fourier analysis coupled with theoretical tensor decomposition frameworks [9] can pave the way on explaining the expressiveness of these methods [2, 35, 75, 129]. In particular, in future work, we can attempt to characterize the approximation error of INR-based functional tensor decomposition methods with respect to their rank parameters by using Fourier basis function representations and the corresponding decay rate of Fourier coefficients [8, 130] in the function space. Meanwhile, we can leverage the function singular value decomposition theory [116] and the decay rate of function singular values to establish the approximation error of INR-based functional decompositions by parameterizing INRs in the function singular value decomposition form. Moreover, we can leverage mathematical tools from functional analysis, such as the Stone-Weierstrass theorem [131] that characterizes the density of a certain function class and the classical universal approximation theory [132] for MLPs, to establish the approximation ability guarantee for INR-based functional decomposition methods.

More specifically, Griebel and Li [116] studied the decay rate of singular values of a group of bivariate functions in the Sobolev space $W^{s,2}(D)$ where $D \subset \mathbb{R}^n$. Given a bivariate function $\kappa(y, x)$, the singular value decomposition (SVD) refers to the expansion

$$\kappa(y, x) = \sum_{n=1}^{\infty} \sqrt{\lambda_n}\phi_n(x)\psi_n(y), \tag{9}$$

where λ_n are eigenvalues of the integral operator $\mathcal{R}$ with associated kernel $R(x, x') = \int_\Omega \kappa(y, x)\kappa(y, x')\, dy$, $\phi_n(x)$ are corresponding eigenfunctions, and $\psi_n(y) = \frac{1}{\sqrt{\lambda_n}} \int_D \kappa(y, x)\phi_n(x)\, dx$. The theory [116] establishes the order $O(M^{-s/d})$ for the truncation error of the SVD series expansion (9) after the M-th term truncation [116]. In signal processing, SVD serves as a fundamental method for dimensional reduction tasks such as PCA and data compression. Building upon this foundation, promising research lies in investigating the SVD truncation theory of INR-based continuous representations to uncover theoretical insights of functional tensor decomposition methods [2, 75].

Following this line of research, Wang et al. [118] proposed the functional tensor SVD (t-SVD) via tensor-tensor product, which extends the classical t-SVD to infinite and continuous feature domains.

Theorem 4 (Functional t-SVD [118])**.** Let $F : \mathcal{X} \times \mathcal{Y} \to \mathbb{R}^K$ be a square-integrable vector-valued function with Lipschitz-smooth domains $\mathcal{X} \subset \mathbb{R}^{D_1}$ and $\mathcal{Y} \subset \mathbb{R}^{D_2}$. Then, there exist sets of functions $\{\phi_i\}_{i=1}^{\infty} \subset L^2(\mathcal{X}; \mathbb{R}^K)$ and $\{\psi_i\}_{i=1}^{\infty} \subset L^2(\mathcal{Y}; \mathbb{R}^K)$, and a sequence of t-scalars $\{\sigma_i\}_{i=1}^{\infty} \subset \mathbb{N}^K$ with $\lim_{i\to\infty} \sigma_i = 0$, satisfying the functional t-singular value decomposition (Ft-SVD):

$$F(x, y) = \sum_{i=1}^{\infty} \phi_i(x) *_M \sigma_i *_M \psi_i(y), \tag{10}$$

where $*_M$ denotes the tensor-tensor product induced by the transform M. The orthonormality conditions $\int_{\mathcal{X}} \phi_i(x) *_M \phi_j(x)\, dx = \delta_{ij} M^{-1}(\mathbf{1})$ and $\int_{\mathcal{Y}} \psi_i(y) *_M \psi_j(y)\, dy = \delta_{ij} M^{-1}(\mathbf{1})$ hold, where $\mathbf{1} \in \mathbb{R}^{1\times 1\times K}$ is the t-scalar with all entries equal to 1, and δ_{ij} is the Kronecker delta.

The theorem states that the vector-valued function F can be decomposed into the t-SVD form in the continuous Lipschitz domain. The authors applied this novel functional tensor decomposition model to the multi-output

regression problem, and resolved the combinatorial distribution shift problem in multi-output regression. They also developed an empirical risk minimization to address the regression problem using Ft-SVD, and demonstrated the theoretical analyses for the performance guarantee of the algorithm.

Han et al. [117] proposed the CP low-rank functional tensor decomposition model, a novel dimension reduction framework for tensors with one functional mode and several tabular modes. Let $\mathcal{Y} \in \mathbb{R}^{p_1 \times p_2 \times [0,1]}$ be the functional tensor with approximately CP rank r, then the CP functional tensor decomposition model of $\mathcal{Y}$ is modeled by

$$\mathcal{Y} = \mathcal{X} + \mathcal{Z}, \quad \mathcal{X} = \sum_{l=1}^{r} \lambda_l \mathbf{a}_l \otimes \mathbf{b}_l \otimes \xi_l \in \mathbb{R}^{p_1 \times p_2 \times [0,1]}, \tag{11}$$

where $\mathbf{a}_l, \mathbf{b}_l$ are factor vectors and ξ_l is the factor function in a reproducing kernel Hilbert space (RKHS) spanned by a positive-definite kernel function. The authors provided the identifiability condition of the CP functional model. Then, an RKHS-based power iteration method was proposed to estimate the model parameters from a discrete tensor, which iteratively updates the tabular factors $\mathbf{a}_l, \mathbf{b}_l$ and the function ξ_l without function parameterization. Finally, the authors developed a non-asymptotic contractive error bound for the proposed power iteration algorithm and applied the algorithm to real tensor data analysis.

Gorodetsky et al. [40] developed a new approximation algorithm for representing and computing with multivariate functions using the functional TT, which replaces the three-dimensional TT cores with univariate matrix-valued functions, similar to that of [70]. They provided parameterization error of using the TT model for approximating a multivariate function, and applied the numerical functional TT algorithm for approximating functions with local features (such as discontinuities) and adaptive integration and differentiation of multivariate functions. Recently, Fageot [133] proposed the theoretical guarantee for the inverse problem of recovering a continuous-domain function from a finite number of noisy linear measurements, where the target function is the sum of a slowly varying trend function and a periodic seasonal function, and the reconstruction is formalized by introducing a convex generalized total variation regularization over functions. These theoretical frameworks provide fundamental insights and performance guarantees for continuous representation methods. In future research, it would be interesting (and more challenging) to further investigate tractable and theoretically guaranteed computation, decomposition, and reconstruction algorithms for multivariate neural continuous functions, such as INRs and NO learning that operates directly on INRs [134, 135].

3.2 Generalization and convergence

In this subsection, we review several NTK-based theoretical frameworks that reveal the underlying generalization and convergence capabilities of continuous representation methods using INRs (and also more general deep neural nets). The NTK describes the behavior of infinitely wide neural networks during gradient descent training using the corresponding kernel gradient descent under the NTK, and also explains several optimization challenges (such as the spectral bias in INRs that the network favors low-frequency information more than high-frequency ones [20, 42]). The NTK measures how a small change in parameters affects the outputs for two network inputs x and x'. For wide enough neural nets, this measure stays fixed, simplifying training analysis.

Jacot et al. [31] firstly introduced the NTK framework for neural network convergence and generalization. During gradient descent on the parameters of a neural network f_θ with depth L, the network follows the kernel gradient of the functional cost with respect to the NTK, where the NTK function is defined as

$$\Theta^{(L)}(\theta) = \sum_{p=1}^{P} \partial_{\theta_p} F^{(L)}(\theta) \otimes \partial_{\theta_p} F^{(L)}(\theta),$$

where $\Theta^{(L)}(\theta)$ is the NTK, $F^{(L)}(\theta)$ is the realization function mapping θ to f_θ, and $\otimes$ is the tensor product between two functions. While the NTK is random at initialization and varies during training of the neural network f_θ, in the infinite-width limit, the NTK $\Theta^{(L)}(\theta)$ converges to an explicit limiting kernel and stays constant during training. These are the two key theoretical results presented in [31].

Theorem 5 (Convergence to the NTK with infinite-width at initialization [31])**.** For a neural network of depth L at initialization, with a Lipschitz nonlinearity σ, and in the limit as the network layers width $n_1, \ldots, n_{L-1} \to \infty$, the NTK $\Theta^{(L)}$ converges in probability to a deterministic limiting kernel $\Theta^{(L)} \to \Theta_\infty^{(L)} \otimes Id_{n_L}$, where $\Theta_\infty^{(L)} : \mathbb{R}^{n_0} \times \mathbb{R}^{n_0} \to \mathbb{R}$ is a scalar kernel and Id_{n_L} is an identity matrix.

Theorem 6 (Convergence to the NTK during training [31]). Assume that σ is a Lipschitz nonlinearity function with bounded second derivative. Under mild assumptions, we have that, uniformly for any training time $t \in [0, T]$, $\Theta^{(L)}(t) \to \Theta_{\infty}^{(L)} \otimes Id_{n_L}$, where $\Theta^{(L)}(t)$ is the NTK at time t.

Since the NTK of an infinite-width neural network converges to a deterministic kernel for both initialization and during training, we can readily describe the convergence and generalization features of this neural network by depicting the corresponding kernel. For instance, Arora et al. [55] proposed the classical fine-grained analysis of convergence and generalization of overparameterized two-layer neural nets based on NTK. They considered a two-layer ReLU-activated neural network f and the corresponding training objective Φ with input-label pairs $\{\mathbf{x}_i, y_i\}$:

$$f_{\mathbf{W},\mathbf{a}}(\mathbf{x}) = \frac{1}{\sqrt{m}} \sum_{r=1}^{m} a_r \sigma\left(\mathbf{w}_r^{\mathrm{T}} \mathbf{x}\right), \ \Phi(\mathbf{W}) = \frac{1}{2} \sum_{i=1}^{n} \left(y_i - f_{\mathbf{W},\mathbf{a}}(\mathbf{x}_i)\right)^2.$$

Using the eigen-decomposition of the NTK matrix $\mathbf{H}^{\infty} = \sum_{i=1}^{n} \lambda_i \mathbf{v}_i \mathbf{v}_i^{\mathrm{T}}$ ($\mathbf{H}^{\infty} \in \mathbb{R}^{n \times n}$ is the evaluation of the NTK function on input data points $\mathbf{x}_1, \ldots, \mathbf{x}_n$), the optimization dynamic and generalization error bound of this neural network can be analyzed.

Theorem 7 (Training convergence rate [55]). Suppose $\mathbf{y} = [y_1, \ldots, y_n]$, $\lambda_0 = \lambda_{\min}(\mathbf{H}^{\infty}) > 0$, $\kappa = O\left(\frac{\epsilon\delta}{\sqrt{n}}\right)$, $m = \Omega\left(\frac{n^7}{\lambda_0^4 \kappa^2 \delta^4 \epsilon^2}\right)$ and $\eta = O\left(\frac{\lambda_0}{n^2}\right)$. Then with probability at least $1 - \delta$ over the random initialization, for all training steps $k = 0, 1, 2, \ldots$ we have the training error follows:

$$\|\mathbf{y} - [f_{\mathbf{W}(k),\mathbf{a}}(\mathbf{x}_1), \ldots, f_{\mathbf{W}(k),\mathbf{a}}(\mathbf{x}_n)]\|_2 = \sqrt{\sum_{i=1}^{n} (1 - \eta\lambda_i)^{2k} \left(\mathbf{v}_i^{\mathrm{T}} \mathbf{y}\right)^2} \pm \epsilon. \tag{12}$$

Following the analysis in [55], we define $\xi_i(k) = (1 - \eta\lambda_i)^{2k} (\mathbf{v}_i^{\mathrm{T}} \mathbf{y})^2$, and each sequence starts at $\xi_i(0) = (\mathbf{v}_i^{\mathrm{T}} \mathbf{y})^2$ and decreases at ratio $(1 - \eta\lambda_i)^2$. In other words, we can think of decomposing the label vector $\mathbf{y}$ into its projections onto all eigenvectors $\mathbf{v}_i$ of $\mathbf{H}^{\infty}$: $\|\mathbf{y}\|_2^2 = \sum_{i=1}^{n} (\mathbf{v}_i^{\mathrm{T}} \mathbf{y})^2 = \sum_{i=1}^{n} \xi_i(0)$, and the i-th portion shrinks exponentially at ratio $(1 - \eta\lambda_i)^2$. The larger λ_i is, the faster $\{\xi_i(k)\}_{k=0}^{\infty}$ decreases to 0. In order to have faster convergence, we would like the projections of $\mathbf{y}$ onto top eigenvectors to be larger. For a set of labels $\mathbf{y}$, if they align with the top eigenvectors, i.e., $(\mathbf{v}_i^{\mathrm{T}} \mathbf{y})^2$ is large for large eigenvalues λ_i, then gradient descent converges quickly. Otherwise, the optimization would converge slowly to components that correspond to smaller eigenvalues. This property induces the well-known spectral bias in neural networks. Addressing the spectral bias issue is the motivation of many INR methods. For instance, the Fourier reparameterized INR method [42] reconfigures the eigenvalue distribution of the NTK through reparameterization of MLP layers, hence enabling more projections onto top eigenvectors, leading to faster convergence towards high-frequency components. The method in [72] alleviates the spectral bias of INR by flexible bandwidth tuning of the NTK through a delicately designed activation function.

Since the training of a neural network using gradient descent mimics the kernel gradient descent with respect to the NTK, we can consider the scenario of using the kernel regression for continuous representation (i.e., mapping coordinates to values using kernel regression). If the kernel $k(x, x')$ is non-diagonal (i.e., input coordinates x and x' that are close to each other do not result in high responses $k(x, x')$), it is hard to use this kernel to fit a good regression model in the continuous space. Otherwise, if the kernel $k(x, x')$ is diagonal and shift-invariant, it would be more suitable. This is the underlying principle of many feature encoding-based INR methods, such as the Fourier feature PE [20] and SIREN [16]. The Fourier feature encoding shifts the NTK of a ReLU-activated neural network from non-diagonal to diagonal, hence enabling effective continuous representation (see Figure 6).

In terms of generalization error bound, Arora et al. [55] developed an NTK-based bound that fully depends on data pairs $\{\mathbf{x}_i, y_i\}$ and the structure of the neural network through the NTK matrix $\mathbf{H}^{\infty}$. The generalization theory states that, suppose the data $S = \{(\mathbf{x}_i, y_i)\}_{i=1}^{n}$ are i.i.d. samples from a distribution D and consider any loss function $\ell : \mathbb{R} \times \mathbb{R} \to [0, 1]$ that is 1-Lipschitz and sufficiently wide neural network, then with high probability $1 - \delta$, the two-layer neural network $f_{\mathbf{W}(k),\mathbf{a}}$ trained by gradient descent has generalization loss $L_D(f_{\mathbf{W}(k),\mathbf{a}}) = \mathbb{E}_{(\mathbf{x},y)\sim D}\left[\ell(f_{\mathbf{W}(k),\mathbf{a}}(\mathbf{x}), y)\right]$ bounded as

$$L_D(f_{\mathbf{W}(k),\mathbf{a}}) \leqslant \sqrt{\frac{2\mathbf{y}^{\mathrm{T}} (\mathbf{H}^{\infty})^{-1} \mathbf{y}}{n}} + O\left(\sqrt{\frac{\log \frac{n}{\lambda_0 \delta}}{n}}\right),$$

where the first term $\sqrt{\frac{2\mathbf{y}^{\mathrm{T}} (\mathbf{H}^{\infty})^{-1} \mathbf{y}}{n}}$ can be viewed as a complexity measure of data that one can use to predict the test accuracy of the learned neural network. This result gives an illustrative example on how to use the

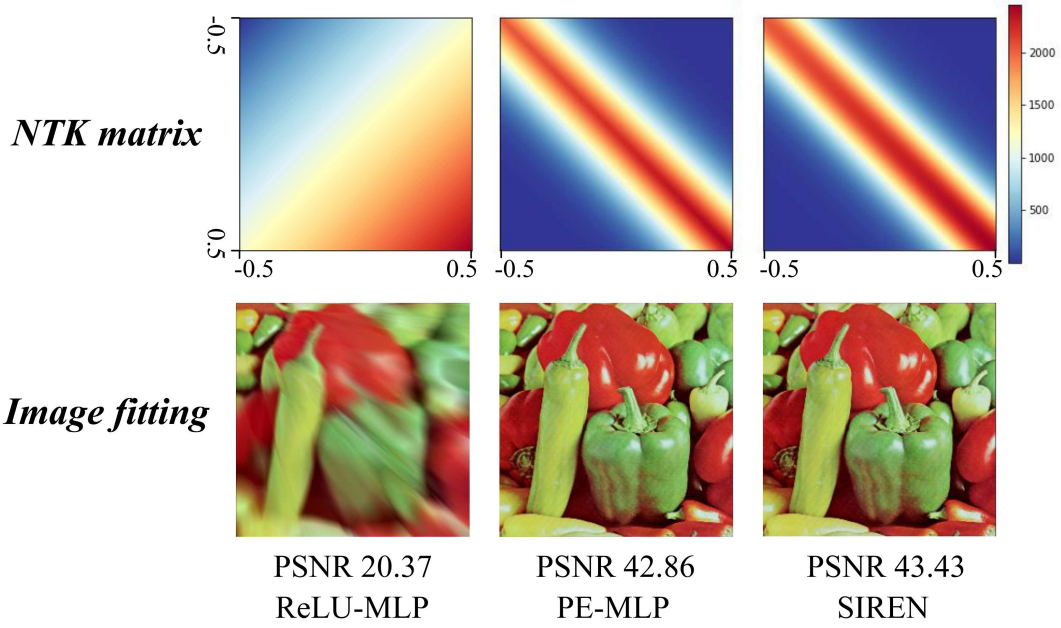

Figure 6 (Color online) Neural tangent kernel diagrams of several neural networks: ReLU-activated MLP, positional encoding MLP (PE-MLP) [20], and SIREN [16]. The INR methods PE-MLP and SIREN shift the NTK matrix from non-diagonal to diagonal, thus enabling more accurate continuous representations of an image.

generalization theory of traditional kernel methods to analyze the generalization behavior of sufficiently wide neural networks, bringing new theoretical tools for neural nets. Indeed, enhancing the generalization capabilities of INRs for unseen coordinates remains a crucial research objective [92]. Rigorous theoretical analysis of generalization error bounds for INR methods is warranted, as it would facilitate the development of principled approaches with provable generalization guarantees.

Many subsequent studies have provided further analysis of NTK-based frameworks. Arora et al. [54] gave the first exact algorithm for computing the NTK of a convolutional neural network, and proposed a non-asymptotic proof that a wide neural network is equivalent to the NTK regression. They also proposed an efficient GPU implementation of this algorithm, and reported a state-of-the-art performance using a pure kernel-based method for image classification. While conventional NTK analysis does not work when there is a standard ℓ_2-norm regularizer (known as weight decay), Wei et al. [119] showed that regularized neural nets have better generalization abilities than the corresponding NTK without regularizer, and developed the convergence of ℓ_2-norm regularized neural nets. Specifically, they proved that for infinite-width two-layer neural nets, gradient descent optimizes the regularized neural net loss to a global minimum. Chen et al. [120] proposed a function-space regularization for training neural nets instead of the conventional ℓ_2-norm regularizer. This method approximates the norm of neural network functions by the RKHS norm under the NTK and uses it as a function-space regularizer. The authors proved that neural networks trained using this regularizer are arbitrarily close to kernel ridge regression solutions under the NTK. Furthermore, they provided a generalization error bound under the RKHS norm regularizer and empirically demonstrated improved generalization on downstream tasks.

While conventional NTK analysis deals with gradient descent with full-batch settings (noise-less setting), understanding the training dynamic of neural nets under stochastic optimization is of crucial importance. Chen et al. [136] proposed a more generalized NTK analysis of two-layer neural net, which considers the setting with noisy gradient descent (e.g., mini-batch) and weight decay, and such a generalized setting also exhibits a "kernel-like" behavior, implying that the training loss converges linearly. This is a more practical optimization setting since full-batch gradient descent is usually computationally heavy in practice. Accelerating the convergence of deep neural nets via preconditioning is also a widely studied topic. For instance, Geifman et al. [121] proposed a family of modified spectrum kernels (MSK's) and introduced the MSK's-based preconditioned gradient descent by altering eigenvalues of NTK for accelerating the convergence of wide neural networks, which gets rid of the dependency of convergence speed on NTK. Shi et al. [137] proposed an inductive gradient adjustment method based on the eigenvalues of the empirical NTK to address the spectral bias of INR. Recently, Chng et al. [138] proposed a stochastic training scheme for INRs by using the curvature-aware diagonal preconditioners for second-order optimization methods, which are especially useful for non-traditional activation-based INR training such as SIREN [16] and WIRE [30].

As relative theoretical frameworks, Alkhouri et al. [32] summarized the theories and algorithms of using untrained DNNs (for instance, untrained neural networks including INRs and deep image priors [139]) for data reconstruction, which establishes NTK dynamics analysis and reconstruction error estimations for such an untrained paradigm. This work connects the broad category of untrained neural net methods with theoretical frameworks of NTK to explain the underlying effectiveness of these unsupervised methods. Recently, Audia et al. [56] demonstrated that grid encoding continuous representations (such as InstantNGP [51]) recovers fine details better than conventional INRs from the NTK eigenvalue perspective. Specifically, they showed that the smallest eigenvalue of the NTK matrix induced by InstantNGP is greater than that of an MLP, and the expressiveness mainly comes from the additional learnable grid parameters, which uncovers the theoretical insights about the stronger representation abilities of grid encoding continuous representation methods.

The NTK provides a powerful framework for analyzing the properties and theoretical advantages of continuous representation models, such as INRs. By leveraging NTK theory, researchers can examine key characteristics of INRs, including analyzing the shift-invariant property of the NTK (a desired property for continuous representation) when passing the input coordinates through a Fourier mapping [20], the bandwidth of NTK and its corresponding parameter configurations/initialization schemes of INR [72], and the desired eigenvalue distribution of NTK for faster convergence of INR [42]. One can utilize the NTK framework for a wider range of analysis involving non-conventional neural structures, such as the theoretical insights of PDE-constrained neural solvers [19] and NO learning [114]. Utilizing the NTK analysis tool to advance fundamental theoretical understanding for various applications such as FWI [108] and computational biology [64] are also promising interdisciplinary research directions in future work.

3.3 Implicit regularization

Implicit regularization [57, 122] refers to the theoretical analysis that characterizes the implicit bias or structure constraint of an optimization algorithm over a parameterization model (e.g., neural networks), even without explicit regularization or constrained conditions. These theoretical analyses, in part, explain the good generalization ability of deep neural networks even with over-parameterization. In particular, continuous representations (e.g., INRs [16, 20]) are representative instances that, even with over-parameterization, could still learn relatively robust and generalizable features (e.g., to unseen coordinates) from limited training data, which can be understood from the implicit regularization perspective of training dynamics.

Gunasekar et al. [140] firstly developed the implicit regularization of gradient descent over the matrix factorization of the form $\mathbf{X} = \mathbf{U}\mathbf{U}^{\mathrm{T}} \in \mathbb{R}^{n\times n}$ where $\mathbf{U} \in \mathbb{R}^{n\times d}$ is an over-parameterized matrix factor (i.e., $n = d$). They showed that with small enough step sizes and initialization close enough to the origin, gradient descent on such a full-dimensional matrix factorization converges to the minimum nuclear norm solution. Consequently, Arora et al. [57] studied the implicit regularization of gradient flow over a deep matrix factorization of the form $\mathbf{X} = \mathbf{W}_N\mathbf{W}_{N-1}\cdots\mathbf{W}_1$, where $\mathbf{W}_n$ are over-parameterized matrix factors. The main result in [57] states that gradient descent over the following matrix sensing minimization problem

$$\min_{\mathbf{W}_1,\ldots,\mathbf{W}_N} \phi(\mathbf{W}_1(t),\ldots,\mathbf{W}_N(t)) := \frac{1}{2}\sum_{i=1}^{m}(y_i - \langle \mathbf{A}_i, \mathbf{W}_N\mathbf{W}_{N-1}\cdots\mathbf{W}_1\rangle)^2 \tag{13}$$

converges to the minimal nuclear norm solution, a conjecture similar to that of [140].

Theorem 8 (Implicit regularization of deep matrix factorization [57]). Let $\mathbf{W}_{\mathrm{deep},\infty}(\alpha) := \lim_{t\to\infty}\mathbf{W}_N(t)\mathbf{W}_{N-1}(t)\cdots\mathbf{W}_1(t)$ where $\mathbf{W}_j(0) = \alpha I$ and $\mathbf{W}_j(t) = -\frac{\partial\phi}{\partial\mathbf{W}_j}(\mathbf{W}_1(t),\ldots,\mathbf{W}_N(t))$ for $t \in \mathbb{R}_{\geqslant 0}$. Suppose $N \geqslant 3$, and that the matrices $\mathbf{A}_1,\ldots,\mathbf{A}_m$ commute. Then, if $\bar{\mathbf{W}}_{\mathrm{deep}} := \lim_{\alpha\to 0}\mathbf{W}_{\mathrm{deep},\infty}(\alpha)$ exists and is a global optimum for (13) with zero loss, then $\bar{\mathbf{W}}_{\mathrm{deep}}$ is a global optimum with minimal nuclear norm.

The tendency of gradient-based optimization over deep matrix factorization towards a low nuclear norm solution sheds light on the generalization mystery of deep neural networks, i.e., a low "complexity" model would generalize better by such implicit regularization of gradient descent. To further distinguish the influence of depth N on the implicit regularization, the authors [57] proposed a dynamical analysis of gradient flow with infinitesimally small learning rate on deep matrix factorizations. They showed that the evolution of singular values of the recovered matrix X is essentially related to the depth N. Specifically, the derivative of the r-th singular value σ_r of the recovered matrix with respect to training time t is formulated by

$$\dot{\sigma}_r(t) = -N\cdot\left(\sigma_r^2(t)\right)^{1-1/N}\cdot\left\langle\nabla\ell(\mathbf{W}(t)), \mathbf{u}_r(t)\mathbf{v}_r^{\mathrm{T}}(t)\right\rangle,$$

where N is the depth, $\nabla\ell(\mathbf{W}(t))$ is the gradient of the loss function, and $\mathbf{u}_r(t), \mathbf{v}_r(t)$ are singular vectors of the recovered matrix at time t. This gives the evolution dynamic of the singular value with respect to time t. We can

see that the dynamic enhances the movement of large singular values, and on the other hand attenuates that of small ones, ultimately leading to a low-rank solution. Moreover, the evolution of singular values depends on the depth N, and the attenuation of singular values becomes more significant as N grows. This theoretically reflects the influence of depth on the convergence rate towards the low nuclear norm solution. It could be noted that the INR [20, 51] can be seen as a special case of the deep matrix factorization with input layer $\mathbf{W}_1$ being coordinate embedding and without nonlinear activation. Further studying the implicit regularization of gradient optimization over INRs is an important theoretical direction towards understanding its effectiveness. The work proposed in [141] studies the landscape analysis for discrete gradient dynamics to explain the implicit regularization underlying deep low-rank matrix factorization. The authors [141] proved that the rank-R deep matrix factorization will converge to a second-order critical point after R stages of saddle point escaping, providing a new theory to analyze implicit regularization in deep learning. For more related studies of the gradient dynamics and implicit regularization, we refer readers to [142–144] and the references therein.

Subsequently, Razin et al. [122] studied the implicit regularization in hierarchical tensor factorization, a model similar to a certain deep convolutional neural network. Through dynamical analysis, they established implicit regularization of the model towards low hierarchical tensor rank, hence translating to an implicit regularization towards locality (i.e., low separation rank) for the associated convolutional network. Here, the separation rank of a function f with respect to an index set I is defined as the smallest number R such that the function can be separated into

$$f\left(\mathbf{x}^{(1)},\ldots,\mathbf{x}^{(N)}\right)=\sum_{r=1}^{R} g_r\left[\left(\mathbf{x}^{(i)}\right)_{i\in I}\right]\cdot \bar{g}_r\left[\left(\mathbf{x}^{(j)}\right)_{j\in[N]\setminus I}\right]$$

with some separated functions $g_r, \bar{g}_r$. The lower the separation rank, the stronger the local (short-range) dependencies between different input regions $\mathbf{x}^{(i)}$ and $\mathbf{x}^{(j)}$. Hence, to counter the locality implicit regularization and enhance the long-range dependency evacuation of the deep network, the authors [122] designed an explicit regularization that discourages locality (i.e., discourages low separation rank), and demonstrated its effectiveness to improve the long-range dependency characterization of a convolutional network for image classification performance.

Similar implicit regularization analyses in deep tensor factorizations are conducted in [33, 123]. Hariz et al. [33] studied implicit regularization in deep tensor CP factorization in the form of

$$\mathcal{W}=\sum_{r=1}^{R}\bigotimes_{n=1}^{N}\prod_{i=1}^{k_n}\mathbf{A}_i^{n,r}\mathbf{w}_r^n,$$

where $\bigotimes$ denotes the outer product and $\mathbf{A}_i^{n,r}, \mathbf{w}_r^n$ are factors of the deep tensor CP factorization, with k_n indicating the depth. They established the training dynamic of the vector component $\bigotimes_{n=1}^{N}\mathbf{w}_r^n(t)$ with respect to the training time t using an infinitely small learning rate of gradient descent, which writes

$$\frac{d}{dt}\left\|\bigotimes_{n=1}^{N}\mathbf{w}_r^n(t)\right\|=N\delta_r(t)\left\|\bigotimes_{n=1}^{N}\mathbf{w}_r^n(t)\right\|^{2-\frac{2}{N}+\frac{k_1+\cdots+k_N}{N}},$$

where $\delta_r(t)$ can be expressed independent of depth. This shows that the evolution rates of the CP component $\bigotimes_{n=1}^{N}\mathbf{w}_r^n(t)$ are proportional to $\left\|\bigotimes_{n=1}^{N}\mathbf{w}_r^n(t)\right\|^{2-\frac{2}{N}+\frac{k_1+\cdots+k_N}{N}}$. This evolution rate is polynomially related to the depth k_n, i.e., when the depth increases, the evolution becomes faster. Since the CP blocks with larger norms decay faster according to the evolution rate, these facts ultimately lead to a low-CP-rank solution, even without explicit low-rank constraints. The implicit low-tensor-rank regularization could yield more accurate estimations and better convergence properties for deep tensor factorizations. Similarly, their later work [123] studied the implicit regularization in deep tensor Tucker factorization, which shows that deep Tucker factorization trained by gradient descent induces a structured sparse regularization, leading to the solution with low-multilinear-rank. The deep Tucker factorization here is tightly connected to a certain deep neural network. These results could draw inspiration for depicting the implicit regularization of a class of functional tensor decomposition methods based on INR [2, 75, 129], since these methods can be exactly formulated as deep tensor factorization models parameterized by deep neural networks, with the input layers being coordinate embedding.

Recently, Bai et al. [145] studied the influence of the connectivity of the graph induced by the observed matrix on the implicit regularization. They showed that disconnected observations lead to low nuclear norm regularization while connected ones lead to low-rank solutions, supported by training dynamic analysis. Except for standard

gradient descent, many studies have developed implicit bias analysis for other popular optimizers in deep learning. For instance, Xie and Li [124] studied the implicit bias of the widely utilized AdamW optimizer, and showed that, under full-batch training, it implicitly performs constrained optimization in terms of ℓ_∞-norm conditioned on the weight decay factor. Future research can combine advanced optimizers with deep matrix/tensor factorizations, and consider more stochastic optimization (such as stochastic gradient descent) to deepen the insights into implicit regularization induced by different models and algorithms, which would be beneficial for explaining some specific deep models, such as continuous representation using INRs.

The implicit regularization encoded in deep models and optimization algorithms can explain the good generalization ability of INRs for unseen coordinates and across different images, such as the generalization of the arbitrary-scale image restoration model [11]. However, most current implicit regularization results rely on pure linear combination, and how to extend the results to scenarios with nonlinearity remains challenging. Moreover, deriving the theoretical implicit regularization of more complex models such as neural TV-induced optimization dynamics [18], differential equations represented by neural nets [19], and NO learning [146] are open areas.

4 Practical applications of continuous representations

This section conducts a systematic review of representative practical applications of continuous representation methods. To provide a coherent overview, we categorize these applications into four major paradigms based on the domain and the nature of the reconstruction problem. (i) Computer vision and graphics, focusing on reconstructing and synthesizing visual data such as images and 3D scenes. Representative fields include scene & shape representation, applications in robotics, and image & video restoration (i.e., low-level vision). (ii) Scientific computing, where continuous representations are leveraged to resolve PDE approximation governed by physical laws. Representative methods include PINN and NO. (iii) Medical imaging and bioinformatics, which leverages the resolution independence and smoothness of continuous representations for biological data analysis, including medical image, computational microscopy, and bioinformatics. (iv) Geosciences and remote sensing, which deal with high-dimensional spatial and temporal geoscience data, including HSI and seismic data analysis. An overview of some representative application studies using continuous representation methods is synthesized in Table 7 [5, 11, 14, 15, 25, 28, 34, 35, 37, 61, 64, 65, 67, 108, 110, 111, 146–153].

4.1 Computer vision and graphics

Utilizing continuous representation models (particularly INRs) for computer vision problems and applications in graphics has attracted extensive attention in recent years due to the continuous and differentiable nature of INRs, which make them especially suitable for representing continuous, resolution-independent, and irregular signals in vision and graphics. The classical INR methods [16,20] were applied to represent images, videos, and surfaces under a unified continuous representation framework, showing strong capability for capturing fine details of visual signals by compressing them into neural representations. Here, we introduce some representative applications of continuous representation in related fields.

4.1.1 *Scene and shape representation*

Around 2020, there were many pioneer studies that developed implicit and continuous methods for 3D scene representation. For instance, Park et al. [61] proposed the first SDF-based implicit representation for shape representation (termed DeepSDF). It utilizes an INR to encode the SDF of a shape, where the SDF is a continuous function that, for a given spatial point in $\mathbb{R}^3$, outputs the point's distance to the closest surface, whose sign encodes whether the point is inside (negative) or outside (positive) of the surface. The underlying shape is implicitly represented by the surface of SDF$=0$. Sitzmann et al. [106] proposed a continuous and 3D structure-aware scene representation that encodes both geometry and appearance by representing 3D scenes as continuous functions that map world coordinates to a feature representation of local scene properties. Jiang et al. [154] proposed local implicit grid representations for 3D scenes, which reconstruct 3D scenes from point clouds via optimization of the latent grid of an implicit network. Mescheder et al. [155] proposed the occupancy network, which implicitly represents the 3D surface as the continuous decision boundary of a deep neural network classifier, allowing to extract 3D meshes at any resolution. Yariv et al. [156] proposed to model the volume density of 3D scenes as a function of the geometry represented by SDF, which produces high-quality geometry reconstructions. Niemeyer et al. [157] proposed the differentiable rendering formulation for implicit shape representations, which learns implicit shape and texture representations directly from RGB images by leveraging the analytic expression of the gradients of depth with

Table 7 Review of some representative applications of continuous representation methods.

Category	Application	Description	Year	Ref.
Vision and graphics	(DeepSDF) Shape representation	Learn SDF of shapes by continuous neural representation that implicitly encodes the boundary.	2019	[61]
	(NeRF) Neural radiance fields	Represent scenes for view synthesis using continuous 5D INR and volume rendering.	2020	[15]
	(LIIF) Arbitrary-scale image super-resolution	Introduce the LIIF using INR for image super-resolution with arbitrary upsampling scales.	2021	[11]
	(PCU) Point cloud upsampling	Self-supervised and arbitrary-scale PCU by seeking nearest projection points on the implicit surface of seed points.	2023	[147]
	Cross-scale image deblurring	Introduce self-supervised method for cross-scale blind image deblurring using INR to represent image and kernel.	2024	[148]
Scientific computing	(DeepONet) Deep operator network	Learning nonlinear operators using two deep neural nets to respectively take input functions and coordinates.	2021	[146]
	(FNO) Fourier NO	Parameterize the function integral kernel in the Fourier space for expressive operator learning.	2021	[37]
	Physical simulation using grid encoding	Utilize InstantNGP for neural physical simulation with a numerical gradient method and fast boundary sampling.	2024	[110]
	InstantNGP for PINN	Use InstantNGP for physics-informed neural nets with finite -difference calculations of derivatives to address discontinuity.	2024	[111]
	Tensor decomposed PINN	Employ CP, Tensor-Train, and Tucker decompositions in PINN for efficient learning of multivariate functions.	2025	[35]
	(D-FNO) Decomposed FNO	Improve the efficiency of FNO ($O(N^3 \log N)$ to $O(NP \log N)$) by tensor decomposition and separability of Fourier transform.	2025	[149]
Medical imaging and bioinformatics	(IREM) INR for MRI Reconstruction	High-resolution 3D MRI reconstruction with arbitrary up-sampling rate using INR.	2021	[150]
	(ArSSR) MRI arbitrary-scale super-resolution	Arbitrary-scale super-resolution for 3D MRI using 3D CNN and local LIIF.	2023	[151]
	Survey of INR for medical imaging	Deliver a comprehensive survey of INR for medical imaging analysis and reconstruction.	2023	[5]
	INR for image registration	Medical image registration using generalized INR with latent modulations obtained by a CNN encoder.	2024	[152]
	(Moner) Undersampled MRI reconstruction	Reconstruct MRI and motion parameters from undersampled measurements using INR and Fourier-slice theorem.	2025	[28]
	(STINR) INR for spatial transcriptomics	Decipher multi-slice ST data using INR and single-cell references.	2025	[64]
	(GASTON) Spatial gene expressions	Analyze spatial gene expressions through spatial gradients and isodepth learned by INR.	2025	[14]
Geosciences and remote sensing	HSI super-resolution using INR	Single HSI super-resolution using INR and a content-aware hypernetwork that produces the weights of INR.	2023	[65]
	(IFWI) Full waveform inversion	Use INR to parameterize the velocity model for full-waveform inversion (FWI) with improved convergence.	2023	[108]
	(SINR) Spectral reconstruction using INR	Continuous spectral amplification process using INR for snapshot spectral imaging with arbitrary recovered spectral bands.	2024	[153]
	Arbitrary-scale HSI super-resolution	Utilize LIIF for HSI arbitrary-scale super-resolution by leveraging and fusing RGB spatial priors.	2024	[34]
	Hyperspectral unmixing	Nonnegative matrix functional factorization parameterized by INRs for hyperspectral unmixing.	2024	[67]
	(NeRSI) Seismic data interpolation	Utilize INR to encode continuous seismic 5D wavefield to infer missing trace amplitudes (interpolation).	2025	[25]

respect to the implicit network parameters. In terms of shape representation, Genova et al. [158] proposed to use structured implicit functions for learning template 3D shapes, and the learned shape templates support downstream applications such as shape exploration, correspondence, and interpolation. Chen and Zhang [159] proposed to use implicit fields for learning generative models of shapes, where an implicit field decoder was developed for improving the visual quality of the generated shapes. Chibane et al. [160] proposed the implicit feature networks for 3D shape reconstruction and completion from 3D inputs (such as sparse voxel), which outputs continuous shapes from implicit functions. Recently, Schirmer et al. [7] presented a comprehensive survey on geometric INR methods for signed distance functions in scene representation.

Continuous representations have been widely utilized in scene representation. In 2018, Eslami et al. [161] introduced the generative query network, which takes images of a scene from different viewpoints as inputs, constructs an internal representation, and uses this representation to predict the appearance of that scene from unobserved viewpoints, paving a pioneer and fundamental way to autonomously make machines understand the world around them. Another famous scene representation model is the NeRF [15]. The NeRF represents a scene using an implicit network, which maps a single continuous 5D coordinate (spatial location (x, y, z) and viewing direction (θ, ϕ)) to the corresponding volume density and view-dependent color. Then the classic volume rendering technique is used to project the output colors and densities into an image to synthesize novel views. The following studies such as InstantNGP [51], PlenOctrees [107], and Plenoxels [73] methods based on grid parametric encoding are more powerful continuous representation methods for scene representation of novel view synthesis based on NeRF. Chen et al. [38] proposed tensorial radiance fields, which decompose NeRF under the tensor block term decomposition to enable faster convergence without neural networks. Tang et al. [162] proposed compressible and composable NeRF via rank residual decomposition. It learns a tensor decomposition model of NeRF, uses a rank-residual learning strategy to encourage the preservation of primary information in lower ranks, and gradually encodes fine details in higher ranks, allowing composition of scenes by concatenating along the rank dimension. Fridovich-Keil et al. [163] proposed the K-planes representation, which represents a d-dimensional scene using C_d^2 2D planes with multi-resolution grids and interpolation. The K-planes induce a natural decomposition of static and dynamic components, achieving state-of-the-art reconstruction fidelity with low memory usage for scene representation. For a detailed and comprehensive survey of NeRF-based methods, please refer to [62].

Recently, 3DGS has emerged as a popular framework for continuous scene representation. Introduced by Kerbl et al. [45] in 2023, this method models radiance fields with a collection of continuous 3D Gaussian basis functions, each parameterized by learnable mean, covariance, color, and opacity. Compared to NeRF, 3DGS offers significant advantages in training efficiency and robust geometry reconstruction, enabling real-time rendering. Following this pioneer work, Wu et al. [164] proposed the 4D Gaussian splatting, a novel explicit representation containing both 3D Gaussians and 4D neural voxels for representing and rendering dynamic scenes. Huang et al. [165] proposed the 2D Gaussian splatting for radiance field reconstruction, which utilizes 2D oriented Gaussian disks instead of 3D Gaussians, thereby providing view-consistent geometry while modeling surfaces intrinsically. Zhang et al. [166] introduced 2D Gaussians and a novel rendering algorithm based on accumulated summation to represent images under the INR framework, which achieves faster rendering and representation performance. Moreover, Zhang et al. [167] proposed the wavelet-based visual primitives and a wavelet-based differentiable rasterizer. This method utilizes wavelet basis functions to represent the continuous fields, demonstrating improved accuracy and efficiency for image and scene representations over Gaussian-based representations. 3DGS has also enabled a variety of applications beyond vision and graphics. For instance, inspired by 3DGS, Kang et al. [112] proposed the physics-informed Gaussians for PDE solutions, which utilize learnable Gaussian feature embeddings and a lightweight neural network to model the physical field. Xu et al. [168] proposed the 3D Gaussian adaptive tomography for Fourier light-field microscopy, which improves the volumetric reconstruction quality while maintaining computational efficiency. Recently, Wu et al. [169] provided a comprehensive survey of recent advances in 3DGS and their applications in 3D reconstruction, 3D editing, and other downstream applications. For a detailed introduction to recent 3DGS methods, we refer readers to this comprehensive review [169] for more information.

4.1.2 *Applications in robotics*

In addition, continuous representation methods proposed in vision and graphics, such as SDF and NeRF, have been widely utilized in the field of robotics. For instance, Ortiz et al. [170] proposed a continual learning system for real-time SDF reconstruction for robot perception, which produces more accurate reconstructions and better approximations of collision costs and gradients useful for downstream applications such as navigation to manipulation. Simeonov et al. [171] proposed the neural descriptor fields (NDFs), which are continuous functions that map 3D spatial coordinates to spatial descriptors, where the descriptors encode the spatial relationship of coordinates

to the salient geometric features of the object. Such an object representation of NDF encodes both points and relative poses between an object and a target via category-level descriptors for object manipulation without relying on expert-labeled keypoints. Li et al. [172] introduced a method that uses deep neural networks to map a video stream of a robot to its visuomotor Jacobian field, enabling the control of robots from only a single camera. In this method, a neural radiance field maps a 3D coordinate to its density and radiance, which serves as a representation of the geometry of the robot. They demonstrated the method on various robot manipulators that vary in actuation, materials, fabrication, and cost [172]. Suresh et al. [173] proposed the NeuralFeels, which encodes object geometry by learning a continuous neural field online and jointly tracks it by optimizing a pose graph problem. The learned neural representation driven by multi-modal sensing can serve as a backbone for advancing robot dexterity. Several survey papers on continuous representations in robotics exist in the literature. Irshad et al. [47] provided a thorough review of neural fields in robotics, including the discussions of several neural fields such as occupancy networks, SDF, NeRF, and Gaussian splatting, and their application in major robotics domains such as pose estimation, manipulation, navigation, physics, and autonomous driving. Ming et al. [174] presented a thorough analysis of how NeRF can be used to enhance the capabilities of autonomous robots, with a focus on perception, localization and navigation, and decision-making modules of autonomous robots. Zhu et al. [175] provided a comprehensive review of 3DGS in the field of robotics, and explored how 3DGS has been utilized in various robotics tasks from scene understanding and interaction perspectives. For more details on the applications of continuous representation methodologies in robotics, we refer readers to these comprehensive reviews [47, 174, 175].

4.1.3 *Low-level vision*

Several studies have explored the application of INR for image restoration tasks in low-level vision. Chen et al. [11] proposed the LIIF for continuous image representation, and applied this representation to arbitrary-scale image super-resolution. The LIIF uses an encoder to obtain high-resolution features and feeds the features with image coordinates into an INR to generate the high-resolution image, enabling resolution-independent representation of an image. Recently, Liu and Tang [41] introduced DiffFNO, a model that integrates the FNO with a diffusion framework for arbitrary-scale image super-resolution. This application of operator learning [37] to image super-resolution illustrates the growing interplay between methodologies from scientific computing and those in the computer vision community. Chen et al. [176] proposed a multi-scale INR network for image deraining, which takes advantage of the continuous representation to construct multi-scale collaborative representations of an image. Nam et al. [177] proposed neural image representations for multi-image fusion and layer separation, which estimate the homography, optical flow, and occlusion scene motions to effectively combine multiple input images into a single canonical view using coordinate-based neural representations. Cheng et al. [13] proposed INRs with imaging geometry for synthetic aperture radar (SAR) target recognition. The target recognition problem can be seen as a view synthesis pipeline that predicts the density and intensity from the input views to render novel views. Zhang et al. [148] applied the INR for cross-scale self-supervised image deblurring with unknown blur kernel, which represents the image and kernel with INRs to encode resolution-free property for image deblurring. Hu et al. [178] proposed an INR-based continuous heatmap regression method for human pose estimation. It can output the predicted heatmaps at arbitrary resolution during inference, which easily achieves sub-pixel localization precision. Yang et al. [179] proposed to use INR for cooperative low-light image enhancement, which unifies the diverse degradation factors of real-world low-light images using an INR normalization pipeline, thus enhancing robustness. Recently, Zhao et al. [147] proposed to use implicit surfaces for arbitrary-scale point cloud upsampling, which seeks the nearest projection points on the implicit surface of seed points to sample dense point clouds at arbitrary-scales.

There is a group of studies that leverage implicit representations for videos in the continuous spatial-temporal domain. For instance, Chen et al. [26] applied the INR for continuous space-time super-resolution of videos by estimating motion flow fields between frames. Chen et al. [180] proposed the neural representations for videos (NeRV), which represent videos as neural networks taking frame index as input and outputting the corresponding RGB image. The NeRV achieves efficient video compression by neural networks. Li et al. [181] proposed the expedited NeRV by decomposing the image-wise INR into separate spatial and temporal contexts, which are fused by convolution stages. It achieves significantly faster speed on convergence as compared with vanilla NeRV for implicit video representations. Similarly, Yan et al. [182] proposed the implicit NeRV with decomposed static and dynamic codes for video representation, which efficiently utilizes redundant static information while maintaining high-frequency details.

There are also several studies that generalize INRs to graph-structured data on non-Euclidean spaces. For instance, Grattarola and Vandergheynst [183] proposed the generalised INR for discrete graph representation on non-Euclidean domains. It utilizes the eigenvectors of the graph Laplacian matrix as the spectral embedding of

INRs, which allows the training of INRs without knowing the underlying continuous domain, a scenario for most real-world graph signals. Xia et al. [184] proposed the implicit graphon neural representation, which parameterizes the adjacency matrix of graphs by INRs and enables efficient and flexible generation of arbitrarily sized graphs.

Representing and reconstructing vision and graphics signals using continuous representation (such as coordinate networks and spherical harmonics on voxel) has led to a group of increasingly popular research fields (NeRF [15], LIIF [11], SDF [61], etc). It is foreseen that there will continue to be a large number of advancing methods developed for continuous signal representation in vision and graphics. For a comprehensive review of related fields, we refer readers to [7, 62].

4.2 Scientific computing

Resolving scientific computing problems in numerical mathematics using continuous representations, particularly numerical PDE solutions, has attracted significant interest in recent years with the emerging of many physics-informed continuous representation methods [185]. Resolving a numerical PDE can be viewed as a data reconstruction paradigm that recovers continuous physical fields from interpretable physical rules or limited observations. We mainly focus on the PINN and NO learning frameworks.

4.2.1 *Physics-informed neural network*

The PINN is a class of continuous representation models designed to solve forward and inverse problems involving PDEs by integrating physical laws. The PINN was introduced by Raissi et al. [186] in 2019, which leverages neural networks to approximate solutions of PDEs. Let a PDE be defined as

$$\mathcal{N}[u(\mathbf{x},t)]=0,\ \mathbf{x}\in\Omega,\ t\in[0,T]$$

with boundary conditions $\mathcal{B}[u(\mathbf{x},t)]=0,\ \mathbf{x}\in\partial\Omega$, where $\mathcal{N}$ is a differential operator, u is the unknown solution, and Ω is the spatial domain. A PINN approximates $u(\mathbf{x},t)$ using a neural network $\hat{u}_\theta(\mathbf{x},t)$, parameterized by learnable weights θ. The network is trained to minimize a composite differential loss function containing several terms $\mathcal{L}(\theta)=\mathcal{L}_{\text{data}}+\lambda_1\mathcal{L}_{\text{PDE}}+\lambda_2\mathcal{L}_{\text{BC}}$, where the data fidelity loss (if labeled data exists) encodes the knowledge of observed data $\mathcal{L}_{\text{data}}=\sum_i|\hat{u}_\theta(\mathbf{x}_i,t_i)-u(\mathbf{x}_i,t_i)|^2$, the PDE loss encodes the physical law $\mathcal{L}_{\text{PDE}}=\sum_j|\mathcal{N}[\hat{u}_\theta(\mathbf{x}_j,t_j)]|^2$, followed by the boundary condition loss $\mathcal{L}_{\text{BC}}=\sum_k|\mathcal{B}[\hat{u}_\theta(\mathbf{x}_k,t_k)]|^2$. The differential loss functions related to $\mathcal{N}[\hat{u}_\theta]$ and $\mathcal{B}[\hat{u}_\theta]$ are computed using automatic differentiation of neural networks, enabling exact gradient calculations without discretization errors. PINNs have been successfully applied to several scientific fields, including fluid dynamics, material modeling, biomedical systems, and climate science. By unifying data and physical laws, PINNs hold the power of physics-guided machine learning in computational science. Notably, the PINN can be seen as an INR [16, 20] operating on a physically interpretable continuous field, with tailored differential loss functions to model these physical fields. The development of PINNs is a broader topic coupling machine learning and numerical mathematics. For comprehensive discussions and reviews of the PINN framework and related methods, we refer readers to [60, 185, 187].

A growing body of recent research has investigated the application of grid encoding parametric models [51] for PINNs by leveraging the multi-resolution grid structures to effectively represent fine details in physical fields. Kang et al. [188] proposed the physics-informed cell representations, which utilize multi-resolution grid encoding [51] with a cosine interpolation kernel for PINNs. Jin et al. [189] proposed the hash grid encoding methods (based on InstantNGP) for PINN using differentiable cubic interpolation, which are combined directly with auto-differentiation of neural nets. Wang et al. [110] proposed the neural physical simulation with multi-resolution hash grid encoding, and used a numerical gradient method for computing high-order derivatives with boundary conditions and a range analysis sample method for fast neural geometry boundary. Huang and Alkhalifah [111] proposed the efficient PINN using hash encoding, which replaces the automatic differentiation with finite-difference calculations of the derivatives to address discontinuity. They also shared the appropriate ranges of hash encoding hyperparameters to obtain robust derivatives. Recently, Kang et al. [112] proposed the physics-informed Gaussians for PDE solutions, which utilize Gaussian mixture models as parametric mesh representations followed by a lightweight neural network, and the derivatives of such a structure can be computed analytically.

4.2.2 *Neural operator*

NO learning [146] serves as a novel architecture designed to learn mappings between infinite-dimensional function spaces, making it particularly suited for solving parametric PDEs. Unlike PINNs, NOs directly operate on functions and thus enjoy generalization abilities by evaluating PDE solutions instantly for new parameter functions. The

advantages of NOs include the fast inference of PDE solutions and the generalization ability between function spaces (see experimental examples in [36, 37]). Let $\mathcal{A}$ and $\mathcal{U}$ be function spaces (e.g., Sobolev spaces). Given observations of input-output function pairs $\{a_j(x), u_j(y)\}_{j=1}^N,\ a_j \in \mathcal{A},\ u_j \in \mathcal{U}$, the goal of NO learning is to learn an operator $\mathcal{G}^\dagger : \mathcal{A} \to \mathcal{U}$ such that $\mathcal{G}^\dagger(a)(y) = u(y)$. For parametric PDEs, $a(x)$ might represent an initial condition or coefficient field, and $u(y)$ the PDE solution. The deep operator network (DeepONet) [146] forms an operator by using a branch net to encode function values and a trunk net to decode locations, which enjoys the universal approximation theorem in function spaces. The DeepONet is formulated as

$$\mathcal{G}(a)(y) = \sum_{k=1}^{p} \underbrace{b_k(a)}_{\text{branch net}} \cdot \underbrace{t_k(y)}_{\text{trunk net}},$$

where b_k encodes the input function, and t_k decodes the output location. Both b_k and t_k could be parameterized by neural nets, and learned through function pairs. The FNO [36,37] maps a function v through the Fourier transform operator and frequency-domain filter. The learnable Fourier operator layer is formulated as

$$\mathcal{K}(a)(y) = \mathcal{F}^{-1}\left[R \cdot \mathcal{F}(a)\right](y),$$

where $\mathcal{F}$ is the Fourier transform operator and R is a learnable frequency-domain filter. Stacking multiple Fourier layers leads to the FNO. As compared with DeepONet, FNO can query both input and output at any positions, and is discretization invariant. The FNO is also grounded with the universal approximation theorem for operators [36]. Liu-Schiaffini et al. [190] proposed the localized integral and differential kernels in FNO to replace the global convolution kernel R, which better capture local features and preserve the resolution-independence. NOs represent a paradigm shift in scientific machine learning, combining numerical analysis with generalizable deep learning to resolve scientific computing problems (especially numerical PDEs) efficiently. For comprehensive discussion and review of NOs, please refer to [191].

Recent studies have explored accelerating techniques and addressing the curse of dimensionality of PINNs and operator learning through tensor decomposition paradigms. Li and Ye [149] proposed the decomposed FNO, which decomposes the high-dimensional latent representation into a series of rank-1 tensor products, and the three-dimensional fast Fourier transform (FFT) is replaced by a series of one-dimensional FFT. This decomposed structure enhances the efficiency for large-scale PDE modeling from $O(N^2 \log N)$ to $O(NP \log N)$, where the separation rank P is much smaller than the grid size N. Cho et al. [129] proposed the separable network architecture for PINNs, which operates on a per-axis basis to significantly reduce the number of network propagations in multi-dimensional PDEs based on tensor decomposition, which shares similarity with tensor functional decomposition methods [2,76]. A similar idea is used in [35], which uses a tensor decomposed structure (e.g., Tucker, CP, and TT) to accelerate numerical PDE based on PINN for internal learning of a multivariate function.

Several studies have investigated operator learning frameworks for generating INR functions. Xu et al. [134] proposed the signal processing paradigm for INR, which maps an INR to another INR by a learned operator parameterized by convolutional neural network. This method inputs the derivatives of an INR into the operator network and generates another INR. It is capable of dealing with several visual problems such as image denoising and classification. Pal et al. [135] proposed the INR via operator learning, which maps input functions (often in the form of Fourier PE functions [20]) to the corresponding signal functions (characterized by conventional INRs that map coordinates to pixels). It achieves theoretical consistency with operator learning and obtains better performances for image regression and robustness in neural weight interpolation.

Efforts to understand the convergence and generalization behaviors of PINN or NO have also been widely explored. For instance, Wang et al. [113] analyzed the training dynamics of PINNs using NTK and proposed a novel NTK-guided gradient descent algorithm for PINN. Bonfanti et al. [19] analyzed the training dynamics of PINN for nonlinear PDEs under the NTK framework. Nguyen and Mücke [114] introduced the NTK regime for two-layer NOs and analyzed their generalization properties. The interplay between PINNs & NOs in scientific computing and the NTK theory from classical neural network analysis underscores promising opportunities for interdisciplinary research. In particular, theoretical tools established in one domain (e.g., NTK in classical neural network analysis) can be leveraged to interpret and inspire the development of efficient algorithms in a different area (e.g., PINNs in scientific computing). Following this direction, further research into the theoretical properties of PINNs and NOs is expected to advance their theoretical foundations and improve algorithmic design. Recently, Dummer et al. [192] proposed to use resolution-independent INR for large deformation diffeomorphic metric mapping (LDDMM) coupled with LDDMM-based statistical latent modeling with applications in computer graphics and the medical domain. This work paves the way for future research into how Riemannian geometry, shape analysis, and continuous learning representations can be combined.

4.3 Medical imaging and bioinformatics

In medical imaging and bioinformatics fields, continuous representation methods (particularly INRs) enable precise and resolution-independent representations of biological data that benefit many downstream tasks [5, 14]. The inherent smoothness of continuous methods preserves interpretable structures in medical scans [193], cellular relationships [64], and tissue organizations [194] in biological specimens. The continuous modeling framework enables natural integration with physical rules, medical imaging processes, and biomedical engineering frameworks for enhanced reconstruction fidelity of diverse types of medical images and biological data.

4.3.1 *Medical imaging*

Image registration is an important computational problem for medical imaging such as MRI and computed tomography (CT) imaging. The image registration aims to establish spatial correspondence between two or more images by applying nonlinear and elastic transformations. There is a group of studies that utilize INRs to address image registration. Wolterink et al. [17] proposed the first INR model for deformable image registration by predicting the transformation between images using an INR. Later, Byra et al. [12] proposed INRs for joint decomposition and registration of gene expression images, which use several implicit networks combined with an image exclusion loss to jointly perform the registration and decompose the image into a support and residual image, where the image decomposition guides the registration to be more accurate. Sideri-Lampretsa et al. [195] proposed a spline-enhanced INR for multi-modal image registration, which parameterizes the continuous deformable transformation represented by an INR using free form deformations, allowing for multi-modal registration while mitigating folding issues. Zimmer et al. [152] proposed the generalized INR for image registration, which encodes the fixed and moving image volumes to latent representations, and uses the latent representations to modulate the INRs to enable generalization across multiple instances.

The medical imaging reconstruction using INRs is another widely studied research direction. For instance, Sun et al. [196] proposed a coordinate-based internal learning paradigm for continuous representation of measurements, with applications in inverse problems of medical imaging. Reed et al. [193] proposed a dynamic CT reconstruction method from limited views with INRs coupled with parametric motion fields. Wu et al. [150] proposed to use INR for high-resolution MRI reconstruction, and further proposed an arbitrary scale super-resolution approach for 3D MRI [151] via 3D convolutional neural networks and INRs. Their recent work [28] proposed an InstantNGP-based model for reconstructing MRI and motion parameters from undersampled measurements. Chu et al. [63] proposed to integrate the prior sampling of a pre-trained diffusion model with INRs for accelerated MRI reconstruction, which incorporates both the diffusion prior and the MRI physical model to ensure high data fidelity. Shen et al. [197] proposed a novel framework named NeuralCMF, which utilizes an INR to model the 3D structure and the comprehensive motion of the heart for continuous 3D myocardial motion tracking, making significant advantages over existing methods in cardiac imaging and motion tracking. Their recent work [198] further proposed the CardiacField, which utilizes the InstantNGP [51]-based INR for reconstructing a 3D cardiac volume from sequential multi-view 2D echocardiography images, enabling accurate and automated heart function estimation.

Advanced model architecture designs were also incorporated into medical imaging processing using INRs. For instance, Vo et al. [199] proposed a sparse-view X-ray CT method by using the regularization-by-denoising (RED) [200, 201] framework to regularize the INR optimization. It enhances the efficiency of INR training for this task by decoupling the post-processing network (RED network) and INR optimization. Similarly, Iskender et al. [202] proposed a continuous neural field to represent the dynamic object with RED, via a learned restoration operator using static supervised training. Yu et al. [203] proposed a bilevel optimization framework for INR, with applications for accelerated MRI reconstruction. This method automatically optimizes the hyperparameters of the INR for a given protocol, enabling a tailored reconstruction without training data. For a comprehensive review of INR methods for medical imaging applications, we refer readers to [5].

4.3.2 *Computational microscopy*

A growing body of studies has successfully applied INRs and neural field representations for the computational microscopy imaging problem, which holds great importance for applications in medical imaging and other scientific fields. For example, Zhu et al. [204] proposed an unsupervised diffractive neural field to reconstruct lensless imaging for microscopic scenes by jointly optimizing the imaging parameter and implicit mapping between spatial coordinates and complex field. Liu et al. [205] proposed the deep continuous refractive index field, which learns a continuous representation of a refractive index volume by using a neural field to map the spatial coordinates to the corresponding complex-valued refractive index values. Zhou et al. [206] proposed a compact framework for represent-

ing and reconstructing Fourier ptychographic microscopy image stacks using INRs, which substantially outperforms traditional Fourier ptychographic microscopy algorithms. Zhang et al. [207] proposed an INR-based single-shot volumetric fluorescence imaging method, which significantly reduces the acquisition time of a conventional fluorescence microscope. Kang et al. [208] applied the INR for joint wavefront estimation and structural information extraction from the input widefield microscopy image stack, which could be applicable to various microscopy modalities. Feng et al. [209] proposed a scanning-free wavefront shaping technique based on INR to reconstruct diffraction-limited images. Cao et al. [210] proposed the neural space-time model via INR to jointly estimate the multi-shot imaging scene and its motion dynamics for computational imaging reconstruction, such as microscopy. Zhou et al. [211] proposed a physics-informed ellipsoidal coordinate encoding INR method for high-resolution volumetric wide-field microscopy, which tackles the challenge of background signal interference and resolution loss in axial scanning image stacks. Zhao et al. [212] introduced a physics-informed neural representation for high-resolution light field microscopy reconstruction, which significantly enhances performance by incorporating an unsupervised and explicit feature representation approach.

4.3.3 *Bioinformatics*

Beyond medical imaging, continuous representation methods have also gained attraction in the field of bioinformatics, demonstrating their applicability across diverse computational biology applications. Zhong et al. [213] proposed the first neural network-based approach for cryo-electron microscopy to determine the structure of proteins under an inverse problem setting. The method leverages coordinate-based deep neural networks with PE to model continuous generative factors of structural heterogeneity within proteins. Another application of continuous models in bioinformatics is the representation of ST data [214]. The ST is a novel technology that enables gene expression profiles within spatial positional context. This approach provides insights into tissue organization and cell-cell interactions in the space, advancing research developments in biology. However, the irregular spatial profile and variability of genes make it challenging to model ST data in a computational framework. There are several recent studies that utilize continuous representation to model the irregular and non-grid structure of ST data. For instance, Song et al. [194] proposed the graph-guided neural tensor decomposition model for reconstructing ST from incomplete measurements, where the model takes the coordinate and gene index as inputs and outputs the corresponding gene expression. The model is regularized by spatial and functional relations-informed graph regularizers. Chitra et al. [14] proposed a coordinate-based neural network to learn a continuous and differentiable function of ST (termed GASTON), which enables gradient and isodepth analysis of ST to accurately identify spatial tissue domains. Li et al. [215] proposed STAGE, a computational framework that generates high-density ST from low-quality measurements by using a spatial coordinate-based generator. This spatial coordinate is generated from the observed ST in an encoder-decoder architecture. Recently, Luo et al. [64] proposed an INR-based ST representation framework (termed STINR), which encodes ST along with single-cell references using an INR. Benefit from the implicit local correlation of INRs, STINR achieves higher accuracy in detecting spatial tissue domains from raw ST data. Zhu et al. [216] introduced SUICA, which models ST in a continuous manner by INRs to improve both the spatial resolution and the gene expression. Overall, continuous representation frameworks, particularly INRs, have emerged as increasingly prominent computational approaches for ST analysis in bioinformatics. It is foreseeable that the continuous representation framework for ST will gain growing attention in future research.

4.4 Geosciences and remote sensing

Continuous function representation methods are increasingly emerging paradigms for geophysical and remote sensing data processing by addressing critical challenges in scenarios including HSI, seismic data analysis, and waveform inversion, by leveraging the inherent advantages of INRs such as parameter efficiency, resolution independence, and seamless integration with physical constraints.

4.4.1 *Hyperspectral imaging*

The HSI community has seen extensive research efforts focusing on leveraging continuous representation and INRs to efficiently encode high-dimensional HSI with hundreds of spectral bands. Zhang et al. [65] proposed to use INR for HSI super-resolution, where a content-aware hypernetwork is employed to produce INR weights for each HSI in a meta-learning manner. Chen et al. [153] proposed a spectral-wise INR method for coded aperture snapshot spectral imaging reconstruction, which can reconstruct an unlimited number of spectral bands. Meng et al. [217] proposed an INR method with progressive high-frequency reconstruction for pan-sharpening by effectively representing and fusing spatial and spectral features in the continuous domain. Chen et al. [34] proposed an arbitrary-scale HSI

super-resolution from a fusion perspective with spatial priors. This method utilizes an RGB encoder trained with high-quality RGB datasets to extract spatial features, and utilizes a spectral transformer for feature fusion, enabling more accurate reconstruction. Liang et al. [218] proposed a Fourier-enhanced INR fusion network for multispectral and hyperspectral image fusion, which utilizes a spatial and frequency implicit fusion function in the Fourier domain to capture high-frequency information and expand the receptive field. Recently, Wang et al. [67] proposed a nonnegative matrix function factorization framework parameterized by INRs for HSI unmixing, which could handle nonuniform spectral sampling due to continuous modeling. Their recent work [115] proposed an hyperspectral and multispectral image fusion method through self-supervised INRs, which could handle observations with arbitrary resolutions.

4.4.2 *Seismic data analysis*

INRs have also been considered in geophysical data processing, such as seismic data. Gao et al. [25] proposed to use INR for 5D seismic data interpolation, which encodes continuous seismic 5D wavefields and infers missing trace amplitudes from their coordinates. Recently, Wang et al. [66] proposed an efficient KAN-empowered neural low-rank representation for seismic denoising, where the model is parameterized by INRs to encode smoothness. The FWI is another important technique in geophysics, which aims to reconstruct the underlying subsurface velocity model from observed seismic data, utilizing various waveforms. Sun et al. [108] proposed the implicit seismic FWI framework by using INR to parameterize the velocity model, and optimize the object

$$\min_{\Theta} \|\mathbf{d}_{\text{obs}} - \mathbf{F}(\mathbf{N}_{\Theta}(\mathbf{x}))\|^2,$$

where $\mathbf{N}_{\Theta}(\mathbf{x})$ is the predicted velocity model parameterized by an INR $\mathbf{N}_{\Theta}$ with input coordinates $\mathbf{x}$, $\mathbf{d}_{\text{obs}}$ is the observed seismic signal, and $\mathbf{F}$ denotes the forward modeling operator for wave propagation. The forward operator $\mathbf{F}$ can be expressed by an acoustic second-order finite difference operator to solve a numerical wave propagation PDE

$$\frac{\partial^2 \mu(x,t)}{\partial t^2} = \mathbf{m}(x)^2 \nabla^2 \mu + f(x,t),$$

where $\mu(x,t)$ is the reconstructed waveform, $\mathbf{m}(x)$ is the velocity model obtained by the INR $\mathbf{N}_{\Theta}(\mathbf{x})$, and $f(x,t)$ is an initial condition. It is shown that the low-frequency preference of INR benefits a more robust and accurate inversion of velocity model under the FWI framework. Their later work [27] applies an INR with GELU activation function to enhance the robustness of implicit FWI with the absence of prior and low-frequency information (such as noisy cases), further enhancing the practical value and robustness of implicit FWI.

The inherent advantages of continuous representations (e.g., parameter efficiency and resolution independence) make them particularly suited for geoscience applications where data acquisition is costly, sparse, or contain noise. These advantages would position continuous methods as transformative tools for important geophysical applications such as multi-parameter inversion, 3D inversion, and uncertainty quantification in Earth system modeling [219] in future developments.

5 Future directions

We have delivered a comprehensive overview of continuous representation methods, theories, and applications. Notably, our analysis reveals substantial cross-pollination interplay between different subareas within the introduced studies. For instance, the interplay between neural representation learning and computational mathematics reveals interdisciplinary parallels, e.g., the arbitrary-scale imaging paradigm [11] shares structural parallels with operator learning frameworks [36, 37] from numerical PDE analysis, as both architectures map low-dimensional positional embeddings (augmented with latent codes/input function responses) to continuous fields through learned operators. Similarly, the tensor factorization paradigms underlying radiance field reconstruction (e.g., TensorRF [38]) demonstrate mathematical similarities with tensor decomposed functional representations [2, 39, 40] developed for high-dimensional data approximation. Classical Fourier basis function approximations [8, 69] are similar to more recent neural representations employing frequency domain feature embeddings [15, 20]. These facts lead to many opportunities to incorporate interdisciplinary research directions, highlighting synergies between machine learning and computational mathematics primitives. Inspired by these intrinsic connections, we propose potential research directions, perspectives, and identify key challenges in developing advanced continuous representation methods and theories for data reconstruction.

5.1 Future directions on continuous representation parametric models

Future research may explore the interdisciplinary integration of diverse parametric models to enhance performance and flexibility of continuous representations. For instance, we can combine statistical modeling techniques with neural representations to better capture periodic and regular patterns in temporal and time-series data. An example was already given in a recent work [21], where the neural representation coupled with statistical modeling shows better performances for tensor recovery. It is promising to incorporate basis function representations into neural frameworks to improve interpretability (e.g., model identifiability), or leverage randomized neural networks [88] under least-squares frameworks to enhance INR efficiency. It would be beneficial to integrate advanced architectures—such as convolutional layers, attention mechanisms, transformers, mamba networks, and MoE models [94]—into neural continuous representations for complex pattern modeling. Integrating continuous representations with generative diffusion priors [63, 220] for more expressive modeling and generation of continuous signals is also an interesting direction.

Though some studies have combined INR with tensor decompositions [2, 77, 129], it would be valuable to further combine INR with more stochastic tensor network decompositions (e.g., TT or tensor-ring), and further learning adaptive tensor network decompositions that automatically determine factor connections through INR's intrinsic knowledge-sharing properties. It is also interesting to explore the integration of tensor decomposition with grid-based parametric models (e.g., InstantNGP [51]) to reduce grid scales and improve computational efficiency. In terms of frequency characterization, we can investigate frequency-aware or frequency-decoupled continuous representation models to enhance multi-frequency modeling abilities for real-world signals.

For image super-resolution, we can develop tensor decomposition-based methodologies to lower the computational complexity of arbitrary-scale super-resolution [11] for large-scale images. It is interesting to further embed physics-informed constraints into INRs and tensor functional networks to learn physically consistent continuous fields while enhancing interpretability. Exploring more in-depth meta-learning strategies to enable the generalization of INRs across datasets, or using continuous representations as meta-learners to enable model generation, are also promising future directions. Furthermore, it would be interesting to investigate model averaging or fusion strategies (e.g., hybridizing Tucker [2] and CP [8] functional models) to adaptively select optimal parametric representations for different samples.

5.2 Future directions on continuous structural modeling methods

Imposing explicit or implicit structural constraints and regularizations for continuous representations are effective for enhancing robustness and interpretability. In future research, we can develop online optimization techniques for continuous models for streaming data analysis [221], with the focus on regularization strategies that can handle irregular data streams, maintain physical consistency of dynamically updated continuous models, and avoid catastrophic forgetting during online optimization.

It is required to generalize existing continuous regularizations to more flexible formulations, such as weighted low-rank factorization models or group sparsity-based continuous regularizations, to boost performances. It is also crucial to extend current continuous regularizations to high-dimensional cases to enhance scalability, such as extending the neural TV [18] to characterize multi-directional local correlations. We can also attempt implementing these continuous regularization methods for various physical models, such as NeRF, SDF fields, and Bayesian statistical frameworks, to enhance structural consistence in real-world applications.

Another potential is to explore continuous neural regularizations for implicit LoRA [105] in large model fine-tuning, where the low-rank weights can be parameterized via continuous representations to enhance the efficiency of fine-tuning large language models. We can further extend the fine-tuning approach to class-incremental continual learning paradigms [222], by employing implicit low-rank function representations to dynamically optimize INR weights for task-adaptive low-rank adapters.

Current tensor function decomposition methods for INRs [2, 75, 129] are inefficient when handling irregular non-grid data. Hence, addressing the efficiency challenges of continuous tensor decomposition methods [2, 75] when processing irregularly sampled data (non-tensor formats) is also important and challenging. This challenge can be resolved through potential integration with grid encoding-based approaches [51] or voxel projection methods, which transform non-grid structured data to grids or voxels to enable efficient processing.

5.3 Future directions on theoretical analysis for continuous methods

Future research on continuous representation methods offers several promising theoretical directions worthy of exploration. We outline some directions to inspire future research on understanding the theoretical effectiveness of

continuous methods. For instance, we can investigate the theoretical properties of neural network-based scientific computing frameworks (e.g., PINNs and neural operators) based on well-established mathematical tools from machine learning, such as implicit regularization and NTK theory. We can study the approximation and representation theories of INR-based matrix/tensor function decomposition models [2, 75, 129], such as low-rank approximation error in the function space and the decay rate of kernel singular values. Furthermore, we can analyze the implicit bias or optimization dynamics induced by explicit continuous regularizations (e.g., neural TV [18], Jacobian regularization [17], or neural nonlocal regularization [80]) beyond their explicit formulations. To exploit this, mathematical tools from NTK-based analyses of differential loss functions in PINNs [19] could provide inspiration.

In practice, many continuous representation models are trained in a mini-batch manner, such as NeRF [15] and LIIF [11]. This may conflict with classical optimization analysis, such as NTK [31] and implicit regularization analysis [57] under full-batch settings. Therefore, it is important to characterize the implicit bias and convergence of optimization methods for continuous models under more practical settings, such as mini-batch algorithms (critical for computationally expensive applications) instead of full-batch optimization. Relevant studies on noisy gradient descent [136] and the implicit bias of mini-batch algorithms [223] provide valuable starting points for future work in analyzing the properties of mini-batch optimization for continuous models like INRs.

On the other hand, the uneven eigenvalue distribution of the NTK matrix of neural networks leads to spectral bias when optimizing INRs, i.e., the tendency of standard INRs to converge rapidly to low-frequency components while struggling with high-frequency details [31, 42, 121]. The spectral bias characterization and alleviation are crucial for understanding and improving continuous INRs. To effectively alleviate spectral bias, future research could prioritize specialized feature mapping/activation functions by extending existing studies [16, 20, 72] to more flexible variants. Another direction is to combine traditional continuous representations with grid encoding-based approaches (e.g., InstantNGP [51]) to enhance the NTK's spectral properties, leading to faster convergence and better detail recovery. Meanwhile, designing efficient preconditioning gradient descent algorithms based on the NTK analysis [121] is also a promising direction for alleviating spectral bias. Moreover, appropriate parameter initialization is crucial for effectively training continuous representation models such as INRs [16, 72]. Despite their importance, existing initialization schemes are typically designed in an architecture-specific manner. Consequently, a promising future direction lies in developing initialization-robust models or unified initialization schemes that generalize across architectures. Potential strategies to mitigate the initialization sensitivity include incorporating principles of effective scaling, batch normalization [101], meta-learning [58], and early stopping for untrained networks [224]. Furthermore, the design of optimization algorithms that are inherently robust to initialization [121, 137] is also a promising future direction for continuous representation methods. Understanding the joint influence of both model architectures and optimization strategies is also important to uncover the scalability of continuous representation methods. The joint influence might be tractable by coupling convergence analysis [31] with implicit bias characterization [57].

With insightful theoretical developments, it is important to develop theoretical-algorithmic co-design, such as using explicit regularizations to counter the implicit and spectral bias [122], developing spectral bias-aware activation functions and rank-adaptive tensor function formats, to establish continuous methods that are both theoretically sound and computationally efficient.

Although implicit regularizations for linear matrix/tensor factorizations have been well-studied [33, 57], establishing distinct implicit regularization theories induced by continuous representation models with smooth inputs (e.g., coordinate inputs in INR frameworks) remains unexplored and challenging. It is important to distinguish continuous representations from conventional deep matrix factorization models [57] to explain their practical performance gap and reveal unique properties of INR-based approaches brought by the continuous paradigm. Also, to interpret the generalization capabilities of continuous representation methods, it is required to incorporate data-dependent and problem-dependent generalization error bounds [225] to theoretically assess the cross-domain and multi-modal modeling capabilities of advanced INR methods, such as the generalization error analysis of INR for FWI [108], arbitrary-scale imaging [11], and view synthesis [15].

Finally, studying the implicit bias from the untrained neural network perspective warrants discussions. For instance, we can consider the double over-parameterization paradigm [226] (over-parameterize both the low-rank matrix and sparse corruption) using implicit low-rank neural representations, and potentially enhance current results using discrete CNNs [226]. We can also investigate the implicit smoothness bias [227] of untrained continuous representation neural networks, and explore the discrepancy principle for early stopping of untrained neural networks [224] to enable stable convergence of continuous representations from randomly initialized neural networks, particularly addressing the initialization sensitivity challenge.

5.4 Future directions on applications of continuous methods

Extending existing continuous representation methods and theoretical frameworks to diverse data representation and reconstruction applications opens up numerous cross-disciplinary research opportunities, warranting further investigation. For example, we can utilize advanced operator learning methods for diverse low-level vision tasks, such as continuous image super-resolution, or conversely, employ grid-encoding-based INRs [51] to solve numerical PDEs and related scientific computing problems. We can also apply the continuous regularization to address the image restoration challenge, such as deraining [4,176], where real-world rain streaks often display explicit or implicit continuous patterns.

In AI for science, INRs [16, 20] and low-rank function representations [2, 75] offer strong potential for processing high-velocity, large-scale real-world data, such as black hole imaging [220], infrared imaging [228], and light-field tensor analysis [229]. These real-world tensor datasets inherently possess local and global structural correlations, which can be efficiently encoded using continuous representation methods.

Future research may integrate computational and interpretability analysis tools, such as gradient-based saliency maps and dimension reduction methods, to balance interpretability with model complexity and identify key features of INRs, thus avoiding redundancy in continuous representation learning. Furthermore, we can leverage pruning, fine-tuning, or adaptive neural architecture search to reduce the model size of continuous representations, thereby improving efficiency.

There are still key challenges in continuous methods for real-world applications, including scalability to high-dimensional data, computational burden, spectral bias toward low-frequency components, and out-of-distribution generalization. Further research on scalability and efficiency is crucial to advancing real-world applications. It is also important to further investigate cross-modal generalization, such as integrating cross-modal priors (e.g., fusing hematoxylin and eosin (H&E) stain imaging [230] with gene expression data [14, 64] under a continuous representation framework to link morphological features with transcriptomics). Exploring unified continuous representation frameworks for heterogeneous data fusion (e.g., hyperspectral and multispectral images, MRI and genomics, infrared and RGB images) is also a promising research direction.

It would be interesting to integrate continuous representation methods with larger models (e.g., contrastive language-image pre-training (CLIP) network and large language models) to broaden the applicability of continuous approaches or to enhance the resolution and modality adaptability of larger-scale models. Recently, D'Orazio [231] proposed an image generation pipeline by integrating an INR with the pre-trained CLIP model [232]. This method optimizes the INR weights to match an input text prompt by minimizing the alignment loss between the generated image of INR and the text prompt in the encoding space of the CLIP, unlocking the capability of INRs for text-to-image generation without altering CLIP's weights. Building on this pioneering work, further in-depth combinations of continuous representations and large models merit investigation. For example, one could employ advanced INR backbones [51, 53, 167] or incorporate geometric properties and regularization techniques [17, 18, 172] into the continuous representation to improve the robustness of INR-based image synthesis. Another promising direction is to combine continuous representations with pre-trained multi-modal models, such as conditional diffusion models [233], to enhance the capability of larger models across various domains, e.g., synthesizing NeRF from text prompts [234]. This integration can be achieved by combining continuous representations with modern optimization techniques, such as diffusion prior sampling [235] and score distillation sampling [234], to better modulate the posterior sampling process in diffusion models.

In summary, future research could consider both theory-guided and application-oriented developments, and couple mathematical analysis with algorithm improvements to enable continuous representation methods for interdisciplinary scientific discovery and applications. It is required to develop deeper collaborations between machine learning, applied mathematics, and domain scientists, with innovative modeling techniques to promote advanced data reconstruction paradigms, therefore addressing multi-modal, multi-scale, and physics-induced data science problems in the era of big data.

Finally, we would like to remark on the novelty of our proposed review from a future research perspective. In particular, by integrating fragmented knowledge under a unified continuous representation framework, we have proposed several novel future research directions by systematically exploiting the interplay among different sub-areas. Our review goes beyond merely identifying such connections by systematically mapping out how these interplays manifest across methodologies, theories, and applications, and, more importantly, by using this framework to propose novel and specific future research directions that are uniquely enabled by these synergies. In particular, in this section, we have articulated several forward-looking research directions that are rooted in the identified interdisciplinary interplay, such as (i) interdisciplinary integration of parametric models, such as combining statistical frameworks with neural representations for temporal data modeling, (ii) theoretical-algorithmic co-design by linking

theories such as NTK analysis with optimization dynamics under more practical settings (e.g., mini-batch training) to improve continuous representation learning, and (iii) integrating continuous representations with larger models (e.g., CLIP, diffusion models) for cross-modal and cross-domain applications. These proposed directions are not merely speculative but are grounded in the methodological and theoretical interplays being uncovered. We believe that these directions could offer novel roadmaps for advancing the field and add novelty and practical value to this review.

6 Conclusion

Continuous representations have achieved significant progress in data representation and reconstruction. This review synthesizes recent research advancements across three dimensions: methodological designs, theoretical foundations, and practical applications. Future studies could prioritize interdisciplinary collaboration, combining advances in neural architectures with domain knowledge (e.g., physical principles) to enhance continuous representation efficiency and real-world applicability. Additionally, integrating these methods with emerging technologies, such as foundation models, multi-modal models, and large language models, could lead to breakthroughs in continuous data reconstruction paradigms. It is essential to establish closer collaboration among machine learning researchers, applied mathematicians, and domain experts. Such efforts would improve existing techniques and provide transformative computational tools for the family of continuous representation methods, benefiting scientific discovery for broader research fields.

Acknowledgements This work was supported by Fundamental and Interdisciplinary Disciplines Breakthrough Plan of the Ministry of Education of China (Grant No. JYB2025XDXM101), National Key R&D Program of China (Grant No. 2025YFA1016400), National Natural Science Foundation of China (Grant Nos. 124B2029, 62272375, 62476214, 12371456, 12171072), Tianyuan Fund for Mathematics of National Natural Science Foundation of China (Grant No. 12426105), and Sichuan Science and Technology Program (Grant Nos. 2024NSFJQ0038, 2024NSFSC0038).

References

1 Elad M, Kawar B, Vaksman G. Image denoising: the deep learning revolution and beyond-a survey paper. SIAM J Imag Sci, 2023, 16: 1594–1654
2 Luo Y, Zhao X, Li Z, et al. Low-rank tensor function representation for multi-dimensional data recovery. IEEE Trans Pattern Anal, 2024, 46: 3351–3369
3 Pragliola M, Calatroni L, Lanza A, et al. On and beyond total variation regularization in imaging: the role of space variance. SIAM Rev, 2023, 65: 601–685
4 Wang H, Wu Y C, Li M H, et al. Survey on rain removal from videos or a single image. Sci China Inf Sci, 2022, 65: 111101
5 Molaei A, Aminimehr A, Tavakoli A, et al. Implicit neural representation in medical imaging: a comparative survey. In: Proceedings of the IEEE/CVF International Conference on Computer Vision (ICCV) Workshops, 2023. 2381–2391
6 Hong D, He W, Yokoya N, et al. Interpretable hyperspectral artificial intelligence: when nonconvex modeling meets hyperspectral remote sensing. IEEE Geosc Rem Sen M, 2021, 9: 52–87
7 Schirmer L, Novello T, da Silva V, et al. Geometric implicit neural representations for signed distance functions. Comput Graph, 2024, 125: 104085
8 Kargas N, Sidiropoulos N D. Supervised learning and canonical decomposition of multivariate functions. IEEE Trans Signal Proces, 2021, 69: 1097–1107
9 Kolda T G, Bader B W. Tensor decompositions and applications. SIAM Rev, 2009, 51: 455–500
10 Zhou X W, Yang C, Zhao H Y, et al. Low-rank modeling and its applications in image analysis. ACM Comput Surv, 2014, 47: 1–33
11 Chen Y, Liu S, Wang X. Learning continuous image representation with local implicit image function. In: Proceedings of IEEE/CVF Conference on Computer Vision and Pattern Recognition, 2021. 8624–8634
12 Byra M, Poon C, Shimogori T, et al. Implicit neural representations for joint decomposition and registration of gene expression images in the marmoset brain. In: Proceedings of Medical Image Computing and Computer Assisted Intervention (MICCAI), 2023. 645–654
13 Cheng Z, Ding Y, Qu C, et al. Implicit neural representation with imaging geometry for SAR target recognition. IEEE Trans Aero Elec Sys, 2025, 61: 7279–7292
14 Chitra U, Arnold B J, Sarkar H, et al. Mapping the topography of spatial gene expression with interpretable deep learning. Nat Methods, 2025, 22: 298–309
15 Mildenhall B, Srinivasan P P, Tancik M, et al. NeRF: representing scenes as neural radiance fields for view synthesis. In: Proceedings of European Conference on Computer Vision, 2020. 405–421
16 Sitzmann V, Martel J, Bergman A, et al. Implicit neural representations with periodic activation functions. In: Proceedings of International Conference on Neural Information Processing Systems, 2020. 7462–7473
17 Wolterink J M, Zwienenberg J C, Brune C. Implicit neural representations for deformable image registration. In: Proceedings of the 5th International Conference on Medical Imaging with Deep Learning, 2022. 1349–1359
18 Luo Y, Zhao X, Ye K, et al. NeurTV: Total variation on the neural domain. SIAM J Imag Sci, 2025, 18: 1101–1140
19 Bonfanti A, Bruno G, Cipriani C. The challenges of the nonlinear regime for physics-informed neural networks. In: Proceedings of Advances in Neural Information Processing Systems, 2024. 41852–41881
20 Tancik M, Srinivasan P, Mildenhall B, et al. Fourier features let networks learn high frequency functions in low dimensional domains. In: Proceedings of International Conference on Neural Information Processing Systems, 2020. 7537–7547
21 Fang S, Yu X, Wang Z, et al. Functional Bayesian Tucker decomposition for continuous-indexed tensor data. In: Proceedings of the 12th International Conference on Learning Representations (ICLR), 2024. 1–18
22 Chen P, Cheng L, Li J, et al. Generalized temporal tensor decomposition with rank-revealing latent-ode. 2025. ArXiv:2502.06164
23 Fang S, Wen Q, Luo Y, et al. BayOTIDE: Bayesian online multivariate time series imputation with functional decomposition. In: Proceedings of the 41st International Conference on Machine Learning (ICML), 2024. 12993–13009
24 Kratsios A. The universal approximation property. Ann Math Artif Intel, 2021, 89: 435–469
25 Gao W, Liu D, Chen W, et al. NeRSI: neural implicit representations for 5D seismic data interpolation. Geophysics, 2025, 90: V29–V42
26 Chen Z, Chen Y, Liu J, et al. Videoinr: learning video implicit neural representation for continuous space-time super-resolution. In: Proceedings of IEEE/CVF Conference on Computer Vision and Pattern Recognition (CVPR), 2022. 2037–2047

27 Du B, Sun J, Jia A, et al. Physics-informed robust and implicit full waveform inversion without prior and low-frequency information. IEEE Trans Geosci Remote, 2024, 62: 1–12
28 Wu Q, Du C, Tian X, et al. Moner: motion correction in undersampled radial MRI with unsupervised neural representation. In: Proceedings of the 13th International Conference on Learning Representations (ICLR), 2025
29 Hashemi B, Trefethen L N. Chebfun in three dimensions. SIAM J Sci Comput, 2017, 39: C341–C363
30 Saragadam V, LeJeune D, Tan J, et al. Wire: wavelet implicit neural representations. In: Proceedings of IEEE/CVF Conference on Computer Vision and Pattern Recognition (CVPR), 2023. 18507–18516
31 Jacot A, Gabriel F, Hongler C. Neural tangent kernel: convergence and generalization in neural networks. In: Proceedings of the 32nd International Conference on Neural Information Processing Systems (NeurIPS), 2018. 8580–8589
32 Alkhouri I, Bell E, Ghosh A, et al. Understanding untrained deep models for inverse problems: algorithms and theory. 2025. ArXiv:2502.18612
33 Hariz K, Kadri H, Ayache S, et al. Implicit regularization with polynomial growth in deep tensor factorization. In: Proceedings of the 39th International Conference on Machine Learning (ICML), 2022. 8484–8501
34 Chen G, Nie J, Wei W, et al. Arbitrary-scale hyperspectral image super-resolution from a fusion perspective with spatial priors. IEEE Trans Geosci Remote, 2024, 62: 1–11
35 Vemuri S K, Büchner T, Niebling J, et al. Functional tensor decompositions for physics-informed neural networks. In: Proceedings of International Conference on Pattern Recognition, 2025. 32–46
36 Kovachki N, Li Z, Liu B, et al. Neural operator: learning maps between function spaces with applications to PDEs. J Mach Learn Res, 2023, 24: 1–97
37 Li Z, Kovachki N B, Azizzadenesheli K, et al. Fourier neural operator for parametric partial differential equations. In: Proceedings of International Conference on Learning Representations, 2021
38 Chen A, Xu Z, Geiger A, et al. Tensorf: tensorial radiance fields. In: Proceedings of the 17th European Conference on Computer Vision (ECCV), 2022. 333–350
39 Sort L, Brusquet L L, Tenenhaus A. Latent functional parafac for modeling multidimensional longitudinal data. 2024. ArXiv:2410.18696
40 Gorodetsky A, Karaman S, Marzouk Y. A continuous analogue of the tensor-train decomposition. Comput Method Appl M, 2019, 347: 59–84
41 Liu X, Tang H. Difffno: diffusion Fourier neural operator. In: Proceedings of IEEE/CVF Conference on Computer Vision and Pattern Recognition (CVPR), 2025. 150–160
42 Shi K, Zhou X, Gu S. Improved implicit neural representation with Fourier reparameterized training. In: Proceedings of IEEE/CVF Conference on Computer Vision and Pattern Recognition (CVPR), 2024. 25985–25994
43 Xie Y, Takikawa T, Saito S, et al. Neural fields in visual computing and beyond. Comput Graph Forum, 2022, 41: 641–676
44 Gao K, Gao Y, He H, et al. Nerf: neural radiance field in 3D vision: a comprehensive review. 2025. ArXiv:2210.00379
45 Kerbl B, Kopanas G, Leimkühler T, et al. 3D Gaussian splatting for real-time radiance field rendering. 2023. ArXiv:2308.04079
46 Essakine A, Cheng Y, Cheng C W, et al. Where do we stand with implicit neural representations? A technical and performance survey. Trans Mach Learn Res, 2025
47 Irshad M Z, Comi M, Lin Y C, et al. Neural fields in robotics: a survey. 2024. ArXiv:2410.20220
48 Sun S, Han K, You C, et al. Medical image registration via neural fields. Med Image Anal, 2024, 97: 103249
49 Liu Z, Wang Y, Vaidya S, et al. KAN: kolmogorov-arnold networks. In: Proceedings of the 13th International Conference on Learning Representations, 2025
50 Vemuri S K, Büchner T, Denzler J. F-INR: functional tensor decomposition for implicit neural representations. 2025. ArXiv:2503.21507
51 Müller T, Evans A, Schied C, et al. Instant neural graphics primitives with a multiresolution hash encoding. ACM Trans Graphic, 2022, 41: 1–15
52 Sun C, Sun M, Chen H T. Direct voxel grid optimization: super-fast convergence for radiance fields reconstruction. In: Proceedings of IEEE/CVF Conference on Computer Vision and Pattern Recognition (CVPR), 2022. 5449–5459
53 Zhu H, Liu F Y, Zhang Q, et al. RHINO: regularizing the hash-based implicit neural representation. Sci China Inf Sci, 2026, 69: 112101
54 Arora S, Du S S, Hu W, et al. On exact computation with an infinitely wide neural net. In: Proceedings of the 33rd International Conference on Neural Information Processing Systems (NeurIPS), 2019. 8141–8150
55 Arora S, Du S, Hu W, et al. Fine-grained analysis of optimization and generalization for overparameterized two-layer neural networks. In: Proceedings of the 36th International Conference on Machine Learning (ICML), 2019. 322–332
56 Audia S, Feizi S, Zwicker M, et al. How learnable grids recover fine detail in low dimensions: a neural tangent kernel analysis of multigrid parametric encodings. In: Proceedings of the 13th International Conference on Learning Representations (ICLR), 2025
57 Arora S, Cohen N, Hu W, et al. Implicit regularization in deep matrix factorization. In: Proceedings of the 33rd International Conference on Neural Information Processing Systems (NeurIPS), 2019. 7413–7424
58 Yüce G, Ortiz-Jiménez G, Besbinar B, et al. A structured dictionary perspective on implicit neural representations. In: Proceedings of the IEEE/CVF Conference on Computer Vision and Pattern Recognition (CVPR), 2022. 19228–19238
59 Roddenberry T M, Saragadam V, de Hoop M V, et al. Implicit neural representations and the algebra of complex wavelets. In: Proceedings of the 12th International Conference on Learning Representations (ICLR), 2024
60 Hu H, Qi L, Chao X. Physics-informed neural networks (PINN) for computational solid mechanics: numerical frameworks and applications. Thin Wall Struct, 2024, 205: 112495
61 Park J J, Florence P, Straub J, et al. Deepsdf: learning continuous signed distance functions for shape representation. In: Proceedings of IEEE/CVF Conference on Computer Vision and Pattern Recognition (CVPR), 2019. 165–174
62 Yao M, Huo Y, Ran Y, et al. Neural radiance field-based visual rendering: a comprehensive review. 2024. ArXiv:2404.00714
63 Chu J, Du C, Lin X, et al. Highly accelerated MRI via implicit neural representation guided posterior sampling of diffusion models. Med Image Anal, 2025, 100: 103398
64 Luo Y, Zhao X, Ye K, et al. Stinr: deciphering spatial transcriptomics via implicit neural representation. In: Proceedings of the IEEE/CVF Conference on Computer Vision and Pattern Recognition (CVPR), 2025
65 Zhang K, Zhu D, Min X, et al. Implicit neural representation learning for hyperspectral image super-resolution. IEEE Trans Geosci Remote, 2023, 61: 1–12
66 Wang S, Luo Y, Li S, et al. Efficient seismic random noise attenuation via kan-empowered neural low-rank representation. IEEE Trans Geosci Remote, 2025, 63: 1–15
67 Wang T, Li J, Ng M K, et al. Nonnegative matrix functional factorization for hyperspectral unmixing with nonuniform spectral sampling. IEEE Trans Geosci Remote, 2024, 62: 1–13
68 Yokota T, Zdunek R, Cichocki A, et al. Smooth nonnegative matrix and tensor factorizations for robust multi-way data analysis. Signal Process, 2015, 113: 234–249
69 Imaizumi M, Hayashi K. Tensor decomposition with smoothness. In: Proceedings of International Conference on Machine Learning, 2017. 1597–1606
70 Gorodetsky A A, Jakeman J D. Gradient-based optimization for regression in the functional tensor-train format. J Comput Phys, 2018, 374: 1219–1238
71 Tancik M, Mildenhall B, Wang T, et al. Learned initializations for optimizing coordinate-based neural representations. In: Proceedings of the IEEE/CVF Conference on Computer Vision and Pattern Recognition (CVPR), 2021. 2846–2855
72 Liu Z, Zhu H, Zhang Q, et al. Finer: flexible spectral-bias tuning in implicit neural representation by variableperiodic activation functions.

In: Proceedings of IEEE/CVF Conference on Computer Vision and Pattern Recognition (CVPR), 2024. 2713–2722
73 Fridovich-Keil S, Yu A, Tancik M, et al. Plenoxels: radiance fields without neural networks. In: Proceedings of IEEE/CVF Conference on Computer Vision and Pattern Recognition (CVPR), 2022. 5491–5500
74 Zhu H, Xie S, Liu Z, et al. Disorder-invariant implicit neural representation. IEEE Trans Pattern Anal, 2024, 46: 5463–5478
75 Liang R, Sun H, Vijaykumar N. CoordX: accelerating implicit neural representation with a split MLP architecture. In: Proceedings of International Conference on Learning Representations (ICLR), 2022
76 Wang J, Zhao X. Functional transform-based low-rank tensor factorization for multi-dimensional data recovery. In: Proceedings of the 18th European Conference on Computer Vision (ECCV), 2024. 39–56
77 Li Y, Zhang X, Luo Y, et al. Deep rank-one tensor functional factorization for multi-dimensional data recovery. In: Proceedings of the AAAI Conference on Artificial Intelligence, 2025. 18539–18547
78 Fang S, Yu X, Li S, et al. Streaming factor trajectory learning for temporal tensor decomposition. In: Proceedings of the 37th International Conference on Neural Information Processing Systems, 2023. 56849–56870
79 Li Z, Wang H, Meng D. Regularize implicit neural representation by itself. In: Proceedings of IEEE/CVF Conference on Computer Vision and Pattern Recognition (CVPR), 2023. 10280–10288
80 Luo Y, Zhao X, Meng D. Revisiting nonlocal self-similarity from continuous representation. IEEE Trans Pattern Anal, 2025, 47: 450–468
81 Heo H, Oh S, Lee J Y, et al. Isometric regularization for manifolds of functional data. In: Proceedings of the 13th International Conference on Learning Representations, 2025
82 Debals O, van Barel M, de Lathauwer L. Nonnegative matrix factorization using nonnegative polynomial approximations. IEEE Signal Proc Let, 2017, 24: 948–952
83 Kargas N, Sidiropoulos N D. Nonlinear system identification via tensor completion. In: Proceedings of the AAAI Conference on Artificial Intelligence, 2020. 4420–4427
84 Kunkel P, Mehrmann V. Smooth factorizations of matrix valued functions and their derivatives. Numer Math, 1991, 60: 115–131
85 Oseledets I V. Constructive representation of functions in low-rank tensor formats. Constr Approx, 2013, 37: 1–18
86 Tichavský P, Straka O. Tensor train approximation of multivariate functions. In: Proceedings of the 32nd European Signal Processing Conference (EUSIPCO), 2024. 2262–2266
87 Chen T, Li H, Yang Q, et al. General functional matrix factorization using gradient boosting. In: Proceedings of the 30th International Conference on Machine Learning (ICML), 2013. 436–444
88 Li Y, Wang F. Local randomized neural networks with finite difference methods for interface problems. J Comput Phys, 2025, 529: 113847
89 Wu T, Fan J. Smooth tensor product for tensor completion. IEEE Trans Image Process, 2024, 33: 6483–6496
90 Fathony R, Sahu A K, Willmott D, et al. Multiplicative filter networks. In: Proceedings of International Conference on Learning Representations, 2021
91 Li J C L, Liu C, Huang B, et al. Learning spatially collaged Fourier bases for implicit neural representation. In: Proceedings of the AAAI Conference on Artificial Intelligence, 2024. 13492–13499
92 Jayasundara D, Zhao H, Labate D, et al. PIN: prolate spheroidal wave function-based implicit neural representations. In: Proceedings of the 13th International Conference on Learning Representations (ICLR), 2025
93 Ramasinghe S, Lucey S. Beyond periodicity: towards a unifying framework for activations in coordinate-MLPs. In: Proceedings of the 17th European Conference on Computer Vision (ECCV), 2022. 142–158
94 Hao Z, Mallya A, Belongie S, et al. Implicit neural representations with levels-of-experts. In: Proceedings of Advances in Neural Information Processing Systems, 2022. 2564–2576
95 Ben-Shabat Y, Hewa Koneputugodage C, Ramasinghe S, et al. Neural experts: mixture of experts for implicit neural representations. In: Proceedings of Advances in Neural Information Processing Systems, 2024. 101641–101670
96 Vyas K, Humayun A I, Dashpute A, et al. Learning transferable features for implicit neural representations. In: Proceedings of the 38th Annual Conference on Neural Information Processing Systems (NeurIPS), 2024. 42268–42291
97 Zhang C, Luo S T S, Li J C L, et al. Nonparametric teaching of implicit neural representations. In: Proceedings of the 41st International Conference on Machine Learning (ICML), 2024. 59435–59458
98 Fang W, Tang Y, Guo H, et al. Cycleinr: cycle implicit neural representation for arbitrary-scale volumetric super-resolution of medical data. In: Proceedings of IEEE/CVF Conference on Computer Vision and Pattern Recognition (CVPR), 2024. 11631–11641
99 Saragadam V, Tan J, Balakrishnan G, et al. Miner: multiscale implicit neural representation. In: Proceedings of the 17th European Conference on Computer Vision (ECCV), 2022. 318–333
100 Li J, Zhao X, Wang J, et al. Superpixel-informed implicit neural representation for multi-dimensional data. In: Proceedings of the 18th European Conference on Computer Vision (ECCV), 2024. 258–276
101 Cai Z, Zhu H, Shen Q, et al. Batch normalization alleviates the spectral bias in coordinate networks. In: Proceedings of IEEE/CVF Conference on Computer Vision and Pattern Recognition (CVPR), 2024. 25160–25171
102 Yu C, Luo Y, Ye K, et al. Cross-frequency implicit neural representation with self-evolving parameters. 2025. ArXiv:2504.10929
103 Kazerouni A, Azad R, Hosseini A, et al. Incode: implicit neural conditioning with prior knowledge embeddings. In: Proceedings of 2024 IEEE/CVF Winter Conference on Applications of Computer Vision (WACV), 2024. 1287–1296
104 Chen Y, Wang X. Transformers as meta-learners for implicit neural representations. In: Proceedings of European Conference on Computer Vision (ECCV), 2022. 170–187
105 Hu E J, Shen Y, Wallis P, et al. LoRA: low-rank adaptation of large language models. 2021. ArXiv:2106.09685
106 Sitzmann V, Zollhöfer M, Wetzstein G. Scene representation networks: continuous 3D-structure-aware neural scene representations. In: Proceedings of the 33rd International Conference on Neural Information Processing Systems, 2019. 1121–1132
107 Yu A, Li R, Tancik M, et al. Plenoctrees for real-time rendering of neural radiance fields. In: Proceedings of IEEE/CVF International Conference on Computer Vision (ICCV), 2021. 5732–5741
108 Sun J, Innanen K, Zhang T, et al. Implicit seismic full waveform inversion with deep neural representation. J Geophys Res Solid Earth, 2023, 128: e2022JB025964
109 Nie T, Qin G, Ma W, et al. Spatiotemporal implicit neural representation as a generalized traffic data learner. Transport Res C-Emer, 2024, 169: 104890
110 Wang H, Yu T, Yang T, et al. Neural physical simulation with multi-resolution hash grid encoding. In: Proceedings of the AAAI Conference on Artificial Intelligence, 2024. 5410–5418
111 Huang X, Alkhalifah T. Efficient physics-informed neural networks using hash encoding. J Comput Phys, 2024, 501: 112760
112 Kang N, Oh J, Hong Y, et al. PIG: physics-informed Gaussians as adaptive parametric mesh representations. In: Proceedings of the 13th International Conference on Learning Representations, 2025
113 Wang S, Yu X, Perdikaris P. When and why PINNs fail to train: a neural tangent kernel perspective. J Comput Phys, 2022, 449: 110768
114 Nguyen M, Mücke N. Optimal convergence rates for neural operators. 2025. ArXiv:2412.17518
115 Wang T, Yan Z P, Li J Z, et al. Hyperspectral and multispectral image fusion with arbitrary resolution through self-supervised representations. Int J Comput Vision, 2025, 133: 7515–7535
116 Griebel M, Li G. On the decay rate of the singular values of bivariate functions. SIAM J Numer Anal, 2018, 56: 974–993
117 Han R, Shi P, Zhang A R. Guaranteed functional tensor singular value decomposition. J Am Stat Assoc, 2024, 119: 995–1007
118 Wang A, Qiu Y, Bai M, et al. Generalized tensor decomposition for understanding multi-output regression under combinatorial shifts. In: Proceedings of Advances in Neural Information Processing Systems, 2024. 47559–47635
119 Wei C, Lee J D, Liu Q, et al. Regularization matters: generalization and optimization of neural nets v.s. their induced kernel. In:

Proceedings of the 33rd International Conference on Neural Information Processing Systems, 2019. 9712–9724
120 Chen Z, Shi X, Rudner T G J, et al. A neural tangent kernel perspective on function-space regularization in neural networks. In: Proceedings of International Conference on Neural Information Processing Systems (NeurIPS) Workshop on Optimization for Machine Learning, 2022
121 Geifman A, Barzilai D, Basri R, et al. Controlling the inductive bias of wide neural networks by modifying the kernel's spectrum. 2024. ArXiv:2307.14531
122 Razin N, Maman A, Cohen N. Implicit regularization in hierarchical tensor factorization and deep convolutional neural networks. In: Proceedings of the 39th International Conference on Machine Learning (ICML), 2022. 18422–18462
123 Hariz K, Kadri H, Ayache S, et al. Implicit regularization in deep Tucker factorization: low-rankness via structured sparsity. In: Proceedings of International Conference on Artificial Intelligence and Statistics (AISTATS), 2024. 2359–2367
124 Xie S, Li Z. Implicit bias of AdamW: ℓ_∞-norm constrained optimization. In: Proceedings of the 41st International Conference on Machine Learning, 2024. 54488–54510
125 Hornik K, Stinchcombe M, White H. Multilayer feedforward networks are universal approximators. Neural Netws, 1989, 2: 359–366
126 Ellacott S W. Aspects of the numerical analysis of neural networks. Acta Numer, 1994, 3: 145–202
127 Plonka G, Potts D, Steidl G, et al. Numerical Fourier Analysis. Hoboken: John Wiley & Sons, 2020. 235–259.
128 Daubechies I. Orthonormal bases of compactly supported wavelets. Commun Pur Appl Math, 1988, 41: 909–996
129 Cho J, Nam S, Yang H, et al. Separable physics-informed neural networks. In: Proceedings of the 37th Conference on Neural Information Processing Systems, 2023. 23761–23788
130 Wang Y, Xie H, Jin P. Tensor neural network and its numerical integration. J Comput Math, 2024, 42: 1714–1742
131 Fedorova V P. The Stone–Weierstrass theorem and spaces of measures. Math Notes, 2002, 72: 417–427
132 Leshno M, Lin V Y, Pinkus A, et al. Multilayer feedforward networks with a nonpolynomial activation function can approximate any function. Neural Netw, 1993, 6: 861–867
133 Fageot J. Variational seasonal-trend decomposition with sparse continuous-domain regularization. 2025. ArXiv:2505.10486
134 Xu D, Wang P, Jiang Y, et al. Signal processing for implicit neural representations. In: Proceedings of Advances in Neural Information Processing Systems, 2022. 13404–13418
135 Pal S, Adepu H, Wang C, et al. Implicit representations via operator learning. In: Proceedings of the 41st International Conference on Machine Learning, 2024. 39022–39041
136 Chen Z, Cao Y, Gu Q, et al. A generalized neural tangent kernel analysis for two-layer neural networks. In: Proceedings of the 34th International Conference on Neural Information Processing Systems (NeurIPS), 2020. 13363–13373
137 Shi K, Chen H, Zhang L, et al. Inductive gradient adjustment for spectral bias in implicit neural representations. In: Proceedings of the 42nd International Conference on Machine Learning, 2025
138 Chng S F, Saratchandran H, Lucey S. Preconditioners for the stochastic training of neural fields. In: Proceedings of the IEEE/CVF Conference on Computer Vision and Pattern Recognition (CVPR), 2025
139 Ulyanov D, Vedaldi A, Lempitsky V. Deep image prior. Int J Comput Vision, 2020, 128: 1867–1888
140 Gunasekar S, Woodworth B E, Bhojanapalli S, et al. Implicit regularization in matrix factorization. In: Proceedings of Advances in Neural Information Processing Systems, 2017. 6152–6160
141 Cao J, Qian C, Huang Y, et al. A dynamics theory of implicit regularization in deep low-rank matrix factorization. 2022. ArXiv:2212.14150
142 Gidel G, Bach F, Lacoste-Julien S. Implicit regularization of discrete gradient dynamics in linear neural networks. 2019. ArXiv:1904.13262
143 Pesme S, Flammarion N. Saddle-to-saddle dynamics in diagonal linear networks. In: Proceedings of the 37th International Conference on Neural Information Processing Systems, 2023. 7475–7505
144 Chou H H, Gieshoff C, Maly J, et al. Gradient descent for deep matrix factorization: dynamics and implicit bias towards low rank. Appl Comput Harmon A, 2024, 68: 101595
145 Bai Z, Zhao J, Zhang Y. Connectivity shapes implicit regularization in matrix factorization models for matrix completion. In: Proceedings of the 38th Annual Conference on Neural Information Processing Systems, 2024. 45914–45955
146 Lu L, Jin P, Pang G, et al. Learning nonlinear operators via DeepONet based on the universal approximation theorem of operators. Nat Mach Intell, 2021, 3: 218–229
147 Zhao W, Liu X, Zhai D, et al. Self-supervised arbitrary-scale implicit point clouds upsampling. IEEE Trans Pattern Anal, 2023, 45: 12394–12407
148 Zhang T, Quan Y, Ji H. Cross-scale self-supervised blind image deblurring via implicit neural representation. In: Proceedings of Advances in Neural Information Processing Systems, 2024. 7060–7094
149 Li K, Ye W. D-FNO: a decomposed Fourier neural operator for large-scale parametric partial differential equations. Comput Method Appl M, 2025, 436: 117732
150 Wu Q, Li Y, Xu L, et al. Irem: high-resolution magnetic resonance image reconstruction via implicit neural representation. In: Proceedings of Medical Image Computing and Computer Assisted Intervention (MICCAI), 2021. 65–74
151 Wu Q, Li Y, Sun Y, et al. An arbitrary scale super-resolution approach for 3D MR images via implicit neural representation. IEEE J Biomed Health, 2023, 27: 1004–1015
152 Zimmer V A, Hammernik K, Sideri-Lampretsa V, et al. Towards generalised neural implicit representations for image registration. In: Proceedings of Medical Image Computing and Computer Assisted Intervention (MICCAI), 2024. 45–55
153 Chen H, Zhao W, Xu T, et al. Spectral-wise implicit neural representation for hyperspectral image reconstruction. IEEE Trans Circ Syst Vid, 2024, 34: 3714–3727
154 Jiang C, Sud A, Makadia A, et al. Local implicit grid representations for 3D scenes. In: Proceedings of IEEE/CVF Conference on Computer Vision and Pattern Recognition (CVPR), 2020. 6000–6009
155 Mescheder L, Oechsle M, Niemeyer M, et al. Occupancy networks: learning 3D reconstruction in function space. In: Proceedings of IEEE/CVF Conference on Computer Vision and Pattern Recognition (CVPR), 2019. 4455–4465
156 Yariv L, Gu J, Kasten Y, et al. Volume rendering of neural implicit surfaces. In: Proceedings of Advances in Neural Information Processing Systems, 2021. 4805–4815
157 Niemeyer M, Mescheder L, Oechsle M, et al. Differentiable volumetric rendering: learning implicit 3D representations without 3D supervision. In: Proceedings of IEEE/CVF Conference on Computer Vision and Pattern Recognition (CVPR), 2020. 3501–3512
158 Genova K, Cole F, Vlasic D, et al. Learning shape templates with structured implicit functions. In: Proceedings of IEEE/CVF International Conference on Computer Vision (ICCV), 2019. 7153–7163
159 Chen Z, Zhang H. Learning implicit fields for generative shape modeling. In: Proceedings of IEEE/CVF Conference on Computer Vision and Pattern Recognition (CVPR), 2019. 5932–5941
160 Chibane J, Alldieck T, Pons-Moll G. Implicit functions in feature space for 3D shape reconstruction and completion. In: Proceedings of IEEE/CVF Conference on Computer Vision and Pattern Recognition (CVPR), 2020. 6968–6979
161 Eslami S M A, Jimenez Rezende D, Besse F, et al. Neural scene representation and rendering. Science, 2018, 360: 1204–1210
162 Tang J, Chen X, Wang J, et al. Compressible-composable NeRF via rank-residual decomposition. In: Proceedings of Advances in Neural Information Processing Systems (NeurIPS), 2022. 14798–14809
163 Fridovich-Keil S, Meanti G, Warburg F R, et al. K-planes: explicit radiance fields in space, time, and appearance. In: Proceedings of IEEE/CVF Conference on Computer Vision and Pattern Recognition (CVPR), 2023. 12479–12488
164 Wu G, Yi T, Fang J, et al. 4D Gaussian splatting for real-time dynamic scene rendering. In: Proceedings of the IEEE/CVF Conference on Computer Vision and Pattern Recognition (CVPR), 2024. 20310–20320

165 Huang B, Yu Z, Chen A, et al. 2D Gaussian splatting for geometrically accurate radiance fields. In: Proceedings of ACM Special Interest Group for Computer Graphics (SIGGRAPH), 2024. 1–11
166 Zhang X, Ge X, Xu T, et al. Gaussianimage: 1000 FPS image representation and compression by 2D Gaussian splatting. In: Proceedings of European Conference on Computer Vision (ECCV), 2024. 327–345
167 Zhang W, Zhu H, Wu D, et al. Wipes: wavelet-based visual primitives. In: Proceedings of International Conference on Computer Vision (ICCV), 2025
168 Xu C, Jin Z, Shen C, et al. 3D Gaussian adaptive reconstruction for Fourier light-field microscopy. 2025. ArXiv:2505.12875
169 Wu T, Yuan Y J, Zhang L X, et al. Recent advances in 3D Gaussian splatting. Comput Vis Media, 2024, 10: 613–642
170 Ortiz J, Clegg A, Dong J, et al. iSDF: real-time neural signed distance fields for robot perception. 2022. ArXiv:2204.02296
171 Simeonov A, Du Y, Tagliasacchi A, et al. Neural descriptor fields: SE(3)-equivariant object representations for manipulation. In: Proceedings of International Conference on Robotics and Automation (ICRA), 2022. 6394–6400
172 Li S L, Zhang A, Chen B, et al. Controlling diverse robots by inferring Jacobian fields with deep networks. Nature, 2025, 643: 89–95
173 Suresh S, Qi H, Wu T, et al. NeuralFeels with neural fields: visuotactile perception for in-hand manipulation. Sci Robot, 2024, 9: eadl0628
174 Ming Y, Yang X, Wang W, et al. Benchmarking neural radiance fields for autonomous robots: an overview. Eng Appl Artif Intel, 2025, 140: 109685
175 Zhu S, Wang G, Kong X, et al. 3D Gaussian splatting in robotics: a survey. 2024. ArXiv:2410.12262
176 Chen X, Pan J, Dong J. Bidirectional multi-scale implicit neural representations for image deraining. In: Proceedings of IEEE/CVF Conference on Computer Vision and Pattern Recognition (CVPR), 2024. 25627–25636
177 Nam S, Brubaker M A, Brown M S. Neural image representations for multi-image fusion and layer separation. In: Proceedings of the 17th European Conference on Computer Vision (ECCV), 2022. 216–232
178 Hu S, Sun H, Wei D, et al. Continuous heatmap regression for pose estimation via implicit neural representation. In: Proceedings of the 38th Annual Conference on Neural Information Processing Systems (NeurIPS), 2024. 102036–102055
179 Yang S, Ding M, Wu Y, et al. Implicit neural representation for cooperative low-light image enhancement. In: Proceedings of IEEE/CVF International Conference on Computer Vision (ICCV), 2023. 12872–12881
180 Chen H, He B, Wang H, et al. NeRV: neural representations for videos. In: Proceedings of Advances in Neural Information Processing Systems, 2021. 21557–21568
181 Li Z, Wang M, Pi H, et al. E-NeRV: expedite neural video representation with disentangled spatial-temporal context. In: Proceedings of the 17th European Conference on Computer Vision (ECCV), 2022. 267–284
182 Yan H, Ke Z, Zhou X, et al. DS-NeRV: implicit neural video representation with decomposed static and dynamic codes. In: Proceedings of IEEE/CVF Conference on Computer Vision and Pattern Recognition (CVPR), 2024. 23019–23029
183 Grattarola D, Vandergheynst P. Generalised implicit neural representations. In: Proceedings of the 36th International Conference on Neural Information Processing Systems, 2022. 30446–30458
184 Xia X, Mishne G, Wang Y. Implicit graphon neural representation. In: Proceedings of the 26th International Conference on Artificial Intelligence and Statistics, 2023. 10619–10634
185 Karniadakis G E, Kevrekidis I G, Lu L, et al. Physics-informed machine learning. Nat Rev Phys, 2021, 3: 422–440
186 Raissi M, Perdikaris P, Karniadakis G E. Physics-informed neural networks: a deep learning framework for solving forward and inverse problems involving nonlinear partial differential equations. J Comput Phys, 2019, 378: 686–707
187 Zhao C, Zhang F, Lou W, et al. A comprehensive review of advances in physics-informed neural networks and their applications in complex fluid dynamics. Phys Fluids, 2024, 36: 101301
188 Kang N, Lee B, Hong Y, et al. PIXEL: physics-informed cell representations for fast and accurate PDE solvers. In: Proceedings of the 37th AAAI Conference on Artificial Intelligence, 2023. 8186–8194
189 Jin G, Wang D, Wong J C, et al. Differentiable hash encoding for physics-informed neural networks. In: Proceedings of IEEE Conference on Artificial Intelligence (CAI), 2024. 444–447
190 Liu-Schiaffini M, Berner J, Bonev B, et al. Neural operators with localized integral and differential kernels. In: Proceedings of the 41st International Conference on Machine Learning, 2024. 32576–32594
191 Azizzadenesheli K, Kovachki N, Li Z, et al. Neural operators for accelerating scientific simulations and design. Nat Rev Phys, 2024, 6: 320–328
192 Dummer S, Strisciuglio N, Brune C. RDA-INR: Riemannian diffeomorphic autoencoding via implicit neural representations. SIAM J Imaging Sci, 2024, 17: 2302–2330
193 Reed A W, Kim H, Anirudh R, et al. Dynamic CT reconstruction from limited views with implicit neural representations and parametric motion fields. In: Proceedings of IEEE/CVF International Conference on Computer Vision (ICCV), 2021. 2238–2248
194 Song T, Broadbent C, Kuang R. GNTD: reconstructing spatial transcriptomes with graph-guided neural tensor decomposition informed by spatial and functional relations. Nat Commun, 2023, 14: 8276
195 Sideri-Lampretsa V, McGinnis J, Qiu H, et al. SINR: spline-enhanced implicit neural representation for multi-modal registration. In: Proceedings of International Conference on Medical Imaging with Deep Learning, 2024
196 Sun Y, Liu J, Xie M, et al. CoIL: coordinate-based internal learning for tomographic imaging. IEEE Trans Comput Imag, 2021, 7: 1400–1412
197 Shen C K, Zhu H, Zhou Y, et al. Continuous 3D myocardial motion tracking via echocardiography. IEEE Trans Med Imaging, 2024, 43: 4236–4252
198 Shen C, Zhu H, Zhou Y, et al. CardiacField: computational echocardiography for automated heart function estimation using two-dimensional echocardiography probes. Eur Heart J-Digit Hl, 2025, 6: 137–146
199 Vo R, Escoda J, Vienne C, et al. Neural field regularization by denoising for 3D sparse-view x-ray computed tomography. In: Proceedings of International Conference on 3D Vision (3DV), 2024. 1166–1176
200 Cohen R, Elad M, Milanfar P. Regularization by denoising via fixed-point projection (RED-PRO). SIAM J Imag Sci, 2021, 14: 1374–1406
201 Reehorst E T, Schniter P. Regularization by denoising: clarifications and new interpretations. IEEE Trans Comput Imag, 2019, 5: 52–67
202 Iskender B, Nakarmi S, Daphalapurkar N, et al. RSR-NF: neural field regularization by static restoration priors for dynamic imaging. 2025. ArXiv:2503.10015
203 Yu H, Fessler J A, Jiang Y. Bilevel optimized implicit neural representation for scan-specific accelerated MRI reconstruction. 2025. ArXiv:2502.21292
204 Zhu H, Liu Z, Zhou Y, et al. DNF: diffractive neural field for lensless microscopic imaging. Opt Express, 2022, 30: 18168–18178
205 Liu R, Sun Y, Zhu J, et al. Recovery of continuous 3D refractive index maps from discrete intensity-only measurements using neural fields. Nat Mach Intell, 2022, 4: 781–791
206 Zhou H, Feng B Y, Guo H, et al. Fourier ptychographic microscopy image stack reconstruction using implicit neural representations. Optica, 2023, 10: 1679–1687
207 Zhang O, Zhou H, Feng B Y, et al. Single-shot volumetric fluorescence imaging with neural fields. Adv Photon, 2025, 7: 026001
208 Kang I, Zhang Q, Yu S X, et al. Coordinate-based neural representations for computational adaptive optics in widefield microscopy. Nat Mach Intell, 2024, 6: 714–725
209 Feng B Y, Guo H, Xie M, et al. NeuWS: neural wavefront shaping for guidestar-free imaging through static and dynamic scattering media. Sci Adv, 2023, 9: eadg4671
210 Cao R, Divekar N S, Nuñez J K, et al. Neural space-time model for dynamic multi-shot imaging. Nat Methods, 2024, 21: 2336–2341

211 Zhou Y, Xu C, Jin Z, et al. Physics-informed ellipsoidal coordinate encoding implicit neural representation for high-resolution volumetric wide-field microscopy. BioRxiv, 2024. 2024.10.17.618813
212 Zhao J, Zhao Z, Wu J, et al. PNR: physics-informed neural representation for high-resolution LFM reconstruction. 2024. ArXiv:2409.18223
213 Zhong E D, Bepler T, Davis J H, et al. Reconstructing continuous distributions of 3D protein structure from cryo-EM images. In: Proceedings of International Conference on Learning Representations, 2020
214 Marx V. Method of the year: spatially resolved transcriptomics. Nat Methods, 2021, 18: 9–14
215 Li S, Gai K, Dong K, et al. High-density generation of spatial transcriptomics with STAGE. Nucleic Acids Res, 2024, 52: 4843–4856
216 Zhu Q, Zheng Y, Sang Y, et al. Suica: learning super-high dimensional sparse implicit neural representations for spatial transcriptomics. 2024. ArXiv:2412.01124
217 Meng G, Huang J, Wang Y, et al. Progressive high-frequency reconstruction for pan-sharpening with implicit neural representation. In: Proceedings of the AAAI Conference on Artificial Intelligence, 2024. 4189–4197
218 Liang Y J, Cao Z, Deng S, et al. Fourier-enhanced implicit neural fusion network for multispectral and hyperspectral image fusion. In: Proceedings of Advances in Neural Information Processing Systems (NeurIPS), 2024. 63441–63465
219 Pan X, Chen D, Pan B, et al. Evolution and prospects of Earth system models: challenges and opportunities. Earth-Sci Rev, 2025, 260: 104986
220 Zheng H, Chu W, Zhang B, et al. Inversebench: benchmarking plug-and-play diffusion priors for inverse problems in physical sciences. In: Proceedings of the 13th International Conference on Learning Representations, 2025
221 Abed-Meraim K, Trung N L, Hafiane A, et al. A contemporary and comprehensive survey on streaming tensor decomposition. IEEE Trans Knowl Data En, 2022, 35: 10897–10921
222 Wu Y, Piao H, Huang L K, et al. SD-loRA: scalable decoupled low-rank adaptation for class incremental learning. In: Proceedings of the 13th International Conference on Learning Representations (ICLR), 2025
223 Cattaneo M D, Klusowski J M, Shigida B. On the implicit bias of Adam. In: Proceedings of the 41st International Conference on Machine Learning, 2024
224 Jahn T, Jin B. Early stopping of untrained convolutional neural networks. SIAM J Imaging Sci, 2024, 17: 2331–2361
225 Li J, Luo X, Qiao M. On generalization error bounds of noisy gradient methods for non-convex learning. In: Proceedings of International Conference on Learning Representations, 2020
226 You C, Zhu Z, Qu Q, et al. Robust recovery via implicit bias of discrepant learning rates for double over-parameterization. In: Proceedings of Advances in Neural Information Processing Systems, 2020. 17733–17744
227 Heckel R, Soltanolkotabi M. Compressive sensing with un-trained neural networks: gradient descent finds a smooth approximation. In: Proceedings of the 37th International Conference on Machine Learning, 2020. 4149–4158
228 Wu F, Liu S, Wang H, et al. Neural spatial-temporal tensor representation for infrared small target detection. 2024. ArXiv:2412.17302
229 Feng B Y, Varshney A. Signet: efficient neural representation for light fields. In: Proceedings of IEEE/CVF International Conference on Computer Vision (ICCV), 2021. 14204–14213
230 Yang Y, Cui Y, Zeng X, et al. STAIG: spatial transcriptomics analysis via image-aided graph contrastive learning for domain exploration and alignment-free integration. Nat Commun, 2025, 16: 1067
231 D'Orazio A, Briglia M R, Crisostomi D, et al. Implicit inversion turns clip into a decoder. 2025. ArXiv:2505.23161
232 Radford A, Kim J W, Hallacy C, et al. Learning transferable visual models from natural language supervision. In: Proceedings of the 38th International Conference on Machine Learning, 2021. 8748–8763
233 Zhu Y, Li Z, Wang T, et al. Conditional text image generation with diffusion models. In: Proceedings of IEEE/CVF Conference on Computer Vision and Pattern Recognition (CVPR), 2023. 14235–14244
234 Poole B, Jain A, Barron J T, et al. Dreamfusion: text-to-3D using 2D diffusion. In: Proceedings of the 11th International Conference on Learning Representations, 2023
235 Chung H, Kim J, Mccann M T, et al. Diffusion posterior sampling for general noisy inverse problems. In: Proceedings of the 11th International Conference on Learning Representations, 2023